The effects of changes in atmospheric mercury deposition on the bioaccumulation of mercury by fish

By

Diane M. Orihel

A Thesis Submitted
In Partial Fulfillment of the
Requirements of the Degree of

Master of Natural Resources Management

Natural Resources Institute
70 Dysart Road
The University of Manitoba
Winnipeg, Manitoba, Canada

THE UNIVERSITY OF MANITOBA

FACULTY OF GRADUATE STUDIES

*****

COPYRIGHT PERMISSION

The effects of changes in atmospheric mercury deposition on the bioaccumulation of mercury by fish

BY

Diane M. Orihel

A Thesis/Practicum submitted to the Faculty of Graduate Studies of The University of Manitoba in partial fulfillment of the requirement of the degree Of Master of Natural Resources Management

ABSTRACT

To improve our understanding of the effects of reductions in mercury (Hg) emissions on concentrations of this contaminant in fish, the present study examined the relationship between the deposition rate of atmospheric Hg and its concentration in the environment and food web of aquatic ecosystems. Different rates of atmospheric Hg deposition (1 to 15 times 7.1 $\mu g\ Hg \cdot m^{-2} \cdot yr^{-1}$) were simulated in large, in-lake mesocosms by adding multiple doses of inorganic Hg (enriched with ^{202}Hg). The experimentally-added Hg was quickly converted to methylmercury and incorporated into all levels of the food web within the 10-week experiment. Concentrations of the experimentally-added Hg in the environment and in the food web were directly proportional to Hg loading rates. This study suggests decreases in atmospheric Hg deposition will: i) immediately remove a pool of Hg from aquatic ecosystems that would otherwise be quickly methylated and bioaccumulated by aquatic biota; and ii) result in proportional changes in the MeHg content in biota that is derived from newly-deposited atmospheric Hg.

ACKNOWLEDGEMENTS

I gratefully acknowledge the support and guidance of my advisor, Drew Bodaly. I wish to thank my committee members Michael Paterson, Norman Kenkel, and Shirley Thompson for providing valuable comments on my thesis. I thank the Natural Resources Institute for welcoming me into their program and expanding the breadth of my graduate experience. I acknowledge the Environmental Science Division of Fisheries & Oceans Canada for engaging me into their research program and sharing their impressive wealth of knowledge with me.

This study was made by possible by the invaluable efforts of:

- Michael Paterson (Fisheries & Oceans Canada) for his role as project director, his insightful advice in all aspects of the study, and his defiant defence of the project;
- Drew Bodaly (Fisheries & Oceans Canada) for his guidance in planning, interpreting and communicating the study, and for promoting the findings to the scientific community;
- Holger Hintelmann (Trent University) and Cynthia Gilmour (Smithsonian Environmental Research Center) for their inputs into the study design, for conducting mercury analyses, and for discussing the intricacies of mercury with me;
- John Rudd and Carol Kelly (Rudd and Kelly Research Inc.) and Reed Harris (Tetra Tech Inc.) for their intellectual contributions to the experimental design and study interpretation;
- Alexandre Poulain and Marc Amyot (Université de Montréal) and George Southworth (Oakridge National Laboratory) for their roles in the evasion component of the project;

- Ken Sandilands, Danielle Godard, Marie-Laure Acolas, Jane Orihel, Marilynn Kullman, Dalila Seckar, Justin Shead, and many other Experimental Lakes Area (ELA) staff and students for their assistance in the field;
- Rick Wastle, John Babaluk, and Sandy Chalanchuk (Fisheries & Oceans Canada) for providing resources and training for ageing fish;
- Cheryl Podemski and Michelle Dobrin (Fisheries & Oceans Canada) for providing equipment and instructions for sampling and processing benthic invertebrates;
- Ray Hesslein (Fisheries & Oceans Canada) for helpful discussions on modelling tritium.

On a personal note, I thank my partner and my family for their incessant encouragement and support of my education. I thank fellow graduate students Lisa Loseto and Dalila Seckar for their friendship and for fostering a sense of community among the graduate students at the Freshwater Institute. I thank Michael Paterson and Drew Bodaly for making many experiences possible that have, and surely will continue to, open doors for me in my career.

Funding for this research was provided by the Collaborative Mercury Research Network (COMERN), a network of the Natural Science and Engineering Research Council of Canada (NSERC). In-kind support was provided by Fisheries & Oceans Canada and the Mercury Experimental to Assess Atmospheric Mercury Loading in Canada and the United States (METAALICUS). Personal funding was provided by the NSERC, the University of Manitoba, and the ELA Graduate Student Fund.

TABLE OF CONTENTS

LIST OF TABLES

LIST OF FIGURES

CHAPTER 1. Introduction

1.1 Mercury – an environmental contaminant of concern

Mercury (Hg) is an environmental contaminant that poses serious health risks to humans and wildlife. The form of this metal of most concern, methylmercury (MeHg), primarily exerts its toxic effect by impairing the function of the central nervous system (Fitzgerald and Clarkson 1991; Wolfe et al. 1998). By binding to sulphydryl groups (-SH), MeHg can disrupt the physiological function of proteins, and consequently impair normal cellular processes (Galli and Restani 1993; Tchounwou et al. 2003). MeHg readily crosses the placental and blood-brain barrier and interferes with fundamental processes of brain development, such as cell division and migration (World Health Organization 1990; United Nations Environment Programme 2002).

The profound effects of MeHg on human health were recognized by tragic poisonings in Japan (1950s – 60s) and Iraq (1971 – 72). Thousands of people in Japan became ill, in some cases fatally, after eating fish and shellfish from coastal waters and rivers receiving effluent from factories inadvertently synthesizing MeHg as a waste product in the manufacture of acetaldehyde (Takizawa 1979). Victims suffered from a neurological disease characterized by numbness in the extremities, incoordination, constriction of visual fields, loss of hearing, and speech impairment (Clarkson 2002). Children of women who consumed fish during pregnancy were born with severe developmental disabilities, including cerebral palsy, mental retardation, and seizures (Davidson et al. 2004). In Iraq, a mass poisoning occurred after farmers and their families ate bread made from seed grains treated with methylmercurial fungicides.

People who consumed the contaminated bread suffered symptoms similar to those observed in the earlier poisoning in Japan (Bakir et al. 1973). Delays in achieving developmental milestones were also documented in children exposed to MeHg *in utero* or by breastfeeding (World Health Organization 1990).

Today, the risk of MeHg toxicity in the general human population primarily arises from chronic, low-dose exposure to MeHg in the diet, primarily from consumption of fish and fish products (World Health Organization 1990). Over the last 20 years, adverse effects of MeHg from fish consumption have been documented in a number of fish-eating communities, including subtle neurological impairments, and to a lesser extent, increased risk of cardiovascular problems (Table 1-1). Indigenous populations and others groups who consume large amounts of contaminated fish or marine mammals are believed to be most at risk (United Nations Environment Programme 2002).

The health risks associated with MeHg exposure not only apply to humans, but also to fish-eating birds and mammals, and to fish themselves. MeHg toxicity in mammals is generally manifested as lethargy, emaciation, incoordination, visual impairments, and later, convulsions and death (Wiener and Spry 1996; Wolfe et al. 1998). Overt MeHg intoxication has been observed in fish downstream of acetaldehyde plants (Wiener et al. 2003), in birds during the widespread use of alkylmercurials as seed fungicides (Chan et al. 2003), and in mink and otter downstream of manufacturers using the chlor-alkali process (Wobeser 1976; Wren 1985). Direct aqueous discharges of high concentrations of Hg have largely been eliminated from industrialized countries, but there is evidence that current environmental concentrations of Hg from diffuse sources are causing harm to fish and wildlife (Wiener et al. 2003). Exposure of fish to

environmentally-relevant concentrations of Hg has been shown to result in diminished foraging behaviour (Fjeld et al. 1998; Samson et al. 2001), impaired predator avoidance (Weis and Weis 1995; Webber and Haines 2003), and reduced reproductive success (Friedmann et al. 1996; Latif et al. 2001; Hammerschmidt et al. 2002). In birds, sublethal effects of MeHg include increased susceptibility to disease (Spauldling et al. 1994), altered chick behaviour (Nocera and Taylor 1998), and reduced reproductive success (Fimbreite 1974; Meyer et al. 1998; Scheuhammer et al. 1998). Scheuhammer and Blancher (1994) estimated that up to 30% of the lakes in Ontario contain small fish with Hg levels sufficiently high to pose a risk to the reproductive success of loons. Further, Hg concentrations in the brains of otter and mink caught in the wild have been within the range ($5 - 10\ \mu g \cdot g^{-1}$ ww) known to produce sublethal effects on mammals in controlled laboratory studies, such as impaired escape and avoidance behaviours and abnormal performance on learning tasks (Wiener et al. 2003).

As studies suggest contemporary levels of Hg in the environment are posing a threat to humans and wildlife, it is critical to understand the sources of Hg contamination. Both natural and anthropogenic sources release Hg to the environment. Inorganic Hg compounds occur naturally in the Earth's crust and mantle, and can be released by degassing (e.g. volcanoes and geothermal vents) and weathering of rocks (Jackson 1997). Mercury is also released from forest fires and evasion from soil, water and vegetation surfaces (Morel et al. 1998; Schroeder and Munthe 1998), but these sources likely represent a mix of natural and anthropogenic Hg (Fitzgerald and Lamborg 2003). Historically, the most important anthropogenic source of Hg was the mining and smelting of cinnabar (HgS) and other Hg ores (Clarkson 1997). For centuries, liquid Hg has been

used to recover gold and silver in mining operations (see "patio process", Fitzgerald and Lamborg 2003), and continues to be used today in many developing countries (Wiener et al. 2003). In the 1950s – 60s, industrial applications of Hg, such as in chlor-alkali plants and pulp and paper mills, were responsible for large releases of Hg to water bodies, but these discharges have largely been curtailed in industrialized countries (Wiener et al. 2003). Presently, the single most important anthropogenic source of Hg is the combustion of fossil fuels, particularly the burning of coal in electric power plants (Jackson 1997), but the incineration of municipal refuse, medical waste, and sewage sludge, as well as metal smelting, refining and manufacturing, are also major sources (Schroeder and Munthe 1998). Global emissions from various anthropogenic sources have recently been estimated by Pacyna and Pacyna (2002) (Table 1-2).

Based on recent global models, emissions of Hg to the atmosphere from anthropogenic sources now exceed emissions from natural sources (Lindqvist et al. 1991; Mason et al. 1994; Hudson et al. 1995; Lamborg et al. 2002). Strong empirical evidence exists that anthropogenic activities have increased the mass of Hg cycling in the environment. Measurements of Hg in air over the Atlantic Ocean during the period of 1977 – 1990 determined that total gaseous Hg concentrations increased by 1.5 and 1.2 % per year in the northern and southern hemispheres, respectively (Slemr and Langer 1992). Further, chronological Hg concentrations in dated lake sediment, peat, terrestrial soil and ice cores from geographically diverse regions indicate that contemporary Hg levels in the environment have increased substantially since the beginning of the Industrial Revolution, with concentrations typically peaking in the late 20th century (Jackson 1997; Fitzgerald 1998). For example, sediment cores collected from numerous locations,

including remote areas not receiving local point source pollution, reveal that modern fluxes of Hg to lake sediments are typically 2 – 4 fold higher than pre-industrial rates (Table 1-3). Recently, a comprehensive 270-year record obtained from ice cores collected from the Upper Fremont Glacier (Wyoming) shows a 20-fold increase in Hg deposition since pre-industrial times (Schuster et al. 2002). They estimate that 70% of Hg accumulated in the ice core over the last century was from anthropogenic sources. The similarities in the timing and magnitude of Hg accumulation over the last 150 years in geographically disparate ecosystems, even in remote regions, strongly indicate that long-range atmospheric transport of Hg from anthropogenic emissions is largely the cause of this contamination (Jackson 1997; Fitzgerald 1998) .

Atmospheric circulation of Hg emissions has caused some degree of Hg contamination in virtually all water bodies (Morel et al. 1998). Many water bodies across North American now contain fish with MeHg concentrations considered unsafe for unrestricted human consumption. In 2003, Hg was responsible for 18 – 67% of consumption restrictions on sport fish in the Great Lakes water system and over 98% of consumption restrictions from inland locations in Ontario (Ontario Ministry of Environment 2003). In the same year, water bodies in 45 US states were under Hg advisories, including 13,068,990 lake acres and 766,872 river miles (U.S. Environmental Protection Agency 2004). The prevalence of Hg contamination in fish has recently prompted health authorities in Canada and the United States to issue warnings to pregnant women and children to limit consumption of particular fish species (Health Canada 2002; U.S. Food and Drug Administration and U.S. Environmental Protection Agency 2004).

1.2 Cycling of mercury in the environment

Mercury has a complex biogeochemical cycle that is driven by natural processes, but has been modified by human activities. For example, natural forces are responsible for dispersing Hg in the atmosphere, controlling air-surface exchanges of Hg, transporting Hg between land and water bodies, transforming inorganic Hg to more toxic organic forms, and incorporating Hg into food chains. Most significantly, humans are modifying the cycling of Hg in the environment by releasing naturally-occurring Hg in the Earth's crust to the atmosphere (e.g. burning fossil fuels, particularly coal), thereby increasing the mass of Hg cycling in the environment today. Humans have also directly released Hg to waterways and caused environmental changes that affect the rate at which natural processes transport or transform Hg in the environment (e.g. reservoir flooding, acid deposition, deforestation).

Mercury emitted to the atmosphere from natural and anthropogenic sources is dispersed by air currents, which can transport Hg great distances away from its source of emission. The speciation of Hg in emissions determines its residence time and transport distance in the atmosphere. Mercury emissions to the atmosphere are operationally defined as: i) elemental Hg vapour [Hg^0]; ii) soluble divalent inorganic Hg species [Hg(II)]; and iii) particulate phase Hg [$Hg_{(p)}$] (Lindqvist 1994; Schroeder and Munthe 1998). Mercury emitted from water, soils, and vegetation is mainly released to the atmosphere as Hg^0 (Cohen et al. 2004), while anthropogenic emissions contain various Hg species depending on the particular processes employed. For example, emissions from coal-fired power plants in Canada and the United States contain, on average, 50% Hg^0, 45% Hg(II), and 5% $Hg_{(p)}$ (Cohen et al. 2004). Elemental Hg is volatile, relatively

unreactive, and sparingly soluble in water (Jackson 1997; Schroeder and Munthe 1998); consequently, Hg^0 has an atmospheric residence time of one year or more (Lindqvist 1994; Porcella 1994; Fitzgerald and Lamborg 2003) and may be transported thousands or even tens of thousands of kilometres away from its source of emission (Lindqvist 1994; Jackson 1997; Schroeder and Munthe 1998). Hg(II) is less volatile, highly reactive and much more soluble (Lin and Pehkonen 1999; Cohen et al. 2004), and therefore remains in the atmosphere for days to weeks (Porcella 1994; Lin and Pehkonen 1999) and may be transported tens to hundreds of kilometres (Schroeder and Munthe 1998). The residence time and transport distance of $Hg_{(p)}$ is dependent on particle size and wind speed (Porcella 1994), but is considered to be intermediate to other forms of Hg (Schroeder and Munthe 1998). Because the various forms of Hg differ in their atmospheric residence times, Hg pollution occurs on local, regional, and global scales. Mason et al. (1994) estimate that approximately half of anthropogenic Hg emissions are deposited locally or regionally, while the other half enter the global atmospheric cycle.

On a global scale, most Hg in the atmosphere is in the form of Hg^0 (> 90%) (Porcella 1994; Lin and Pehkonen 1999; Fitzgerald and Lamborg 2003; Cohen et al. 2004), yet Hg is removed from the atmosphere and returns to the Earth's surface largely in oxidized forms (Porcella 1994). An important chemical process in the atmosphere is the oxidation of Hg^0 to Hg(II), as this may subsequently result in removal from the atmosphere. Oxidation of Hg^0 is thought to occur in clouds and scavenging aerosols (Mason et al. 1994). Hg^0 is known to be oxidized by ozone, hydrogen peroxide, chlorine, and hydroxyl radicals in the gas phase, and by ozone, hydroxyl radicals, hydrochlorous acid and hypochlorite ions in the aqueous phase (e.g. cloud droplets) (Cohen et al. 2004).

The relative importance of different oxidation pathways in the atmosphere, however, is yet to be determined (Fitzgerald and Lamborg 2003).

Hg in the atmosphere can be incorporated into water droplets and returned to the Earth's surface in precipitation (wet deposition). Alternatively, random turbulent air motions can transfer Hg from the atmosphere to water, vegetation, and land surfaces (dry deposition). Wet and dry processes can act on Hg^0, Hg(II), or $Hg_{(p)}$ (Schroeder and Munthe 1998), but the susceptibility of each form depends on its specific chemical and physical properties. Mercury in wet deposition consists mostly of Hg(II) and $Hg_{(p)}$ forms (Cohen et al. 2004). Hg^0 is not efficiently incorporated into wet deposition as it is only sparingly soluble in water (Cohen et al. 2004). Hg(II) is about 10^5 times more soluble than Hg^0 (Lindberg and Stratton 1998) and readily dissolves in atmospheric waters (Lin and Pehkonen 1999) either within or below clouds (Cohen et al. 2004). $Hg_{(p)}$ can be wet-deposited if its host particles are scavenged by precipitating clouds (Cohen et al. 2004). Small amounts of MeHg have also been reported in precipitation, but the source of this MeHg is not known (Schroeder and Munthe 1998).

Wet deposition is often the dominant process removing Hg from the atmosphere (Morel et al. 1998; Lamborg et al. 2002), but dry deposition can be important in forested areas (Schroeder and Munthe 1998), over the open ocean (Mason et al. 2003), and close to emission sources (Fitzgerald and Lamborg 2003). Plants, particularly trees, are believed to play an important role in the dry deposition of atmospheric Hg. In particular, plant surfaces are involved with dry deposition via the adsorption and oxidation of gaseous Hg, the uptake of gaseous Hg by stomata, and the adsorption of Hg(II) and $Hg_{(p)}$ (Schroeder and Munthe 1998). Hg associated with plant surfaces may be washed off by

precipitation (Fitzgerald and Lamborg 2003) or retained by leaves and deposited to the forest floor in senescing leaves (Schroeder and Munthe 1998).

Atmospheric Hg may be deposited directly to the surface of a lake (direct deposition), or may be deposited to a lake's watershed and subsequently transferred to the lake (indirect deposition) (Cohen et al. 2004). Mercury deposited to watersheds is transported to downstream water bodies in streams, direct runoff, or groundwater (Mierle 1990; Sellers et al. 1996), largely in association with dissolved organic carbon (DOC) (Morel et al. 1998). Atmospheric Hg deposited to land tends to be sequestered by surface soils, where it accumulates and is only slowly released to water bodies (Mason et al. 1994).

Once atmospheric Hg is deposited to aquatic systems, it undergoes a complex biogeochemical cycle. Watras et al. (1994) identify three important pathways for atmospheric Hg in lakes: i) reduction to elemental Hg and subsequent re-emission to the atmosphere (evasion); ii) particle scavenging and sedimentation; and iii) conversion to MeHg (methylation) and subsequent bioaccumulation in aquatic organisms or demethylation. Different pathways compete for the available Hg, and the balance among these pathways is determined by a complex suite of environmental variables (Watras et al. 1994).

In surface waters, Hg(II) can be reduced to its elemental form [referred to as "dissolved gaseous mercury" (DGM)] by photochemical and bacterial processes (Morel et al. 1998; Fitzgerald and Lamborg 2003; Tseng et al. 2004). Because the reverse reaction [oxidation of Hg(0) to Hg(II)] can also occur, DGM concentrations are controlled by the balance between oxidation and reduction processes (Siciliano et al.

2002). A distinct diel pattern in DGM concentrations has been observed in many aquatic systems, with a maximum concentration around noon and a minimum concentration during the night, often just before sunrise (Amyot et al. 1994; Krabbenhoft et al. 1998; Lindberg and Zhang 2000; O'Driscoll et al. 2003). Surface waters of a large majority of aquatic systems are supersaturated with DGM (Schroeder and Munthe 1998; Fitzgerald and Lamborg 2003), which creates a concentration gradient across the air-water interface and drives the evasion of Hg to the atmosphere. Hg evasion is not only controlled by the concentration of DGM across the air-water interface, but also by ambient environmental factors, such as solar radiation, wind speed, water temperature, and DOC (Lindberg and Zhang 2000; Tseng et al. 2004).

A significant proportion of Hg deposited to water bodies is re-emitted to the atmosphere, although estimates are variable among systems. Mason et al. (1994) estimated that Hg evasion from the ocean to the atmosphere is approximately equal to the amount of Hg deposited to the ocean. Similarly, Tseng et al. (2004) determined that Hg evasion from Arctic lakes during ice-free periods is similar to atmospheric Hg inputs. Fitzgerald et al. (1991) estimated that in Little Rock Lake, Wisconsin, Hg evasion to the atmosphere represents 7 – 14% of annual Hg deposition, while Krabbenhoft et al. (1998) determined that Hg evasion from the Florida Everglades is equal to 10% of Hg deposition. The extent of DGM production and evasion in a system is critical because this pathway decreases the reactive Hg pool available for methylation and uptake by biota (Fitzgerald et al. 1991).

Another important pathway by which atmospheric Hg is removed from the water column of aquatic systems is particle scavenging and sedimentation. Mercury has a high

tendency to be sorbed to particles (Ullrich et al. 2001). In fact, most of the Hg in natural waters is bound to organic matter (U.S. Environmental Protection Agency 1997). Specifically, inorganic Hg binds strongly to mineral particles and organic detritus in the water column (Morel et al. 1998; Ullrich et al. 2001). The association of Hg in the water column to suspended particles largely controls the distribution of this element in freshwaters, as sedimentation processes acting on particles in the water column can transport Hg to the lake bottom (Ullrich et al. 2001). For example, settling of particulate matter is the most important mechanism delivering Hg to the sediment-water interface in Little Rock Lake, Wisconsin (Watras et al. 1994). Particle scavenging in surface waters and subsequent particulate dissolution at the redox boundary is responsible for the accumulation of Hg in the hypolimnion of this lake (Hurley et al. 1994). Similarly, the most important loss of Hg from the water column of Lake Velenje, Slovenia, is the settling of particulate matter (Kotnik et al. 2002). Sediments are important sites for MeHg production (as discussed below), hence sedimentation of particulate Hg increases the pool of inorganic Hg at potential sites of methylation. Alternatively, sedimentation of particulate Hg can result in burial in sediments, thereby removing the Hg, at least temporarily, from circulating within the lake.

Methylation of inorganic Hg is a critical process in aquatic systems because this reaction increases the bioavailability and toxicity of Hg (Wiener et al. 2003). In the methylation process, a methyl group ($-CH_3$) is transferred from an organic compound to a Hg ion (Hg^{2+}), usually producing monomethylmercury (CH_3Hg^+) (Morel et al. 1998). Methylation of inorganic Hg occurs through both abiotic and biotic pathways, but biological methylation is considered to be more important in natural systems (Winfrey

and Rudd 1990; Ullrich et al. 2001; Benoit et al. 2003; Fitzgerald and Lamborg 2003). Sulphate-reducing bacteria have been identified as the primary methylating agents in estuarine (Compeau and Bartha 1985) and freshwater sediments (Gilmour et al. 1992). The mechanism by which Hg(II) enters bacterial cells is not well-established, but Benoit et al. (1999; 2001) hypothesize that uptake occurs by passive diffusion of small, neutral hydrophobic Hg complexes, likely HgS^0. Alternatively, Golding et al. (2002), propose that uptake of Hg(II) by bacteria occurs via facilitated transport. Further evidence for the facilitated transport hypothesis is provided by a recent study of Hg(II) uptake in an aquatic bacterium using a Hg(II)-specific bioreporter (Kelly et al. 2003).

The formation of MeHg by microbes is probably an accidental process (Ullrich et al. 2001), but little is known about the biochemical mechanisms involved (Ekstrom et al. 2003). *Desulfovibrio desulfuricans* LS, a sulphate-reducing bacteria, has been shown to methylate inorganic Hg via methylcobalamin (a vitamin B_{12} derivative), in association with the acetyl-coenzyme A (CoA) synthase pathway (Choi and Bartha 1993; Choi et al. 1994). However, Ekstrom et al. (2003) determined that methylation can also occur independent of the acetyl-CoA pathway in several strains of bacteria, and may not require vitamin B_{12}.

Methylation of inorganic Hg can take place both within lakes and in their watersheds. The most important sites of microbial methylation of inorganic Hg are oxic-anoxic interfaces of sediments and wetlands (Ullrich et al. 2001; Fitzgerald and Lamborg 2003; Wiener et al. 2003). Epilimnetic sediments have been identified as key sites of in-lake methylation, at least in oligotrophic lakes of the Canadian Shield (Ramlal et al. 1993). A recent study suggests that considerable amounts of MeHg are produced in the

water column, particularly under anoxic conditions (Eckley et al. 2005). Minor amounts of MeHg are also formed in floating periphyton mats and roots of certain aquatic plants, and in the intestine and slime layer of fish (Wiener et al. 2003). In the watershed, wetlands and peatlands actively produce MeHg (Ullrich et al. 2001). For example, St. Louis et al. (1994) compared yields of MeHg from different types of boreal forest catchments, and determined that wetlands export 26 – 79 times more MeHg per unit area than upland areas. MeHg formed within watersheds can be transported to lakes by streams or direct runoff (Sellers et al. 2001).

The relative importance of different sources of MeHg to aquatic systems has been examined in several studies. Internal sources of MeHg to lakes include any in-lake methylation processes, while external sources include direct deposition of atmospheric MeHg, and the export of MeHg from the surrounding watershed (Sellers et al. 2001). In a boreal lake in northwestern Ontario, Sellers et al. (2001) determined that in-lake methylation was at least one order of magnitude greater than import from the watershed, and 30-fold greater than atmospheric deposition. Verta et al. (1994) concluded that watershed export was the main source of MeHg to drainage lakes in Finland, while atmospheric deposition and in-lake production was more important in seepage lakes. Based on a series of modelling exercises, Rudd (1995) concludes that atmospheric deposition, watershed export, and in-lake production can all be important sources of MeHg to lakes under different circumstances. Specifically, he suggests that the relative importance of the three sources of MeHg varies with the rate of atmospheric deposition, lake type, percentage of wetlands in watershed, and the percentage of water surface area that covers flooded terrain.

Demethylation, the conversion of MeHg to inorganic Hg, occurs in near-surface sediments via microbial processes and in the water column via biotic or abiotic processes (Wiener et al. 2003). Some microbes demethylate Hg using an active detoxification pathway, which is encoded by the *mer* operon. The *mer* gene sequence encodes for enzymes that are responsible for cleaving the C-Hg bond, and subsequently reducing Hg(II) to Hg(0) (Benoit et al. 2003). Microbes can also break down MeHg by oxidative demethylation, which is not an active detoxification pathway (Benoit et al. 2003). Marvin-DiPasquale et al. (2000) suggest oxidative demethylation is the dominant mechanism in less contaminated sites, while the *mer*-detoxification pathway is active in severely contaminated environments. MeHg can also be decomposed abiotically by photodegradation in surface waters (Sellers et al. 1996). Photodegradation of MeHg can represent a significant flux in the mass balance of lakes (Sellers et al. 2001).

Net methylation (i.e. the balance of methylation and demethylation) is controlled by a number of environmental factors, including temperature, dissolved oxygen, sulphate, pH, and organic carbon. These factors can affect either the bioavailability of inorganic Hg for uptake or the activity of the microbes (Fitzgerald and Lamborg 2003). Because methylation is stimulated by higher water temperatures, while low water temperatures favour demethylation, net methylation is greater at higher temperatures (Wright and Hamilton 1982; Bodaly et al. 1993; Ramlal et al. 1993). Most studies indicate that methylation:demethylation ratios are less than one in aerobic conditions, and greater than one in anaerobic conditions (Gilmour and Henry 1991). Gilmour et al. (1992) report that the addition of sulphate (SO_4^{2-}, a substrate required by sulphate-reducing bacteria to break down organic matter) stimulates methylation in sediments at low concentrations,

but above an optimal concentration, methylation is inhibited by the production of sulphide (S^{2-}, a metabolic by-product of sulphate reduction). Benoit et al. (1999; 2001) suggest that sulphide inhibits methylation by shifting the speciation of Hg(II) from neutral species to more polar species, thereby decreasing the bioavailability of Hg(II) for passive diffusion into the bacterium. Acidity has been shown to both stimulate and inhibit methylation (Gilmour and Henry 1991), but low pH generally enhances net methylation in lake water and at the sediment-water interface, and depresses net methylation in anoxic sediments (Ullrich et al. 2001). Uptake of Hg(II) by one bacterial strain has been shown to increase in direct proportion to hydrogen ion concentration (Kelly et al. 2003). The relationship between organic carbon and net methylation is complex, as organic carbon stimulates microbial activity but decreases the bioavailability of Hg(II) for uptake by bacteria (Ullrich et al. 2001). According to Gilmour and Henry (1991), organic carbon increases methylation in the water column, but decreases methylation in the sediments.

1.3 Mercury bioaccumulation in aquatic food webs

The problem of Hg in the environment has largely focused on fish, as these animals play the pivotal role of transferring MeHg from aquatic systems to humans and other mammals. Because fish obtain the majority of their MeHg from their diet, the importance of the aquatic food web as a whole needs to be considered. The dynamics of Hg uptake into the base of the food web and the subsequent transfer of Hg between trophic levels influences MeHg levels in fish, and by corollary, exposure to humans and wildlife.

1.3.1 Organisms at the base of aquatic food webs

The uptake of Hg into the base of the aquatic food chain is critical to its subsequent bioaccumulation and biomagnification in the food web (Mason et al. 1996; Lawson and Mason 1998; Watras et al. 1998; Moye et al. 2002; Chen and Folt 2005). Unfortunately, our understanding of the dynamics of MeHg in the lower food web is inadequate (Moye et al. 2002).

MeHg has a strong tendency to bioaccumulate in lower food web organisms. The bioaccumulation capacity of a contaminant is usually expressed in terms of its concentration in biota relative to its concentration in water:

$$BAF = (C_{biota} / C_{water})$$

where BAF is the bioaccumulation factor of the contaminant (usually expressed in $\log_{10}$ units), C_{biota} is the concentration of the contaminant in biota, and C_{water} is the concentration of the contaminant in the dissolved phase of water. Field and lab studies have reported BAFs for MeHg over 10^5, for both seston and periphyton (Table 1-4), demonstrating the highly efficient bioaccumulation of MeHg by organisms at the base of aquatic food webs.

Inorganic Hg also bioaccumulates in lower trophic organisms of natural systems, but to a lesser extent than MeHg (Table 1-4). The lower bioaccumulation of Hg(II) by seston and periphyton in field studies may result from organisms having a lower affinity for Hg(II), and/or from Hg(II) having a greater tendency to form complexes that are not available for uptake by biota (Watras et al. 1998). The latter explanation is more likely

for two reasons. First, Hg(II) and MeHg uptake rates by microorganisms in controlled laboratory studies are not substantially different (Boudou and Ribeyre 1981; Hintelmann et al. 1993). Second, Hg(II) is estimated to bind to DOC more strongly than MeHg (Dyrssen and Wedborg 1991), and as DOC-Hg complexes are thought to inhibit Hg uptake by phytoplankton (Mason et al. 1996; Moye et al. 2002), the higher affinity of DOC for Hg(II) may explain the depressed bioaccumulation of Hg(II) in natural systems.

Previously, it was presumed that Hg bioaccumulates in organisms because of a high lipid solubility, analogous to hydrophobic organic pollutants, such as polychlorinated biphenyls (Mason et al. 1995; 1996). The rationale behind this hypothesis was that hydrophobic compounds readily pass through the lipid bilayer of cell membranes. The lipid solubility of MeHg and Hg(II) complexes, however, has been determined to be several orders of magnitude less than organic pollutants with similar BAFs (Mason et al. 1995). The high bioaccumulation capacity of Hg, despite its low hydrophobicity, has been attributed to the strong binding of Hg(II) and MeHg to intracellular ligands (Mason et al. 1996). To support this hypothesis, Mason et al. (1996) exposed broken diatom cells to dissolved Hg(II) and MeHg. Both Hg(II) and MeHg were rapidly and efficiently removed from solution, suggesting that this metal is highly reactive with intracellular ligands.

It is not well-understood how microorganisms assimilate Hg from their environment. Metal contaminants typically cross cell membranes via transport systems of nutrient metals, but if metals form uncharged, nonpolar complexes, they can also enter cells by passive diffusion (Sunda and Huntsman 1998). Mason et al. (1995; 1996) suggest that Hg uptake by phytoplankton occurs by passive diffusion of neutral Hg

complexes across the cell membrane, based on the observation that uptake rates of both Hg(II) and MeHg into the diatom *Thalassiosira weissflogii* were positively correlated with the calculated proportions of uncharged Hg complexes in solution. In contrast, Moye et al. (2002) conclude that uptake of MeHg by phytoplankton is more characteristic of active transport, as uptake by four species of algae was not related to the surface area-volume ratio of the cells and was partly depressed by metabolic inhibitors, exposure to γ-radiation, and darkness. Watras et al. (1998) also conclude that MeHg uptake by phytoplankton and bacterioplankton is likely dominated by active transport, based on the finding that the calculated aqueous concentration of the free MeHg ion was a better predictor of seston BAFs among Wisconsin lakes than concentrations of neutral MeHg complexes.

Just as the mechanisms of Hg uptake by biota at the base of aquatic food webs are still being elucidated, our understanding of the environmental factors controlling Hg accumulation in these organisms is only in its infancy. If Hg is taken up by passive diffusion, then water chemistry parameters that determine Hg speciation, such as pH and chloride concentration, will be important factors governing Hg uptake (Mason et al. 1995; 1996). On the contrary, if Hg is taken up by active transport, then environmental factors that affect an organism's metabolism, such as light levels (for autotrophs) and temperature, will affect Hg uptake rates (Moye et al. 2002). Two environmental factors that appear to play important roles in Hg uptake by phytoplankton are organic carbon and phytoplankton biomass.

The inhibitory effect of organic carbon on Hg uptake by phytoplankton has been observed in both laboratory and field experiments. For example, when natural organic

matter was added to algal cultures spiked with MeHg, uptake was significantly reduced relative to control cultures (Moye et al. 2002). Further, seston BAFs for both Hg(II) and MeHg were negatively correlated with lake DOC concentrations in two field studies (Back and Watras 1995; Watras et al. 1998). In the study by Watras et al. (1998), DOC concentrations explained over half of the variation in Hg(II) and MeHg bioaccumulation by seston in 15 Wisconsin lakes.

The importance of phytoplankton biomass on Hg accumulation has been suggested by both controlled experiments and surveys of natural systems. Riisgard and Hansen (1990) report that the accumulation of Hg(II) by the alga *Phaeodactylum tricornutum* was approximately four times greater in cell cultures of 60,000 cells·mL^{-1}, than at 200,000 cells·mL^{-1}. Pickhardt et al. (2002) added stable Hg isotopes of Hg(II) or MeHg to microcosms inoculated with phytoplankton at different nutrient levels. Based on the observation that Hg concentrations in phytoplankton were lower in microcosms with higher nutrient inputs, the authors conclude that algal blooms can "dilute" Hg bioaccumulation in phytoplankton. Similarly, Chen and Folt (2005) determined that phytoplankton Hg levels were negatively correlated with lake-specific chlorophyll densities (a surrogate measure for algal biomass) in northeastern US lakes.

1.3.2 Aquatic invertebrates

When lower trophic organisms are fed upon by invertebrates, some of the Hg bound to the prey organism is transferred to the consumer organism – a process referred to as "trophic transfer". While there is relatively little discrimination between Hg(II) and MeHg in uptake by algae and bacteria, the efficiency by which these two Hg forms are transferred between these organisms and their invertebrate consumers are considerably

different. Controlled experiments have consistently demonstrated that the trophic transfer of MeHg to zooplankton and benthic invertebrates is much more efficient for MeHg than Hg(II) (Boudou and Ribeyre 1981; Riisgard and Hansen 1990; Mason et al. 1995; Mason et al. 1996; Lawson and Mason 1998). For example, over 60% of MeHg in phytoplankton is assimilated by invertebrate grazers, while less than 40% of Hg(II) is assimilated (Table 1-5).

The differential trophic transfer of MeHg and Hg(II) between phytoplankton and invertebrates may be the consequence of the distribution of these forms in the phytoplankton cell. As copepods are believed to digest phytoplankton by breaking open algal cells and assimilating the soluble cellular material of the cytoplasm, metals associated with the cytoplasm of phytoplankton are more readily assimilated by zooplankton predators than metals associated with cellular membranes (Reinfelder and Fisher 1991). Mason et al. (1995; 1996) hypothesized that zooplankton assimilate MeHg from phytoplankton more efficiently than Hg(II) because of their differential fractionation in the phytoplankton cell. To test this hypothesis, cultures of the marine diatom *Thalassiosira weissflogii* were exposed to either Hg(II) or MeHg. The majority of MeHg accumulated by diatoms was in the cytoplasm, while almost all of the Hg(II) was associated with the cell membrane. When these diatoms were fed to adult calanoid copepods, the assimilation efficiency of MeHg and Hg(II) (62 and 15%, respectively) closely corresponded to the percentage of each Hg form in the cytoplasm of the diatom (62 and 9%, respectively).

Concentrations of MeHg in zooplankton and benthic invertebrates can be higher than their respective prey. This is termed "biomagnification", and is frequently expressed in terms of a biomagnification factor (BMF):

$$BMF = (C_{predator} / C_{prey})$$

where BMF is the biomagnification factor of the contaminant (usually expressed in $\log_{10}$ units), $C_{predator}$ is the concentration of the contaminant in the predator, and C_{prey} is the concentration of the contaminant in the prey. Biomagnification results when consumers taken in contaminants and carbon from their food and then respire carbon at a faster rate than they eliminate the contaminant.

In natural systems, biomagnification of MeHg commonly occurs between seston and zooplankton (Table 1-6). Likewise, benthic invertebrates in two Maryland streams had MeHg levels 3 – 10 times higher than the periphyton/plant material in their diet (Mason et al. 2000). It is important to emphasize that the biomagnification of MeHg between invertebrates and their algal prey rarely exceeds 10^1, while bioaccumulation of MeHg between water and algae is commonly greater than 10^6. In contrast to MeHg, zooplankton BMFs for Hg(II) suggest little biomagnification in natural systems (Table 1-6). Because MeHg biomagnifies between lower trophic organisms and invertebrate consumers to a greater degree than Hg(II), MeHg accounts for a greater proportion of Hg in zooplankton and zoobenthos than their respective prey (Watras and Bloom 1992; Watras et al. 1998; Mason et al. 2000). In other words, trophic transfer tends to result in a relative concentration of MeHg over Hg(II).

Only a few studies have rigorously examined the pathways by which zooplankton absorb Hg from their environment. Furthermore, the relative importance of these pathways in natural systems is poorly understood. Zooplankton have been shown to absorb MeHg and Hg(II) from both water and food under laboratory conditions (Monson and Brezonik 1999; Tsui and Wang 2004b). Tsui and Wang (2004b) developed a simple model to examine the relative importance of MeHg and Hg(II) uptake by zooplankton from food and water in natural systems. They modelled zooplankton bioaccumulation using experimentally-derived influx rates and assimilation efficiencies for *D. magna*, along with literature values for phytoplankton BAFs and ingestion rates. Within the typical range of ingestion rates, their model predicted that zooplankton derive more than 50% of their MeHg from food when phytoplankton BAFs are above 10^5, and more than 90% from food when phytoplankton BAFs are above 10^6. Tsui and Wang (2004b) predicted that 50% or more of Hg(II) accumulated by zooplankton in natural systems is usually derived from water when phytoplankton BAFs are below $10^{4.7}$, regardless of ingestion rate. However, food was predicted to become a more important source of Hg(II) for zooplankton at greater phytoplankton BAFs, particularly at higher ingestion rates.

For benthic invertebrates, the situation is even more complicated, as a greater number of exposure routes are possible. Benthic organisms are potentially exposed to Hg in water overlying sediments and in sediment porewater, as well as Hg associated with sediment particles and particulate matter suspended in the water column. Lawrence and Mason (2001) conducted a series of microcosm experiments with the amphipod *Leptocheirus plumulosus*, in which Hg(II) and MeHg were spiked to either water,

sediment, algae, or both sediment and algae. They conclude diet was the most important route of uptake of Hg(II) and MeHg by *L. plumulosus*. Parks et al. (1988) observed that Hg concentrations in caged crayfish in a Hg-contaminated river and a non-contaminated river were similar when fed the same diet, demonstrating that waterborne Hg concentration had little or no effect on Hg bioaccumulation in these animals. Furthermore, crayfish fed a high-Hg diet had concentrations 20 times higher than those fed a low-Hg diet at the same site, indicating the importance of diet in Hg bioaccumulation.

Some factors affecting trophic transfer of Hg to invertebrates have been identified in laboratory experiments. First, food quantity has been shown to affect Hg assimilation efficiency. Tsui and Wang (2004b) observed that the assimilation efficiencies of both Hg(II) and MeHg in *D. magna* exponentially declined with increasing food availability. Second, the concentration of Hg in food may affect its assimilation efficiency. The assimilation efficiencies of Hg(II) and MeHg of *D. magna* both appeared to decline with higher Hg concentrations in food, but the relationship was only statistically significant for MeHg (Tsui and Wang 2004b). Third, species-specific feeding adaptations can affect Hg assimilation efficiencies for a given prey item. Lawson and Mason (1998) observed that the benthic species *Hyallela azteca* assimilated MeHg more efficiently than the planktonic species *Eurytemora affinis* when feeding on diatoms previously exposed to MeHg, particularly after diatom cultures were degraded. The authors suggest *H. azteca* has evolved strategies to more efficiently extract nutrients from its food. Finally, the diet of different invertebrate species may be important. While most studies focus on trophic transfer between algal cells and invertebrates, many invertebrates are predatory, feeding

on heterotrophic protists or smaller invertebrates. Twining and Fisher (2004) observed that copepods generally assimilated metals more efficiently when feeding on protozoans than when feeding on diatoms, which the authors attribute to the different fractionation of metals in these two groups of organisms.

Controlled experiments have also identified environmental factors controlling the uptake of Hg from water by invertebrates. In one study, Hg(II) and MeHg uptake from water by *D. magna* was determined to be temperature-dependent (Tsui and Wang 2004a). The concentration of Hg in water also appears to affect uptake rates by invertebrates. For example, *D. magna* bioaccumulated proportionately less Hg from water at higher dissolved Hg(II) or MeHg concentrations (Tsui and Wang 2004b). Similar to phytoplankton, humic substances have been observed to inhibit uptake of Hg by invertebrates. Monson and Brezonik (1999) exposed *D. magna* to MeHg at two levels of aquatic humus, and observed less uptake of MeHg at the higher DOC concentration. Similarly, when the amphipod *L. plumulosus* was exposed to the same concentration of dissolved Hg(II) or MeHg, but different levels of DOC, BAFs for both Hg forms were depressed by higher DOC levels (Lawrence and Mason 2001).

1.3.3 Fish

While our knowledge of Hg bioaccumulation in lower trophic levels is relatively limited, considerably greater effort has been focused on Hg bioaccumulation in fish, both in controlled experiments and in surveys of natural systems. This section begins by discussing laboratory studies on the uptake and elimination of Hg(II) and MeHg by fish, and then uses the findings of these studies to explain the salient features of Hg bioaccumulation in fish inhabiting natural systems.

As was the case for invertebrates, fish preferentially absorb MeHg over Hg(II) from their food. It has been determined from controlled feeding experiments that fish assimilate between 20 – 90% of MeHg from food, while assimilation efficiencies for Hg(II) do not exceed 10% (Table 1-7). The large range in assimilation efficiencies for MeHg is thought to be related to the digestibility of food items, as Hg associated with non-digestible components is poorly assimilated (Phillips and Buhler 1978; Phillips and Gregory 1979).

Lawson and Mason (1998) suggest that the differential assimilation of Hg(II) and MeHg by fish is related to the distribution of the two Hg forms in their prey. In this study, sheepshead minnow larvae (*Cyprinodon variegatus*) assimilated three times more MeHg than Hg(II) after feeding on Hg-contaminated copepods, which the authors attribute to the observation that all of the MeHg in the copepod was associated with its soft tissues, while the Hg(II) in the copepod was distributed between the soft tissues (85%) and the exoskeleton (15%).

Boudou et al. (1991) propose that the differential assimilation of Hg(II) and MeHg by fish is related to the relative permeability of the gut wall to these two forms. They suggest that the intestinal wall is a "biological barrier" to Hg(II), as large amounts of Hg(II) accumulated in the intestine of rainbow trout (*Salmo gairdneri*) after consuming food contaminated with Hg(II), but very little (5 – 10%) was transferred across the intestinal membrane. In contrast, rainbow trout fed food contaminated with MeHg accumulated little MeHg in their gut, as most of the MeHg (76 – 86%) crossed the intestinal membrane. This study suggests that while Hg(II) in food is largely adsorbed to the intestinal wall of fish, MeHg easily permeates the intestinal membrane.

Laboratory experiments exposing fish to high aqueous Hg concentrations have established that fish rapidly absorb Hg(II) from water (Olson et al. 1973; Cuvin and Furness 1988; Boudou et al. 1991; James et al. 1993; Oliveira Ribeiro et al. 1996; Oliveira Ribeiro et al. 2000). Similarly, fish exposed to high levels of waterborne MeHg in laboratory experiments also rapidly absorb MeHg (Dickenson Burrows and Krenkel 1973; Olson et al. 1973; McKim et al. 1976; Boudou and Ribeyre 1983; Boudou et al. 1991). While fish could potentially absorb waterborne Hg through their skin, gills, or intestinal tract, studies have established that the primary route of Hg uptake from water is through the gill membrane (Olson et al. 1973; Oliveira Ribeiro et al. 1996).

Studies exposing fish to equal concentrations of Hg(II) and MeHg in water indicate that MeHg is bioaccumulated to a greater extent than Hg(II) (Olson et al. 1973; Boudou and Ribeyre 1983). It is unclear if this simply reflects a higher retention of MeHg, or also a more efficient assimilation of MeHg from water. According to the interpretation of Boudou and Ribeyre (1983), MeHg penetrates the gill membrane more easily than Hg(II). The assimilation efficiency of MeHg from water has been reported to be 8 – 10% in at least one fish species (Phillips and Buhler 1978; Rodgers and Beamish 1981), which is substantially lower than assimilation efficiency of MeHg from food (Table 1-7). To my knowledge, there are no published assimilation efficiencies of Hg(II) from water.

After Hg is absorbed through the intestine (food exposure) or gills (water exposure), the blood carries the assimilated Hg(II) and MeHg to other tissues in the fish body (Boudou and Ribeyre 1983; Oliveira Ribeiro et al. 1999). The distribution of assimilated Hg among different fish tissues is independent of the route of exposure

(McKim et al. 1976; Boudou and Ribeyre 1983). The available evidence suggests the distribution kinetics of Hg in the body of fish are relatively slow, at least for larger fish. For example, in arctic charr (*Salvelinus alpinus*) fed radioactive MeHg, it took over 7 days for all of the MeHg to be transferred from the gut to the blood and viscera, and it took 48 days to complete the transfer to the rest of the body (Oliveira Ribeiro et al. 1999). In sheepshead minnows (*Cyprinodon variegatus*), however, 85% of the assimilated MeHg dose was partitioned from the intestine to the rest of the body within five days (Leaner and Mason 2004). A large proportion of the assimilated Hg(II) or MeHg is eventually sequestered in the muscle (Pentreath 1976; Boudou and Ribeyre 1983; Oliveira Ribeiro et al. 1999), which is believed to function as the primary storage organ (Giblin and Massaro 1973).

Over time, Hg is lost from the body of the fish, but this process is poorly understood. The liver and kidney are believed to be the primary organs involved with Hg elimination (Dickenson Burrows and Krenkel 1973; McKim et al. 1976; Boudou and Ribeyre 1983; Oliveira Ribeiro et al. 1996). It is thought that MeHg is demethylated to Hg(II) prior to elimination from the body (Dickenson Burrows and Krenkel 1973; Riisgard and Hansen 1990), but the precise mechanism of elimination is still not known. The feces are considered to be the main route of elimination (Giblin and Massaro 1973; Boudou et al. 1991). The elimination of Hg from the body of the fish is biphasic, reflecting a slow depuration of Hg from the muscle and a fast depuration of Hg from other tissues in the body (Giblin and Massaro 1973; Sharpe et al. 1977).

Fish eliminate Hg(II) from their bodies faster than they eliminate MeHg, regardless of whether the Hg is assimilated from food or water (Table 1-8). In general,

experiments show that fish eliminate half of their assimilated Hg(II) ("half-life") within weeks, while it can take months to years to eliminate the same proportion of MeHg. The notable exception is the study by Boudou & Ribeyre (1983), which reports that rainbow trout exposed to waterborne Hg(II) eliminated only 28% of their Hg(II) burden after more than eight months in clean water. Trudel and Rasmussen (1997) synthesized the findings of published studies on Hg elimination in fish and conclude that elimination rates of Hg(II) are three times faster than those of MeHg.

The absolute rates of elimination presented in Table 1-8 must be considered with caution, as most experiments briefly expose fish to high doses of Hg and observe elimination for short periods under unnatural conditions. The two studies examining elimination of Hg from fish in natural systems (Lockhart et al. 1972; Laarman et al. 1976) report half-lives of more than two years for MeHg.

In summary, controlled uptake and elimination experiments have determined: i) fish efficiently assimilate MeHg from food, while only a few percent of Hg(II) in food is assimilated across the intestinal membrane; ii) fish can rapidly absorb Hg(II) and MeHg from water, but assimilation efficiencies are not well-established; and iii) fish eliminate MeHg very slowly, while Hg(II) is eliminated at a much faster rate. Evidently, MeHg has a greater capacity to bioaccumulate in fish than Hg(II) because of its greater assimilation efficiency and slower elimination rate.

In natural systems, uptake of Hg from water generally contributes a small amount to the bioaccumulation of this metal in fish. First, Hg concentrations in the water column are very low, as compared to food. Natural waters with no point source of Hg pollution typically contain less than 5 $ng \cdot L^{-1}$ (parts per trillion) (Ullrich et al. 2001). Second, most

of Hg in the water column occurs as inorganic Hg(II) complexes (Ullrich et al. 2001), which are not readily bioaccumulated in fish because of their poor assimilation or rapid elimination. MeHg is present in the water column at low concentrations (e.g. 0.04 – 0.8 $ng \cdot L^{-1}$; Wiener et al. 2003), but the uptake of waterborne MeHg is believed to be minor in comparison to the uptake of MeHg from the diet. Bioenergetics-based bioaccumulation models predict that uptake of MeHg from water contributes a small proportion (< 10%, according to more recent models) of the total MeHg uptake in wild fish (Table 1-9). Further, in a field enclosure experiment designed to assess the relative importance of food and water to MeHg bioaccumulation in finescale dace (*Phoxinus neogaeus*), Hall et al. (1997) conclude that uptake from water represented at most 15% of the total MeHg bioaccumulated by *P. neogaeus*. While MeHg uptake from water is not the dominant pathway of MeHg uptake in fish, it is still an important component of MeHg bioaccumulation in wild fish (Power et al. 2002), particularly in young fish during the cooler months of the year (Post et al. 1996).

Hg in the diet of wild fish differs from Hg in the water column in two respects. First, the diet of wild fish usually contains higher Hg concentrations than water, because of the efficient bioaccumulation of Hg(II) and MeHg in microorganisms at the base of aquatic food webs (Table 1-4) and the subsequent biomagnification of MeHg up the food chain (Table 1-10). Second, MeHg constitutes a much greater proportion of Hg in the diet of wild fish than Hg in water, because of the differential trophic transfer of Hg(II) and MeHg through the food chain (Table 1-10). Therefore, fish are exposed through their diet to relatively high concentrations of the form of Hg that is both efficiently assimilated and effectively retained within the body.

A fish's feeding strategy strongly influences its Hg concentrations (Table 1-11). Because MeHg biomagnifies in aquatic food webs, fish preying on organisms higher in the food chain are usually exposed to higher Hg concentrations in their diet than fish feeding lower in the food chain. Consequently, Hg concentrations in fish are closely related to their trophic level (i.e. primary consumer, secondary consumer, etc.). In general, Hg concentrations in fish are lowest in planktivorous species, intermediate in omnivorous species, and highest in piscivorous species (Tables 1-10, 1-11). A more quantitative measure of a fish's trophic position in the food chain is provided by its stable nitrogen isotope ratio ($^{15}N/^{14}N$; $\delta^{15}N$). Positive relationships have been reported in fish communities between the trophic position of fish species (as measured by $\delta^{15}N$) and their Hg concentration (Kidd et al. 1995; Power et al. 2002).

Many fish species undergo ontogenetic diet shifts, usually resulting in an increase in trophic position and a corresponding increase in Hg uptake. For example, MacCrimmon et al. (1983) attributed a 7-fold increase in Hg concentrations between age 5+ and 6+ lake trout (*Salvelinus namaycush*) to a diet shift from invertebrates to forage fish. In addition, Hg concentrations are often positively correlated with body size or age in fish species exhibiting ontogenetic diet shifts, but not in species that do not change their trophic position (Kidd et al. 1995; Snodgrass et al. 2000; Power et al. 2002).

A fish's diet also affects its relative uptake of Hg(II) and MeHg. The differential trophic transfer of the two Hg forms causes the percent MeHg (i.e. MeHg/Hg) in aquatic organisms to increase up the food chain (Table 1-10). In most fish species, virtually all (> 95%) of the Hg in muscle is in the form of MeHg (Bloom 1992). Percent MeHg in fish may be affected by diet as fish feeding on organisms lower in the food chain are

exposed to proportionately less MeHg in their diet than fish preying on upper trophic organisms. As demonstrated in the study by Bowles et al. (2001), percent MeHg is lowest in planktivorous fish species and greatest in piscivorous fish species (Table 1-10). Increases in percent MeHg have also been observed in fish species exhibiting ontogenetic diet shifts. For example, Mason et al. (2000) observed that the average percent MeHg in age 1+ brook trout (*Salvelinus fontinalis*) was 60%, but increased to 100% by age 3+, corresponding to a diet from only invertebrates to a diet including small fish.

Differences in food chain length can affect the trophic position of a fish species among lakes. For example, lake trout vary in their trophic position depending on the presence of the megazooplankton species *Mysis relicta* and/or pelagic forage fish species. Rasmussen et al. (1990) devised a classification system to characterize lake trout food chains as short (both *Mysis* and pelagic forage fish absent), intermediate (*Mysis* absent, but pelagic forage fish present), or long (both *Mysis* and pelagic forage fish present). Using this classification system for 96 Ontario lakes, Cabana et al. (1994) determined that Hg concentrations in lake trout increase significantly with food chain length. Average Hg concentrations in lake trout were 0.18, 0.47, and 0.65 $ug \cdot g^{-1}$ in the short, intermediate and long food chain lakes. Similarly, Futter (1994) concludes that lake trout of a given size are eight times more likely to have Hg concentrations above consumption guidelines (0.5 ppm) in lakes with forage fish than in lakes without forage fish.

An important factor modifying Hg bioaccumulation in fish is growth rate, as the bioaccumulation is dependent on fluxes of both Hg and biomass. Specifically, the concentration of a contaminant in an organism is dependent on: i) the uptake of the contaminant into the body; ii) the elimination of the contaminant from the body; and iii)

the growth of the organism (which is determined by the amount of carbon intake and the relative allocation of carbon among respiration, growth, reproduction and excretion) (Meili 1997). Changes in contaminant concentration can result from a change in any one, or all, of these factors.

To illustrate the effect of growth on Hg bioaccumulation, consider a hypothetical fish with an initial body burden of 100 ng Hg and a body weight of 5 g. The initial concentration of Hg in this fish is 20 $ng \cdot g^{-1}$. Assuming no net change in Hg burden, if the fish grows and increases its body weight to 7 g, the concentration of Hg in the fish will decrease to 14 $ng \cdot g^{-1}$ ("growth biodilution"), but if the fish starves and decreases its body weight to 4 g, the concentration of Hg in the fish will increase to 25 $ng \cdot g^{-1}$ ("starvation concentration").

Low Hg concentration in fish have been attributed, in part, to growth biodilution in intensively-fished lakes (Verta 1990) and eutrophic lakes (Essington and Houser 2003). High Hg concentrations in fish have been attributed to starvation concentration in Lake Mead (Cizdziel et al. 2002), where Hg concentration in striped bass (*Morone saxitilis*) were inversely correlated with fish condition factor (an indicator of overall nutritional status of fish). Similarly, Hg concentrations have been reported to be inversely correlated with fish condition in yellow perch (*Perca flavscens*) (Suns and Hitchin 1990; Greenfield et al. 2001) and northern pike (*Esox lucius*) (Olsson 1976). In the scorpion fish *Pontinus kuhlii*, Hg concentration in females have been observed to be higher than in males of the same age, which was attributed to the much faster growth rates of the males (Monteiro et al. 1991). In contrast, Stafford and Haines (2001) report little or no relationship between fish growth and Hg concentration in two piscivorous fish

populations, and suggest that substantial changes in growth result in only modest changes in Hg concentrations in fish.

1.4 Issue statement and research objectives

Humans have created a serious environmental problem by modifying the cycling of mercury (Hg) in the environment. Hg is a naturally-occurring trace metal in the Earth's crust, but anthropogenic activities have released large amounts of this metal to the atmosphere. Humans emit Hg to the atmosphere largely from fossil fuel combustion, mining and smelting of metal ores, and waste incineration. Depending on its chemical form, Hg remains in the atmosphere for days to years. During this time, atmospheric circulation disperses Hg from 10s – 10,000s km away from its source of emission. The long-range transport of Hg in the atmosphere has resulted in widespread contamination, even in remote areas with no point sources of Hg pollution. Atmospheric Hg is deposited to the Earth's surface in rain or snow or adsorbed to dry particles. Hg may be deposited directly to the surface of a lake, or may be deposited to a lake's watershed and subsequently transferred to the lake in runoff or groundwater. Most of the Hg deposited is inorganic, but natural processes in aquatic systems convert these inorganic forms to methylmercury (MeHg). Methylation of inorganic Hg is mediated by microbes and occurs largely at oxic-anoxic interfaces of lake sediments and wetlands. MeHg production is an extremely important process because it increases both the bioavailability and toxicity of Hg to aquatic organisms.

MeHg is efficiently bioaccumulated by organisms at the base of aquatic food webs and tends to biomagnify between successive levels of the food chain, resulting in

high levels in fish. Organisms at the base of aquatic food webs bioaccumulate MeHg from the water column to such a high degree that levels of MeHg in these organisms are commonly 100,000 times greater than in water. When these organisms are consumed by higher trophic organisms, the MeHg contained within their cells is efficiently assimilated and retained. Consequently, concentrations of MeHg in consumers can be up to 10-fold higher than those in their prey. Because the same principle applies between trophic transfers at higher levels of the food chain, increasing concentrations of MeHg are often found with each successive trophic level in aquatic food chains. Because fish occupy high trophic levels in aquatic food webs, their MeHg levels are often 1,000,000 higher than their environment.

MeHg levels in wild fish are commonly at such high levels that their flesh is considered hazardous for consumption by humans and wildlife. MeHg is a potent toxin known to produce adverse health effects at environmentally-relevant concentrations. In humans, consumption of Hg-contaminated fish has been linked to neurological, psychological, and cardiovascular impairments. MeHg is believed to reduce reproductive success and impair foraging and escape behaviour in fish-eating birds and mammals, and also in fish themselves. Unsafe Hg levels in fish are widespread, as indicated by the prevalence of fish consumption advisories for this contaminant in North America. There are fish consumption advisories for Hg in nearly every state in the United States, and Hg is responsible for almost all fish consumption advisories on inland lakes in Ontario. The governments of both countries have also issued warnings to pregnant women and young children to limit the consumption of particular fish species because of their high Hg content.

As contemporary levels of MeHg in fish pose a health risk to humans and wildlife, there is a serious need for urgent action. The governments of Canada, United States, and Mexico have agreed to "attain a 50 percent reduction nationally in mercury emissions by the year 2006 from existing stationary sources based on 1990 or equivalent emission inventories" (North American Implementation Task Force on Mercury 2000). The United States recently announced that it plans to reduce Hg emissions from coal-fired power plants by 70% from 1999 levels (U.S. Environmental Protection Agency 2005). Unfortunately, the effects of Hg emission reductions on MeHg levels in fish are poorly understood, in terms of both the timing and magnitude of the response, and thus the adequacy of these control measures is not known. The link between atmospheric emissions, atmospheric deposition, and MeHg concentrations in fish has not been substantiated (Pilgrim et al. 2000), which makes it extremely difficult to produce sound emission reduction policies and weakens the political will for Hg emission reductions.

The purpose of this study was to improve our understanding of the effects of changes in atmospheric Hg deposition on concentrations of MeHg in fish. Specifically, this study simulated different rates of atmospheric Hg deposition in large mesocosms situated within a single lake to determine the empirical relationship between the rate of inorganic Hg loading to aquatic systems and MeHg concentrations in fish and their associated food web. Enriched stable isotopes of Hg were added to the mesocosms, which allowed the experimentally-added Hg to be traced through the environment and the food web of the mesocosms.

This thesis is organized into two manuscripts. The first manuscript (Chapter 2) examines the effect of loading rate on the fate of Hg in the environment. The second

manuscript (Chapter 3) examines the relationship between the loading rate of Hg to aquatic systems and its bioaccumulation in fish and their associated food web. A synthesis of research findings and implications for Hg emission reductions are provided in Chapter 4.

Table 1-1. Adverse health effects associated with mercury exposure in fish-eating human populations.

Location	Age	Observed effects	Reference
Northern Quebec	children	abnormal tendon reflex (boys only)	McKeown-Eyssen et al. (1983)
Faroe Islands	children	altered cardiovascular measures	Sorensen et al. (1999)
Faroe Islands	children	neuropsychological dysfunctions	Grandjean et al. (1997)
New Zealand	children	impaired neurodevelopment	Kjellstrom et al. (1986,1989), in World Health Organization (1990)
Amazon Basin	adults	impaired motor and visual functions	Lebel et al. (1998)
Northern Quebec	adults	mild neurological abnormalities	McKeown-Eyssen and Ruedy (1983)
Eastern Finland	adults	increased risk of cardiovascular disease	Salonen et al. (1995), in Clarkson (2002)

Table 1-2. Global emission of mercury from major anthropogenic sources in 1995. Adapted from Pacyna and Pacyna (2002).

Source	Global emissions (tonnes)
Stationary combustion	1474.5
Non-ferrous metal production	165.6
Pig iron and steel production	29.1
Cement production	132.4
Waste disposal	111.2
Total	1912.8

Table 1-3. Pre-industrial and modern fluxes of mercury to lake sediments from various regions (n = number of study lakes). Also shown is the enrichment factor, which is the ratio of modern to pre-industrial flux.

Location	Pre-industrial flux ($\mu g \cdot m^{-2} \cdot y^{-1}$)	Modern flux ($\mu g \cdot m^{-2} \cdot y^{-1}$)	Enrichment factor range (mean)	Reference
Minnesota/ Wisconsin (n=7)	4.5 – 9.0	16 – 32	3.2 – 4.9 (3.7)	Swain et al. (1992)
Northern Canada (n=7)	0.7 – 14.5	3.8 – 28.4	1.1 – 7.0 (2.4)	Lockhart et al. (1995)
Central/Northern Canada (n=18)	1.1 – 52.7	2.1 – 114	0 – 2.8 (1.6)	Lockhart et al. (1998)
New York (n=8)	3.1 – 23.8	4.9 – 64.3	1.6 – 5.7 (3.5)	Lorey and Driscoll (1999)
Scotland (n=1)	8	17.6	2.2	Yang et al. (2002)

Table 1-4. Bioaccumulation factors (BAF) of methylmercury (MeHg) and inorganic mercury [Hg(II)] for organisms at the base of aquatic food webs. BAF is expressed as a ratio of the Hg concentration in an organism (wet weight) to the dissolved Hg concentration in the water column. BAFs calculated in field studies approximate "true" BAFs for algae and bacteria, as seston and periphyton invariably contain some proportion of non-living material.

Organism	Location	MeHg Log BAF	Hg(II) Log BAF	Reference
Phytoplankton	laboratory	6.0 – 6.7[a]		Miles et al. (2001)
Microbial biofilms	laboratory	4.3 – 4.7[b]		Hintelmann et al. (1993)
Seston	Wisconsin lakes (n=12)	5.4 – 7.6[a]		Back and Watras (1995)
Seston	Lake Murray, Papua New Guinea	5.4		Bowles et al. (2001)
Seston	Little Rock Lake, Wisconsin (acidified basin)	5.2	4.4	Watras and Bloom (1992)
Seston	Little Rock Lake, Wisconsin (reference basin)	4.9	4.6	Watras and Bloom (1992)
Seston	Wisconsin lakes (n=15)	5.6 – 7.0[a]	5.5 – 6.7[a]	Watras et al. (1998)
Periphyton	Everglades, Florida	ca. 4 – 5		Cleckner et al. (1999)
Periphyton	Hinds Creek, Tennessee	5.2	3.3	Hill et al. (1996)

[a] reported in paper as dry weight, converted to wet weight assuming 85% moisture; [b] expressed as (mg MeHg·g $^{-1}$ carbohydrate)/(mg MeHg·kg $^{-1}$ solution).

Table 1-5. Assimilation of dietary methylmercury (MeHg) and inorganic mercury [Hg(II)] by various invertebrates. Assimilation efficiency (AE) is the ratio of the amount of Hg assimilated to the amount of Hg ingested.

Invertebrate	Prey	MeHg AE (%)	Hg(II) AE (%)	Reference
Acartia tonsa, Temora longicornis, Centropeges sp. (copepods)	*Thalassiosira weissflogii* (diatom)	62	15	Mason et al. (1995; 1996)
Eurytemora affinis (copepod)	*Thalassiosira weissflogii* (diatom)	~75	~40	Lawson and Mason (1998)
Daphnia magna (cladoceran)	*Chlamydomonas reinhardtii, Chlorella vulgaris* (green algae)	>60	<50	Tsui and Wang (2004b)
Hyallela azteca (amphipod)	*Thalassiosira weissflogii* (diatom)	~95	~35	Lawson and Mason (1998)
Mytilus edulis (mussel)	*Phaeodactylum tricornutum* (diatom)		5	Riisgard and Hansen (1990)

Table 1-6. Zooplankton biomagnification factors (BMFs) for methylmercury (MeHg) and inorganic mercury [Hg(II)] in field studies. BMF is the ratio of Hg concentration in zooplankton to Hg concentration in seston.

Location	MeHg Log BMF	Hg(II) Log BMF	Reference
Wisconsin lakes (n=12)	-0.3 – 1.2		Back and Watras (1995)
Lake Michigan	0.5	-0.5[a]	Mason and Sullivan (1997)
Lake 979, ELA, Ontario	-0.3 – 0.4		Paterson et al. (1998)
Northern Quebec lakes and reservoirs	~0.4 – 0.5		Tremblay et al. (1998)
Little Rock Lake, Wisconsin (acidified basin)	0.6	-0.1[a]	Watras and Bloom (1992)
Little Rock Lake, Wisconisin (reference basin)	0.7	0.1[a]	Watras and Bloom (1992)
Wisconsin lakes (n=15)	0.2	-0.8	Watras et al. (1998)

[a] assuming Hg(II) is equal to (Hg - MeHg)

Table 1-7. Assimilation of dietary inorganic mercury [Hg(II)] and methylmercury (MeHg) by various fish species in laboratory experiments. Assimilation efficiency (AE) is the ratio of the amount of Hg assimilated to the amount of Hg ingested by the fish.

Fish species	Common name	Exposure route	Hg(II) AE (%)	MeHg AE (%)	Reference
Ictalurus punctatus	channel catfish	food pellets		29 – 33	McCloskey et al. (1998)
Salvelinus alpinus	arctic charr	food pellets	4	90	Oliveira Ribeiro et al. (1999)
Pleuronectes platessa	plaice	food pellets	<10	>90	Pentreath (1976)
Oncorhynchus mykiss	rainbow trout	food pellets		70 – 80	Rodgers and Beamish (1982)
Carassius auratus	goldfish	food pellets		70 – 90	Sharpe et al. (1977)
Oncorhynchus mykiss	rainbow trout	gastric injection		73	Giblin and Massaro (1973)
Platichthys flesus	flounder	gastric injection	1	34	Riisgard & Hansen (1990)
Ctenophatyngodon idella	carp	natural plant	2	18	Simon and Boudou (2001)
Oncorhynchus mykiss	rainbow trout	natural prey	6	86	Boudou & Ribeyre (1985)
Pleuronectes platessa	plaice	natural prey	3 – 5	80 – 85	Pentreath (1976)
Oncorhynchus mykiss	rainbow trout	natural prey		68	Phillips & Buhler (1978)
Esox lucius	northern pike	natural prey		19	Phillips & Gregory (1979)

Table 1-8. Elimination of inorganic mercury [Hg(II)] and methylmercury (MeHg) by various fish species. Elimination of Hg is studied by transferring fish previously exposed to Hg to a relatively uncontaminated environment. Experiments were performed in the laboratory, unless otherwise specified. Biological half-life is the amount of time required to eliminate half of the Hg burden in the fish.

Fish species	Common Name	Exposure route	Experiment duration	Hg(II) half-life (days)	MeHg half-life (days)	Reference
Pleuronectes platessa	plaice	food	24 days	26 – 43	147 – 257	Pentreath (1976)
Oncorhynchus mykiss	rainbow trout	food	60 days	<10	>60	Boudou & Ribeyre (1983)
Carassius auratus	goldfish	food	60 days		53 – 161	Sharpe et al. (1977)
Oncorhynchus mykiss	rainbow trout	food	100 days		>200	Giblin and Massaro (1973)
Anguilla anguilla	eel	food	100 days		910 – 1030	Jarvenpaa et al. (1970)
Esox lucius	northern pike	food	100 days		640 – 750	Jarvenpaa et al. (1970)
Oncorhynchus mykiss	rainbow trout	food	100 days		204 – 516	Ruohtula & Miettinen (1975)
Platichthys flesus	flounder	food	130 days		700 – 780	Jarvenpaa et al. (1970)
Gambusia affinus	mosquito fish	water	38 days	45		Schoper (1974)
Phoxinus phoxinus	minnow	water	49 days	45		Cuvin & Furness (1988)
Lepomis macrochirus	bluegill	water	100 days		130	Dickenson Burrows & Krenkel (1973)
Oncorhynchus mykiss	rainbow trout	water	100 days		268	Ruohtula & Miettinen (1975)
Salvalinus fontinalus	brook trout	water	112 days		>112	McKim et al. (1976)
Oncorhynchus mykiss	rainbow trout	water	250 days	>250	>250	Boudou & Ribeyre (1983)
Esox lucius	northern pike	food/water	360 days		~720	Lockhart et al. (1972)[a]
Perca flavescens	yellow perch	food/water	780 days		>780	Laarman et al. (1976)[a]
Ambloplites rupestris	rock bass	food/water	780 days		>780	Laarman et al. (1976)[a]

[a] conducted in natural systems

Table 1-9. Relative contributions of water and diet to methylmercury uptake in wild fish predicted from bioenergetics-based bioaccumulation models.

Fish species	Common name	% Uptake from water	% Uptake from food	Reference
Sander vitreum	walleye	<5	>95	Harris and Bodaly (1998)
Perca flavescens	yellow perch	<10	>90	Harris and Bodaly (1998)
Salvelinus namaycush	lake trout	2	98	Rodgers (1994)
Perca flavescens	yellow perch	5	95	Rodgers (1994)
Sander vitreum	walleye	<1	>99	Harris & Snodgrass (1993)
Perca flavescens	yellow perch	<5	>95	Harris & Snodgrass (1993)
Perca flavescens	yellow perch	38	62	Rodgers and Qadri (1982)
Perca flavescens	yellow perch	37 – 41	59 – 63	Norstom et al. (1976)

Table 1-10. Concentrations of methylmercury (MeHg), total mercury (Hg), and % MeHg (i.e. MeHg/Hg) in various trophic levels of aquatic food chains. Note the biomagnification of methylmercury (MeHg) up aquatic food chains, and the increase in the % MeHg with increasing trophic level.

Location	Trophic level	Species or name	MeHg ($ng \cdot g^{-1}$ ww)	Hg ($ng \cdot g^{-1}$ ww)	% MeHg	Reference
Little Rock Lake, Wisconsin (reference basin)	seston		4	30	13	Watras and Bloom (1992)
	zooplankton		20	56	29	
Wisconsin lakes (n=15)	seston		7	40	18	Watras et al. (1998)[b]
	zooplankton		11	17	57	
	small fish		97	102	95	
Lake Michigan (pelagic)	seston		1	33	1-3	Mason and Sullivan (1997)[b]
	herbivorous zooplankton	*Diaoptamus*	2	13	18	
	predatory zooplankton	*Mysis*	10	8	103	
	planktivorous fish	bloater	40	40	100[a]	
	piscivorous fish	lake trout	108	108	100[a]	
Lake Michigan (benthic)	amphipod	*Diporeia*	16	5	35	Mason and Sullivan (1997)[b]
	fish	sculpin	18	18	100[a]	
Lake Murray, New Guinea	seston		15	-	-	Bowles et al. (2001)
	planktivorous fish	*Nematalosa flyensis*	26	49	54	
	planktivorous fish	*Nematalosa papuensis*	26	48	56	
	omnivorous fish	*Arius berneyi*	180	230	75	
	omnivorous fish	*Toxotes chatareus*	290	360	80	
	piscivorous fish	*Strongylura kreffi*	380	380	94	
	piscivorous fish	*Thryssa scratchleyi*	340	380	79	
	piscivorous fish	*Lates calcarifer*	460	500	88	

[a] assumed to be 100%; [b] Hg concentrations reported in paper as per gram dry weight; converted to per gram wet weight by assuming 1g ww=0.2 g dw

Table 1-11. Total mercury (Hg) levels in muscle of various fish species in relation to their diet.

Location	Species name	Common name	Diet	Hg ($ug \cdot g^{-1}$ ww)	Reference
Savannah River, S. Carolina	*Lepomis auritus*	red-breasted sunfish	medium-large invertebrates	130	Burger et al. (2001)
	Lepomis macrochirus	bluegill sunfish	medium-large invertebrates	140	
	Anguilla rostrata	american eel	detritus/invertebrates/fish	150	
	Ictalurus punctatus	channel catfish	large invertebrates/ fish	200	
	Lepomismicrolophus	shellcracker	medium-large invertebrates	230	
	Pomoxis nigromaculatus	black crappie	large invertebrates/ small fish	240	
	Minytrema melanops	spotted sucker	plant and invertebrate	270	
	Perca flavescens	yellow perch	large invertebrates/ small fish	280	
	Esox niger	chain pickerel	large invertebrates/ fish	360	
	Micropterus salmoides	largemouth bass	fish	460	
	Amia calva	bowfin	fish	940	
Enid Lake, N. Mississippi	*Cyprinidae* spp.	carp	scavenger	630	Huggett et al. (2001)
	Arius felius	hardhead catfish	scavenger	820	
	Micropterus salmoides	largemouth bass	predator	1400	
	Pomoxis nigromaculatus	black crappie	predator	1690	
	Lepisosteus spp.	gar	predator	1890	
Carolina wetlands (n=9)	*Erimyzon sucetta*	lake chubsucker	benthic detritus	56	Snodgrass et al. (2000)[a]
	Acantharchus pomotis	mud sunfish	macroinvertebrates, fish	74	
	Esox americanus	redfin pickerel	macroinvertebrates, fish	90	
Lake Mead, Nevada	*Oreochromis aureus*	blue tilapia	herbivore	8	Cizdziel et al. (2002)
	Lepomis macrochius	bluegill	insectivore	95	
	Micropterus salmoides	largemouth bass	carnivore	179	
	Ictalurus punctatus	channel catfish	omnivore	181	
	Morone saxitilis	striped bass	piscivore	329	

[a] Hg concentrations reported in paper as per gram dry weight; converted to per gram wet weight by assuming 1g ww=0.2 g dw

CHAPTER 2. The effect of deposition rate on the fate of mercury in aquatic ecosystems

2.1 Introduction

Mercury (Hg) contamination of aquatic systems has become a serious concern because consuming fish with high levels of this metal can be toxic to humans and wildlife. Hg is a naturally occurring element in the earth's crust and mantle, but anthropogenic activities, particularly the combustion of fossil fuels, have released large stores of this metal to the atmosphere (Pacyna and Pacyna 2002). Atmospheric circulation disperses Hg far from its sources of emission (Lindqvist 1994). Consequently, virtually all water bodies are contaminated to some degree with Hg derived from anthropogenic emissions (Jackson 1997; Fitzgerald 1998). While atmospheric Hg is deposited to the earth's surface largely in inorganic forms, natural processes in lakes and their watershed convert inorganic Hg to methylmercury (MeHg), which is efficiently bioaccumulated and is highly toxic (Chapter 1). High levels of MeHg in recreational and commercial fish species have prompted government agencies to issue fish consumption advisories in many water bodies (e.g. U.S. Environmental Protection Agency 2004).

To address the problem of Hg contamination in aquatic systems, reductions in anthropogenic Hg emissions have been issued or proposed by some countries (e.g. North American Implementation Task Force on Mercury 2000), but it is not known if these emission reductions will result in significant reductions of MeHg in fish. The effects of

reductions in anthropogenic Hg emissions on MeHg concentrations in fish are not sufficiently understood (Pilgrim et al. 2000), which makes it difficult to produce sound emission policies and certainly weakens the political will for Hg emission reductions. In order to develop effective Hg emission controls, policy makers need to understand both the magnitude and timing of the response of aquatic ecosystems to changes in Hg deposition. For example, will a 50% reduction in atmospheric Hg deposition result in a 50% reduction in MeHg concentrations in fish ("magnitude of response"), and over what time scale will this response happen – years, decades, or centuries ("timing of response")?

Atmospheric Hg deposited to aquatic ecosystems undergoes a complex biogeochemical cycle involving several competing pathways. For example, atmospheric Hg deposited to aquatic ecosystems may be reduced to elemental mercury (referred to as dissolved gaseous mercury, or DGM) and subsequently re-emitted to the atmosphere, scavenged by particles and subjected to sedimentation, or converted to MeHg and subsequently demethylated or bioaccumulated by aquatic organisms (Watras et al. 1994). The timing of different pathways determines when atmospheric Hg deposited to an aquatic system is available to biota, while the balance among these pathways controls what proportion of atmospheric Hg is ultimately available to aquatic organisms.

The timing and relative importance of biogeochemical processes acting on atmospheric Hg soon after deposition to aquatic ecosystems (hereafter referred to as new Hg) are poorly understood, yet are obviously critical to the response of MeHg concentrations in fish to changes in Hg deposition. Furthermore, it is virtually unknown whether the fate of new Hg changes under different Hg deposition regimes. For example,

does Hg deposition rate affect the balance among biogeochemical pathways, and by corollary, the availability of new Hg for uptake by biota? Until recently, no technique has existed to differentiate new Hg in aquatic ecosystems from the large pool of previously-deposited Hg stored in sediments or slowly draining from terrestrial soils, so these issues remain unresolved.

The use of stable Hg isotopes is a powerful new tool for studying the fate of Hg in the environment. The recent development of sensitive analytical techniques to measure stable Hg isotopes has made the prospect of conducting stable Hg isotope tracer experiments possible (Hintelmann and Ogrinc 2003). This type of experiment involves adding one or more stable Hg isotopes to a system and monitoring the isotopic composition in compartments of interest. Because the relative proportions of the seven stable Hg isotopes are essentially constant in nature, any deviation from these standard ratios in a sample indicates an enrichment of experimentally-added Hg (Hintelmann and Ogrinc 2003). This technique allows experimentally-added Hg to be differentiated from the background Hg in a system, which makes it an excellent tool for studying the fate of new Hg in the environment

A research program has begun at the Experimental Lakes Area (ELA), northwestern Ontario, in which enriched stable Hg isotopes are being applied for the first time to natural ecosystems to improve our understanding of the fate and behaviour of new Hg in the environment – a research initiative called the Mercury Experiment To Assess Atmospheric Loading in Canada and the United States (METAALICUS). Pilot studies in the terrestrial and aquatic environment have been completed (Hintelmann et al. 2002; Babiarz et al. 2003; Amyot et al. 2004; Paterson et al. in prep.) and a whole-ecosystem

experiment began in 2001 (Harris et al. 2004). In the whole-ecosystem experiment, enriched stable Hg isotopes are being applied to the lake surface and watershed of Lake 658 to increase Hg loading by 3 – 4 fold. While the whole-ecosystem experiment is examining the response of an aquatic ecosystem to one Hg loading level, it is important to understand if the response differs at different Hg loading rates.

To address this knowledge gap, enriched stable Hg isotopes were added to *in situ* mesocosms at different loading levels to simulate a broad range of atmospheric Hg deposition rates. The primary purpose of this study was to determine the relationship between the rate of Hg loading and the bioaccumulation of this contaminant in fish and their associated food web. As the uptake of Hg by aquatic organisms is probably dependent on the supply and bioavailability of Hg in their environment, the effect of Hg deposition rate on the balance of biogeochemical pathways is critical to understanding the response of the food web. This chapter describes the fate of the experimentally-added Hg in the mesocosms over ten weeks, determines the relationship between Hg loading rate and concentrations of experimentally-added Hg in the water column and sediments, and tests the null hypothesis that the fate of Hg in the aquatic environment is not dependent on its rate of deposition.

2.2 Methods

2.2.1 Study site and mesocosm specifications

This study was conducted in Lake 240 at the ELA (Ontario, Canada), a remote site on the Precambrian Shield where a number of lakes and streams have been designated for scientific research (Johnson and Vallentyne 1971). Lake 240 (49°40'N,

93°44'W) has a surface area of 0.44 km^2, and a mean and maximum depth of 6.1 and 13.1 m (Brunskill and Schindler 1971). The water in Lake 240 is soft, circumneutral and nutrient-poor, and the sediments are sandy with low organic content (Appendix II).

On 11 June 2002, eleven mesocosms (littoral enclosures) were installed in Lake 240 (Figure 2-1). Each mesocosm consisted of a 10-m diameter floating ring, from which a translucent cylindrical curtain (woven poly laminated plastic) hung vertically to the sediments (approximately 2 m deep). The mesocosms were installed by lowering the curtains to the lake bottom and carefully sealing the flared base of the curtains to the sediments with sandbags. For sampling purposes, each mesocosm contained a floating raft (1.8 x 1.8 m) constructed from untreated lumber and Styrofoam. The initial water volumes of the mesocosms ranged from 129,779 – 155,452 L, and water leakage was minimal during the experiment (Appendix I).

2.2.2 Stable Hg isotope additions

To simulate atmospheric Hg deposition, multiple doses of enriched stable Hg isotopes were added to ten mesocosms. The eleventh mesocosm (control) received no Hg additions. Using a regression-based experimental design (Cottingham et al. 2005), each of the ten mesocosms was assigned a different Hg loading rate ranging from 1 – 15 times 7.1 $\mu g\ Hg \cdot m^{-2} \cdot y^{-1}$, which is the annual rate of wet deposition at the ELA (St. Louis et al. 2001) (Table 2-1). Loading rates were randomly assigned to the mesocosms (Figure 2-1). Each mesocosm received eight equal additions of stable Hg isotopes. Additions were performed every seven days between 26 June – 14 August 2002. The amount of Hg received each week is presented in Table 2-1.

A standard protocol for Hg additions to the mesocosms was developed based on procedures in place for the companion whole-lake experiment (METAALICUS). A stock solution was prepared by mixing a ^{202}Hg-enriched preparation (Table 2-2) into 5% nitric acid to achieve a concentration of 86.1 µg Hg·mL^{-1}. Prior to each Hg addition, ten 500 mL Teflon bottles were filled with water from Lake 240 and stored overnight in a cooler. The next morning, the appropriate amount of stock solution was pipetted into the Teflon bottles to produce the spiking solutions. The bottles were stored in a cooler until evening. To deliver the spiking solutions to the mesocosms, an acid-cleaned Teflon tube was attached to a small trolling motor such that the lower end of the tube was near the propeller and the upper end extended above the water surface. With the motor running, the spiking solution was injected with a plastic syringe down the tube. After the bottle was emptied of its spiking solution, it was filled with water from the mesocosm and rinsed down the tube three times. The motor was run for approximately 10 min to mix the spiking solution into the water column.

2.2.3 Sample collection

Water and sediment samples were collected from all eleven mesocosms for Hg or MeHg determinations between June – September 2002. Samples were collected more frequently in three mesocosms (2x, 5x, and 12x), which are referred to as "intensive mesocosms". To minimize contamination of samples, ultraclean techniques were strictly followed during sample collection and processing. Prior to each sampling event, plastic or glass sampling equipment was acid-cleaned (10 – 20% HCl) and rinsed three times with Milli-Q water, and all other equipment was rigorously washed with detergent and tap water. During a sampling event, equipment was thoroughly rinsed in Lake 240

between mesocosms. Preservatives were added to all samples no more than five hours after collection. During sample processing in the laboratory, all equipment was discarded, acid-cleaned, or rigorously rinsed with low-Hg water between samples. Samples were handled with clean, non-powdered gloves at all times and stored in new or acid-cleaned containers.

Dissolved and particulate Hg – Water samples for Hg determination were collected before and after each Hg addition and two weeks after the last Hg addition in the intensive mesocosms, and on seven dates in the remaining mesocosms. Water sampling for Hg was performed using the clean hands/dirty hands protocol. Water was collected for dissolved and particulate Hg analyses near the center of each mesocosm from a depth of 1 m, using a battery-powered pump (CanSun Electronics, Winnipeg, Manitoba). Prior to sampling each mesocosm, water from the mesocosm was circulated through the pump and tubing for 2 min. An in-line filter cartridge containing an ultra-high purity quartz microfibre filter (Whatman QM-A, nominal 0.7 µm pore size) was attached to the outlet tube of the pump. A 250 mL glass bottle was first rinsed, then filled with the filtrate, for analysis of dissolved Hg. A predetermined volume of water was passed through the filter for analysis of particulate Hg. The filter was removed from its cartridge and transferred to a polyethylene Petri dish. All filters and Petri dishes were pre-cleaned as described in Hintelmann and Ogrinc (2003), individually double-bagged, and stored in a cooler while in the field. Upon return to the field station, filters were immediately frozen, and 1 mL concentrated HCl ($\leq$ 0.0008 ng Hg·mL^{-1}) was added to each filtered water sample in a clean room under a laminar flow hood.

Dissolved gaseous mercury (DGM) – Samples of surface water for DGM analysis were collected in the intensive mesocosms only. DGM concentrations were monitored before and after four Hg additions. Samples were collected at noon on the day of the Hg addition, and one and three days after the Hg addition. Duplicate grab samples were collected in 1L Teflon bottles, ensuring no headspace was left in the bottles. In the laboratory, 500 mL of each sample was poured into an amber glass bubbler and sparged for 20 min with ultra pure argon. Elemental mercury was collected on gold traps, which were subsequently sealed with Teflon plugs and stored in a tightly closed glass jar purged with ultra pure nitrogen.

Sediment Hg and MeHg – Sediment samples for Hg and MeHg analyses were collected from three random locations in a mesocosm after the first, third, and last Hg addition. Intact sediment cores were manually collected in clear polycarbonate tubes (4.8 cm diameter). Sediment samples were held vertically on ice and in darkness until processing. In the laboratory, water in the core tube above the sediment surface was siphoned off, ensuring the sediment surface was not disturbed. A plunger was then inserted into the bottom of the core tube to extrude the top 2 cm of the sediment core, which was transferred into a 120 mL polypropylene container and stored frozen until analysis. To determine dry weights and ash weights of sediments, sample aliquots were dried at 60°C to constant weight and then ashed at 450°C.

2.2.4 Hg analyses

All samples were analyzed by inductively coupled plasma mass spectrometry (ICP/MS), to determine individual Hg isotope concentrations (Hintelmann and Ogrinc 2003).

Filtered water, suspended particles, and gold traps (DGM samples) were analyzed for Hg by H. Hintelmann (Trent University, Peterborough, ON). Sample digestions of water and particles were performed using 0.2 N $BrCl_2$ as described by Hintelmann and Ogrinc (2003). Hg contents of sample digests were analyzed by a continuous flow cold vapor generation technique, using $SnCl_2$ as a reductant. Generated Hg(0) was continuously purged into the ICP/MS (Thermo-Finnigan Element2). Gold traps were purged directly into the ICP/MS for quantification of Hg isotopes. For each batch of samples, a suite of blanks and suitable certified reference materials (MESS-3 for Hg on particles) were analyzed. Typical procedural detection limits were 0.2 $ng \cdot L^{-1}$ and 0.1 $ng \cdot L^{-1}$ for dissolved Hg and particulate Hg, respectively, and as little as 1 pg Hg was detectable on gold traps (H. Hintelmann, pers. comm.).

Sediment samples were analyzed for Hg and MeHg by C. Gilmour (Academy of Natural Sciences, St. Leonard, MD). Sediments (1-2 g) were digested with 5 mL HNO_3/H_2SO_4 (7:4 v/v), and heated until their vapours lost their color (usually 2-3 hours). Samples were analyzed using a Perkin Elmer ELAN DRC 6100, as described in Gilmour et al. (1998).

2.2.5 Terminology

As the application of stable Hg isotopes to environmental studies is a relatively new field, standard terminology has not been established. Previous studies have referred to the Hg in a sample derived from a stable Hg isotope addition as "^{202}Hg", for example, if a ^{202}Hg-enriched preparation was added to the experimental system. This terminology is inadequate because it ignores the ^{202}Hg naturally present in the sample, and does not

consider the small contributions of other experimentally-added Hg isotopes (derived from impurities in the preparation).

In this thesis, all Hg in a sample originating from the stable Hg isotope additions is collectively referred to as "spike Hg". Spike Hg is a derived parameter that is determined from the relative abundances of individual Hg isotopes measured in a sample. Using the known isotope ratios of different stable Hg isotopes in nature, the isotope ratios in the Hg preparation, and the isotope ratios measured in the sample, the amount of ^{202}Hg isotope in the sample "in excess" of its natural abundance can be calculated using matrix algebra (Hintelmann and Ogrinc 2003). The concentration of spike Hg in a sample is then determined by dividing the excess ^{202}Hg concentration in the sample by the proportion of ^{202}Hg isotope in the Hg preparation (e.g. 0.90 in this study).

The limit of detection (LOD) of spike Hg in a sample is dependent on the concentration of "ambient Hg" in the sample. "Ambient Hg" refers to all Hg in a sample not originating from the stable Hg isotope additions. Based on procedural tests performed at the laboratories, the LOD of spike Hg in a sample was set to 0.5% of ambient Hg in a sample. Where spike Hg concentrations were below the LOD, concentrations were estimated as half of the LOD and marked with an "E".

2.2.6 Data analysis

All data analyses were performed with STATISTICA 6.1 (StatSoft, Inc.). Simple linear regression was used to model the relationship between Hg loading rate and spike Hg or MeHg concentrations in various environmental media. All variables were $\log_{10}$-transformed, and residuals were examined to ensure the assumptions of linear regression were valid. The control mesocosm was not included in regression analyses.

F-tests were performed to test the significance of the regression models. When the F statistic was significant at an α-level of 0.05, the null hypothesis (i.e. there is no relationship between Hg loading and spike Hg or MeHg concentrations in the environmental medium of interest) was rejected. This test indicates whether or not there was a statistically significant relationship between Hg loading rate and spike Hg or MeHg concentration in the environmental medium of interest.

Two-tailed t-tests were performed to test whether the slopes of the log-log regression lines were significantly different than 1. A slope of 1 is a special case of the log-log relationship with two useful properties. First, a slope of 1 in a log-log regression indicates that the relationship between the variables in their untransformed state is linear. Any other slope indicates the relationship between the variables in their untransformed state is non-linear. Second, a slope of 1 in a log-log regression indicates that the relationship between the variables in their untransformed state is directly proportional (1:1). For example, a 50% increase in the independent variable will result in a 50% increase in the dependent variable. If the t statistic was not significant at an α-level of 0.05, the slope was assumed to be 1, suggesting the relationship between Hg loading rate and Hg or MeHg concentration in the environmental media of interest was linear and proportional. To facilitate visual comparisons among log-log regressions, all graphs were scaled such that a regression line with a slope of 1 would have an angle of 45°.

2.2.7 Mass balance model

To examine the relative partitioning of Hg in the environment under different Hg loading rates, a mass balance model for spike Hg was constructed for each mesocosm. This model contained four components: i) flux of spike Hg to the atmosphere; ii) pool of

spike Hg in the dissolved phase of the water column; iii) pool of spike Hg on suspended particles in the water column; and iv) pool of spike Hg in surface sediments.

i) *Flux of spike Hg to the atmosphere* – Evasion of spike DGM from the intensive mesocosms was estimated by A. Poulain (University of Montreal) based on the thin boundary layer model (Liss and Slater 1974). His methods are provided in Appendix III.

ii) *Pool of spike Hg in the dissolved phase of the water column* – The mass of spike Hg in the dissolved phase of the water column was estimated by multiplying the concentration of spike Hg in a filtered water sample (collected at a depth of 1 m) by the volume of water in the mesocosm on the day the sample was collected. The method used to estimate water volumes of the mesocosms is presented in Appendix I.

iii) *Pool of spike Hg on suspended particles in the water column* – The mass of spike Hg in the particulate phase of the water column was estimated by multiplying the concentration of spike Hg on a filter (through which a predetermined volume of water from a depth of 1 m was passed) by the volume of water in the mesocosm on the day the sample was collected.

iv) *Pool of spike Hg in surface sediments* – The mass of spike Hg in surface sediments was estimated by multiplying the average mass of spike Hg in three sediment samples by the nominal volume of the 0 – 2 cm sediment layer of the mesocosm. The mass of spike Hg in a sediment sample was calculated by multiplying its spike Hg concentration by its density.

2.3 Results

2.3.1 Hg dissolved in the water column

Concentrations of spike Hg in the dissolved phase of the water column changed rapidly after each Hg addition (Figure 2-2, solid circles), indicating the short residence time of new Hg in this compartment. While increases in dissolved spike Hg concentrations were usually observed after each stable Hg isotope addition, spike Hg was efficiently removed from this phase in subsequent days. For example, concentrations of dissolved spike Hg decreased by 16 – 44% in all mesocosms in the week following the first stable Hg isotope addition. Furthermore, significant declines in dissolved spike Hg concentrations were observed in all mesocosms after Hg loading had stopped. As the processes removing spike Hg from the dissolved phase apparently occurred rapidly and efficiently, there was little tendency for spike Hg to accumulate in this compartment during the experiment.

The relationship between Hg loading rate and concentration of dissolved spike Hg was highly significant on all dates sampled during the period of Hg additions (Figure 2-3A-D). On these dates, Hg loading rate explained most (> 75%) of the variation in dissolved spike Hg concentrations among mesocosms. After Hg additions stopped, this relationship was weak or non-significant (Figure 2-3E-F). The slopes of these log-log regressions were not significantly different from 1 on any of the sampling dates (Table 2-3A), suggesting the relationship between Hg loading and dissolved concentrations of new Hg in the water column was linear and proportional in this experiment.

2.3.2 Hg associated with suspended particles

Spike Hg was quickly associated with suspended particles in the water column. All particulate samples collected from the mesocosms ca. 12 hours after the first stable Hg isotope addition contained detectable levels of spike Hg. Concentrations of spike Hg on suspended particles generally increased after each Hg addition (Figure 2-2, open circles), as was observed for the dissolved phase. The percent of spike Hg in water in the particulate phase was ca. 10% one day after the first Hg addition in all mesocosms, but increased during the course of the experiment, reaching 38%, on average, by 3 September. Concentrations of spike Hg on suspended particles decreased following the last Hg addition, concomitant to the decline in dissolved spike Hg.

A strong relationship between Hg loading and particulate spike Hg concentrations (expressed as ng $Hg \cdot g^{-1}$ C) was observed on all sampling dates, both during the period of Hg additions (Figure 2-4A-D) and after Hg loading stopped (Figure 2-4E-F). On these sampling dates, Hg loading explained between 85 – 98% of the variation in particulate spike Hg among mesocosms. The slope of the log-log relationship between Hg loading and particulate spike Hg concentration was not significantly different from 1 on five of the six sampling dates (Table 2-3B).

2.3.3 DGM formation

The addition of stable Hg isotopes to the mesocosms stimulated the production of dissolved gaseous mercury (DGM), a volatile form of Hg that readily evades to the atmosphere. In the intensive mesocosms, concentrations of spike DGM in surface waters were substantially higher (up to 225%) on the day after a Hg addition, compared to concentrations on the previous day. These high levels of spike DGM were short-lived, as

concentrations three to five days after a Hg addition were considerably lower. Accordingly, temporal changes in spike DGM concentrations typically exhibited a saw-tooth pattern (Figure 2-2, solid triangles). Spike DGM accumulated in the surface waters of each mesocosm over the 47-day sampling period, but this accumulation appeared to level off over time.

Concentrations of spike DGM in surface waters were strongly related to the rate of Hg loading to the mesocosms. Spike DGM concentrations ranged from 0.04 – 0.27 $ng \cdot L^{-1}$ in Mesocosm 2x, 0.09 – 1.09 $ng \cdot L^{-1}$ in Mesocosm 5x, and 0.26 – 1.47 $ng \cdot L^{-1}$ in Mesocosm 12x. Concentrations of spike DGM in Mesocosm 5x were, on average, 3.2 times higher than those in Mesocosm 2x, which is similar to the expected value if DGM formation was directly proportional to Hg loading rates (i.e. 2.5). Likewise, concentrations in Mesocosm 12x were, on average, 6.5 times and 2.2 times higher than Mesocosms 2x and 5x, respectively (compared to the expected values of 6.0 and 2.4). Because DGM was monitored in only three mesocosms, the relationship between Hg loading and spike DGM concentrations was examined by plotting spike DGM concentrations in these mesocosms on the afternoon preceding each of the four Hg additions as a function of cumulative Hg load (i.e. the Hg load received to date). There was a significant relationship between cumulative Hg load and spike DGM concentrations (Figure 2-5). The slope of this relationship was not significantly different than 1 (Table 2-3C), suggesting that this relationship was linear and proportional. While the error terms in this model are non-independent, it is supported by the strong linear relationship between Hg loading and total dissolved Hg concentrations (Figure 2-3).

Taken together, these results suggest there was a linear and proportional relationship between Hg loading and DGM concentrations in surface waters.

2.3.4 Hg and MeHg associated with surface sediments

Spike Hg accumulated in the surface sediments of the mesocosms during the experiment. Spike Hg concentrations in surface sediments (0 – 2 cm) collected from the intensive mesocosms four days after the first Hg addition were all below the limit of detection, with increasing concentrations observed after three and seven weeks (Figure 2-6, open bars). By the final sampling period (18 – 19 August), sediment concentrations of spike Hg ranged from 0.034 – 0.53 $ng \cdot g^{-1}$ dw, and were significantly related to the rate of Hg loading to the mesocosm (Figure 2-7A). The log-log relationship between Hg loading rate and spike Hg concentrations in surface sediments on 18 – 19 August was not significantly different than 1 (Table 2-3D).

While spike Hg was added to the mesocosms in an inorganic form, it was observed in an organic form (i.e. MeHg) in surface sediments. On 17 July, spike MeHg was detected in the surface sediments of Mesocosm 12x (Figure 2-6, solid bars), demonstrating that inorganic Hg added to a littoral mesocosm was methylated *in situ* and accumulated to detectable levels within three weeks. Furthermore, spike MeHg was detected in sediment samples from all mesocosms on 18 – 19 August (except for samples from Mesocosm 1x). On this date, spike MeHg accounted for an average of 3% (range: 0.2 – 11%) of spike Hg in surface sediments. Spike MeHg and spike Hg concentrations in surface sediments were positively correlated across mesocosms ($r = 0.90$, $p = 0.004$).

The concentration of spike MeHg in surface sediments on 18 – 19 August was significantly related to the Hg loading rate to the mesocosm (Figure 2-7B). The slope of

this log-log relationship was not significantly different from 1 (Table 2-3E), suggesting that the amount of new MeHg in surface sediments was directly proportional to the rate at which inorganic Hg was added to the mesocosms.

2.3.5 Mass balance

The relative distribution of spike Hg among the different ecosystem compartments of each intensive mesocosm over the 10-week experiment is presented in Figure 2-8. At the beginning of the experiment, the majority of the spike Hg load was dissolved in the water column of these mesocosms. Over time, however, spike Hg partitioned from the dissolved phase, causing the percent of the spike Hg load in this compartment to decrease over time. Evasion was responsible for a significant proportion of this decline (Figure 2-8). By the last Hg addition, approximately 50% of the spike Hg added to the intensive mesocosms was lost to the atmosphere. The percent of the spike Hg load associated with suspended particles in the water column did not exceed 20% in the intensive mesocosms on any of the sampling dates, and tended to decrease over time. Spike Hg associated with surface sediments accounted for 8 – 16% of the Hg added to the intensive mesocosms on 17 July. Approximately the same percent of the spike Hg load was observed in surface sediments of the intensive mesocosms on 18 – 19 August. The sum of spike Hg lost to evasion, dissolved in the water column, associated with suspended particles, and associated with surface sediments on a particular day was consistently less than the amount of Hg added.

The rate at which stable Hg isotopes were added to a mesocosm had no apparent effect on the relative partitioning of Hg in the environment. The proportional amounts of spike Hg in the different ecosystem compartments of each mesocosm on 18 – 20 August

are presented in Table 2-4. It is evident from these mass balances that the distribution of spike Hg among the compartments showed no consistent trend with the Hg loading rate to the mesocosm. In addition, changes in the percent of the spike Hg load dissolved in the water column or associated with suspended particles over time were similar among mesocosms (Figure 2-9A-B). Most importantly, the variation among mesocosms on a given sampling day observed in Figure 2-9A-B, could not be explained by differences in Hg loading rates (Figure 2-9C-H).

2.4 Discussion

2.4.1 Timing

By adding Hg enriched with the ^{202}Hg isotope to littoral mesocosms, it was possible to trace the fate of new Hg in these systems and gain insights into the timing of key biogeochemical processes occurring in the aquatic environment. The timing of these processes is relevant to the question of how quickly aquatic ecosystems will respond to changes in Hg deposition.

This study clearly demonstrated the short residence time of new Hg in the water column, as concentrations of the experimentally-added Hg (i.e. "spike Hg") were highly sensitive to changes in Hg loading. The sawtooth pattern in dissolved spike Hg in the water column observed in this study also occurred after stable Hg isotopes were added to littoral enclosures in an earlier pilot study (Paterson et al. in prep.), and has been consistently observed in the epilimnion of Lake 658, where stable Hg isotope additions have been applied for the last four years on a whole-ecosystem scale (Harris et al. 2004). After a single addition of a radioactive Hg isotope (^{203}Hg) to Lake 224 at the ELA,

concentrations of the isotope in the epilimnion declined exponentially over time, with an estimated half-life of 14.3 days. Similarly, the residence time of ^{203}Hg in an enclosure study in Clay Lake was estimated to be about 20 days (Rudd et al. 1983). The sensitivity of Hg concentrations in surface waters to changes in natural Hg deposition has seldom been studied, but convincing evidence comes from Little Rock Lake – a shallow, precipitation-dominant seepage lake in Wisconsin. Epilimnetic Hg concentrations in Little Rock Lake follow seasonal patterns in Hg deposition (Watras et al. 2002), and have decreased by 39% between 1988 – 1999, corresponding to a decline in Hg deposition (Watras et al. 2000). Taken together, these studies suggest Hg concentrations in shallow lakes and the epilimnion of stratified lakes will respond quickly to changes in deposition regimes, with the caveat that resuspension from sediments or watershed inputs may buffer this response in some aquatic ecosystems.

Significant increases in spike DGM concentrations were observed in the surface waters of the mesocosms after additions of stable Hg isotopes, which is consistent with the pilot study in Lake 239 (Amyot et al. 2004) and Lake 658 (Harris et al. 2004). Increases in DGM concentrations are also observed in natural systems during and after a rainfall event (Lindberg et al. 2000). In all of these studies, the stimulation of DGM production after the addition of new Hg is short-lived, with DGM concentrations on the decline within hours or days. Evidently, new Hg deposited to aquatic ecosystems provides a readily reducible pool of Hg that stimulates DGM production, but only for a limited amount of time. The eventual decline in DGM concentrations may be caused by: i) the evasion of DGM to the atmosphere; ii) the depletion of the reducible pool of Hg; and/or iii) the oxidation of DGM back to Hg(II). Based on these observations, it is

reasonable to expect DGM concentrations in surface waters, and hence evasion rates, to quickly respond to changes in Hg deposition.

Because epilimnetic sediments are known to be important sites of methylation in oligotrophic lakes (Ramlal et al. 1993), the time it takes for Hg deposited to a water body to be transported to the sediments is an important factor influencing when new Hg becomes available to the aquatic food web in the methyl form. The dominant pathway of Hg transfer from the water column to the sediments is thought to occur in two steps: i) suspended particles in the water column scavenge Hg from the dissolved phase; and ii) sedimentation of these particles vertically transports Hg to the sediment surface. In this study, spike Hg was detected on suspended particles within hours of the first Hg addition and was observed in surface sediments within the next three weeks, confirming that the processes transporting new Hg to potential sites of methylation act on short-time scales. These observations concur with previous studies using stable or radioactive isotopes of Hg in aquatic systems (Rudd et al. 1983; Harris et al. 2004).

Detectable levels of spike MeHg were observed in surface sediments of the mesocosms between 3 – 8 weeks after the first Hg addition, demonstrating that inorganic Hg added to these aquatic systems was quickly converted to a methylated form. Similarly, inorganic Hg added to Lake 658 was detected in littoral sediments as MeHg within 2 – 3 months (C. Gilmour, pers. comm.). Together, these studies strongly suggest that inorganic Hg deposited to aquatic ecosystems is quickly transported to sites of methylation and transformed to the form of Hg that biomagnifies in aquatic food webs and is of toxicological significance to fish-eating wildlife and humans.

2.4.2 Magnitude

Statistically significant relationships between Hg loading rate and concentrations of spike Hg dissolved in the water column, on suspended particles, and associated with surface sediments were consistently observed during the period that stable Hg isotopes were added to the mesocosms. Furthermore, analyses strongly support that these relationships were linear and proportional across the range of Hg loading rates examined. Analyses also support that the concentration of spike MeHg in surface sediments was a linear, proportional function of the rate of inorganic Hg loading to the mesocosms.

Because spike Hg concentrations in all ecosystem compartments examined were directly proportional to Hg loading rates, the relative distribution of spike Hg among these compartments was not affected by the amount of Hg added to a mesocosm. Any variability among mesocosms in the percent of the spike Hg load in a compartment could not be explained by Hg loading rates. Therefore, this study supports the null hypothesis that the fate of new Hg in the aquatic environment is not dependent on its rate of deposition. No previous studies have examined this question.

These findings are quite surprising, given the number of steps in the biogeochemical Hg cycle in aquatic systems that could potentially be saturated by an increase in Hg deposition. The biogeochemical processes that are responsible for the movement and conversion of Hg could by limited by, for example, the availability of chemical substrates and/or number of organisms involved in the process. If these rate-limiting factors are finite in the environment, the addition of new Hg to an aquatic system would not result in a proportional response in Hg concentrations in all ecosystem components if one or more of the processes were rate-limited by these factors. However,

even in mesocosms loaded with Hg at rates 12 – 15x the ambient rate of deposition, there was no evidence that the partitioning of spike Hg onto suspended particles, the formation of DGM in surface waters, the partitioning of inorganic Hg into sediments, or the production of MeHg was saturated by the availability of the new pool of Hg. Therefore, the amount of Hg available in the environment was the limiting factor for these biogeochemical processes. However, it is unclear to what extent this would be true if the experiment was conducted on a longer time scale, in another location, or with higher loading rates.

The findings of this experiment suggest that concentrations of new Hg in the aquatic environment will respond in direct proportion to the change in atmospheric deposition. The importance of this implication becomes more apparent when the alternative is considered (i.e. if concentrations in the environment were not directly proportional to Hg loading rates). For example, if DGM production was, hypothetically, saturated at high levels of Hg deposition, proportionately more of the new Hg would be evaded back to the atmosphere at lower Hg loading rates. Consequently, decreases in atmospheric deposition would be highly effective, as a smaller proportion of the new Hg deposited to aquatic systems would be retained, making less Hg available for methylation and uptake by biota. In addition, the effectiveness of Hg reductions on lowering Hg concentrations in the environment would vary depending on the deposition rate, with greater effectiveness at higher Hg loading rates. If MeHg production was, hypothetically, saturated at high levels of Hg deposition, proportionately more of the new Hg would be methylated at lower Hg loading rates. Decreases in atmospheric deposition would not be as effective, as a greater proportion of the new Hg deposited to aquatic systems would be

methylated and available for uptake by biota. Effectiveness of Hg reductions would vary depending on the deposition rate, with less effectiveness at lower Hg loading rates. In contrast to these two hypothetical scenarios, the findings of this study suggest that concentrations of new Hg in aquatic systems will change in direct proportion to changes in Hg deposition. Furthermore, Hg reductions would be equally effective across a broad range of deposition rates.

2.4.3 Mass balance

The mass balance model consistently underestimated the total amount of spike Hg in each mesocosm (i.e. the sum of the masses of spike Hg in the four compartments of the model was less than 100% of the Hg load to the mesocosm). Possible explanations for this observation are:

i) The amount of spike Hg added to the mesocosms was less than intended;

ii) An important pool of spike Hg in the mesocosms or flux of spike Hg out of the mesocosms was not included in the model;

iii) There was an error estimating the mass of spike Hg in one or more of the modelled compartments.

Explanation (i) is not likely because the amount of Hg added was based on the measured concentration of stock solution. Hg concentrations of duplicate subsamples of stock solution were in good agreement (86 and 87 $\mu g\ Hg \cdot mL^{-1}$). It is possible that some Hg could have been lost to the spiking apparatus, but all equipment in contact with the spiking solution was thoroughly rinsed into the mesocosm after each Hg addition. Furthermore, one empty spike bottle was sent for analysis to check if Hg was adsorbed to the inside walls of the bottle, and the amount of Hg measured was negligible.

With respect to explanation (ii), possible pools of spike Hg in the mesocosms not included in the model were biota, mesocosm walls, raft floats, and deep sediments (> 2 cm depth). The biota in the mesocosm accounted for only a small percent of the spike Hg added to the mesocosms. The mass of spike Hg in zooplankton or fish in the mesocosms was much less than 1% of the spike Hg load, and the mass of spike Hg in periphyton growing on the walls of the mesocosm accounted for, at most, 2% of the spike Hg load. Samples of wall material and raft floats were sent for analysis to check if Hg was adsorbed to these materials, and the amount measured was negligible to the mass balance. It is unlikely spike Hg moved into deep sediment layers during the period of the experiment. In Lake 658, no spike Hg was observed below the 0 – 2 cm horizon in most cores collected during the first year of Hg additions (C. Gilmour, pers. comm.).

A possible flux of spike Hg out of the mesocosms not included in the model was leakage (e.g. from a hole in the wall or an incomplete seal to the sediments). To assess leakage, a tracer (^{3}H) was added to the mesocosms at the beginning of the experiment and its concentration was monitored over time. Changes in ^{3}H concentrations over time were similar among all mesocosms and these changes in concentration could largely be accounted for by evaporation, sediment diffusion, and precipitation (Appendix I). Consequently, the flux of spike Hg out of the mesocosms as a result of leakage is considered to be minimal.

Explanation (iii) is the most probable cause for the underestimation of spike Hg in the mesocosms. The most likely source of error in the mass balance model is in the estimate of evasion. First, evasion rates were not measured, but rather, predicted from DGM concentrations using a mass transfer coefficient (Appendix III). Second, the mass

transfer coefficient for DGM was derived from the loss rate of SF_6 from the mesocosms (Appendix III). Third, it was necessary to interpolate DGM values between sampling dates and use the mean mass transfer coefficient between SF_6 sampling periods to estimate the evasion of spike Hg over the time period of interest (Appendix III). A second possible source of error in the model lies in the assumption that the compartments (water, suspended particles, and surface sediments) were homogeneous. Because the mesocosms were not stratified, it is reasonable to assume the water column was well-mixed. However, it may have taken a few days for the spike Hg added to the mesocosms to be mixed throughout the water column, particularly if there was little wind following a Hg addition. The distribution of suspended particles in the mesocosm was likely not homogenous if a large fraction of particles was phytoplankton, as presumably, these organisms are more concentrated higher in the water column (more light penetration). If particles were in fact more concentrated above 1 m depth in the water column, the model consistently underestimated the mass of spike Hg in this compartment. Sediments tend to be fairly heterogeneous, so triplicate cores were taken from each mesocosm during each sampling period to capture this variability. Because sediment cores were taken randomly in the mesocosms, this is not a consistent bias in the model.

2.4.4 Applicability

The applicability of this study is potentially constrained by three major assumptions. First, the method of Hg additions used in this study is a reasonable simulation of atmospheric Hg deposition. Second, the mesocosms are realistic models for Hg cycling in natural systems. Third, the response of aquatic systems to increases in

Hg loading can be extrapolated to the response of aquatic systems to decreases in Hg loading.

To satisfy the first assumption, a great deal of effort was put into developing a method of Hg addition for the METAALICUS study. Because the speciation of Hg in rain is poorly understood, the development of a realistic method was challenging. A series of controlled experiments were conducted by the METAALICUS team to find a method of Hg addition that simulated the behaviour of natural Hg from precipitation once deposited to the lake. Briefly, these experiments suggest that the bioavailability of stable Hg isotopes added to lake water is similar to that of Hg in rain added to lake water. A full account of the methods testing is provided in Sandilands et al. (2005).

In regard to the second assumption, the mesocosms in this study are probably realistic of some, but not all natural aquatic ecosystems. The mesocosms were situated in the littoral zone of a natural lake, were open to the atmosphere and sediments, but did not interact with the hypolimnion or watershed of the lake. As such, these mesocosms are a reasonable model for shallow seepage lakes, and possibly, the epilimnion of stratified lakes.

The validity of the third assumption is dependent on whether previously-deposited "old Hg" stored in lakes and watersheds continues to be a part of the Hg cycle for many years. If old Hg remains in the aquatic Hg cycle for long periods of time, then changes in Hg concentration in aquatic ecosystems will not be proportional to decreases in Hg deposition, at least not initially. However, if old Hg is quickly removed from the aquatic Hg cycle, then it is likely that changes in Hg deposition will result in proportional changes in Hg concentrations in aquatic ecosystems on short time-scales.

Table 2-1. Loading rates of stable Hg isotopes to the ten mesocosms, shown with the amount of Hg received during each of the eight weekly additions. An eleventh mesocosm (control) received no Hg additions.

Mesocosm	Hg loading rate ($\mu g \cdot m^{-2} \cdot y^{-1}$)	Hg load per addition ($\mu g \cdot week^{-1}$)
1x	7	67
2x	14	134
3x	21	202
4x	29	269
5x	36	336
6x	43	403
7x	50	471
8x	57	538
12x	86	807
15x	107	1009

Table 2-2. Composition of the ^{202}Hg-enriched preparation ($HgCl_2$; 99.9% purity).

Isotope	Enrichment (%)
Hg^{196}	0.05 ± 0.01
Hg^{198}	0.70 ± 0.03
Hg^{199}	1.50 ± 0.05
Hg^{200}	4.35 ± 0.10
Hg^{201}	1.65 ± 0.05
Hg^{202}	90.9 ± 0.15
Hg^{204}	0.85 ± 0.03

Table 2-3. Proportionality of the relationship between Hg loading rate and spike Hg or MeHg concentrations in various environmental media (A-D). Simple linear regression models for these relationships are illustrated in Figures 2-3, 2-4, 2-5, and 2-7. All variables were $\log_{10}$-transformed. This table presents the slopes (b_1) of these relationships, with their standard errors (SE), and the results of t-tests (t, p) examining the null hypothesis that the slope is not significantly different from 1. A slope not significantly different than 1 suggests the relationship between the two variables in their untransformed state is linear and proportional.

	Variable	Date	Slope		H_o: Slope = 1	
			b_1	SE	t	p
A.	Dissolved Hg	27 Jun	0.95	0.05	-0.95	0.37
		2 Jul	1.00	0.07	0.06	0.95
		25 Jul	0.97	0.19	-0.14	0.89
		30 Jul	0.96	0.14	-0.32	0.75
		20 Aug	1.01	0.29	0.05	0.96
		3 Sep	0.81	0.40	-0.48	0.65
B.	Particulate Hg	27 Jun	1.03	0.06	0.54	0.61
		2 Jul	1.06	0.11	0.55	0.60
		25 Jul	0.93	0.11	-0.67	0.52
		30 Jul	0.88	0.12	-0.95	0.37
		20 Aug	0.91	0.10	-0.89	0.40
		3 Sep	0.85	0.07	-2.33	0.05
C.	DGM	day 0[a]	0.91	0.09	-0.98	0.36
D.	Sediment Hg	18-19 Aug	1.09	0.17	0.54	0.60
E.	Sediment MeHg	18-19 Aug	0.97	0.15	-0.18	0.86

[a] afternoon before each of the four Hg additions monitored for DGM concentrations.

Table 2-4. Spike Hg mass balance for each mesocosm on 18 – 20 August. The amount of spike Hg in each compartment is expressed as the percent (by weight) of the Hg load added to the mesocosm. By this date, mesocosms had received all eight stable Hg isotope additions. See Table 2-1 for the amount of Hg added to each mesocosm.

	Percent of spike Hg load (%)									
Mesocosm:	1x	2x	3x	4x	5x	6x	7x	8x	12x	15x
Lost to evasion[a]	-	49	-	-	57	-	-	-	47	-
Dissolved in water column	7	16	9	7	6	3	32	7	7	12
Associated with suspended particles	8	3	4	4	6	7	4	8	5	2
Associated with surface sediments	6	10	5	5	8	7	7	19	14	8
Total		78			77				73	

[a] evasion fluxes provided by A. Poulain (unpubl. data).

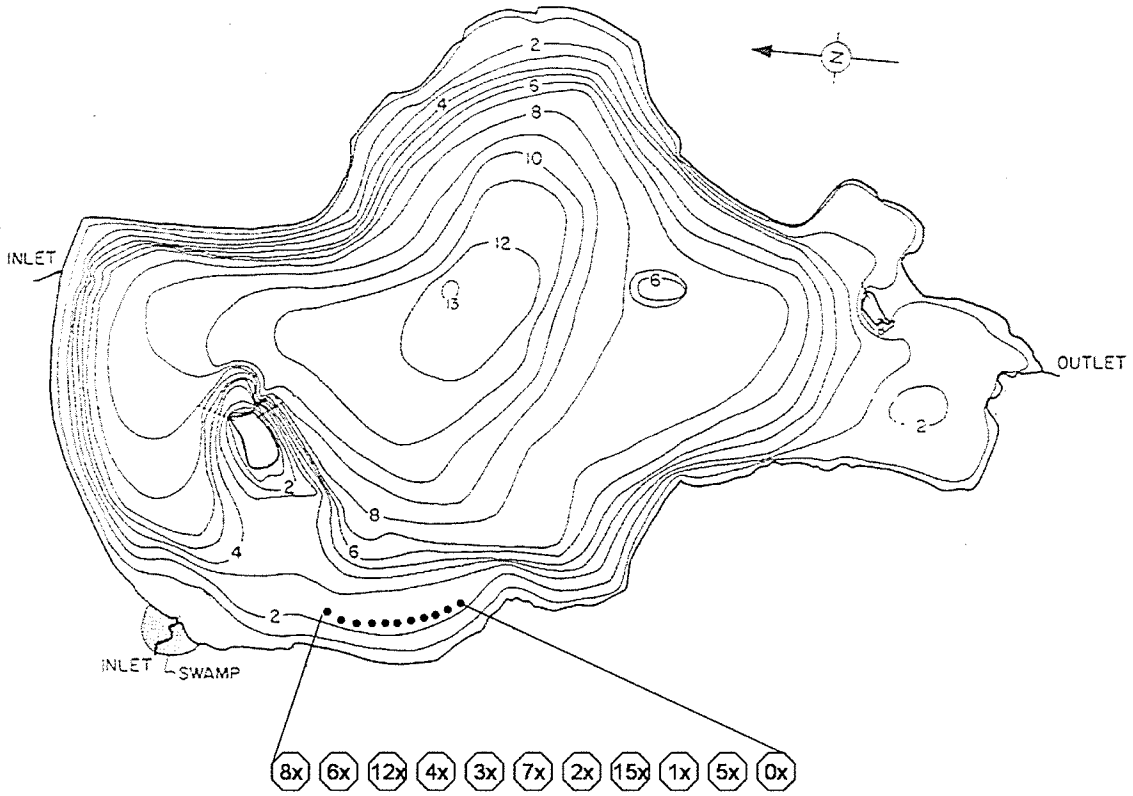

Figure 2-1. Map of Lake 240, Experimental Lakes Area (Ontario, Canada). The approximate locations of the eleven mesocosms are indicated with solid circles. The relative Hg loading rates of the mesocosms are indicated in the expanded view. Modified from Brunskill and Schindler (1971).

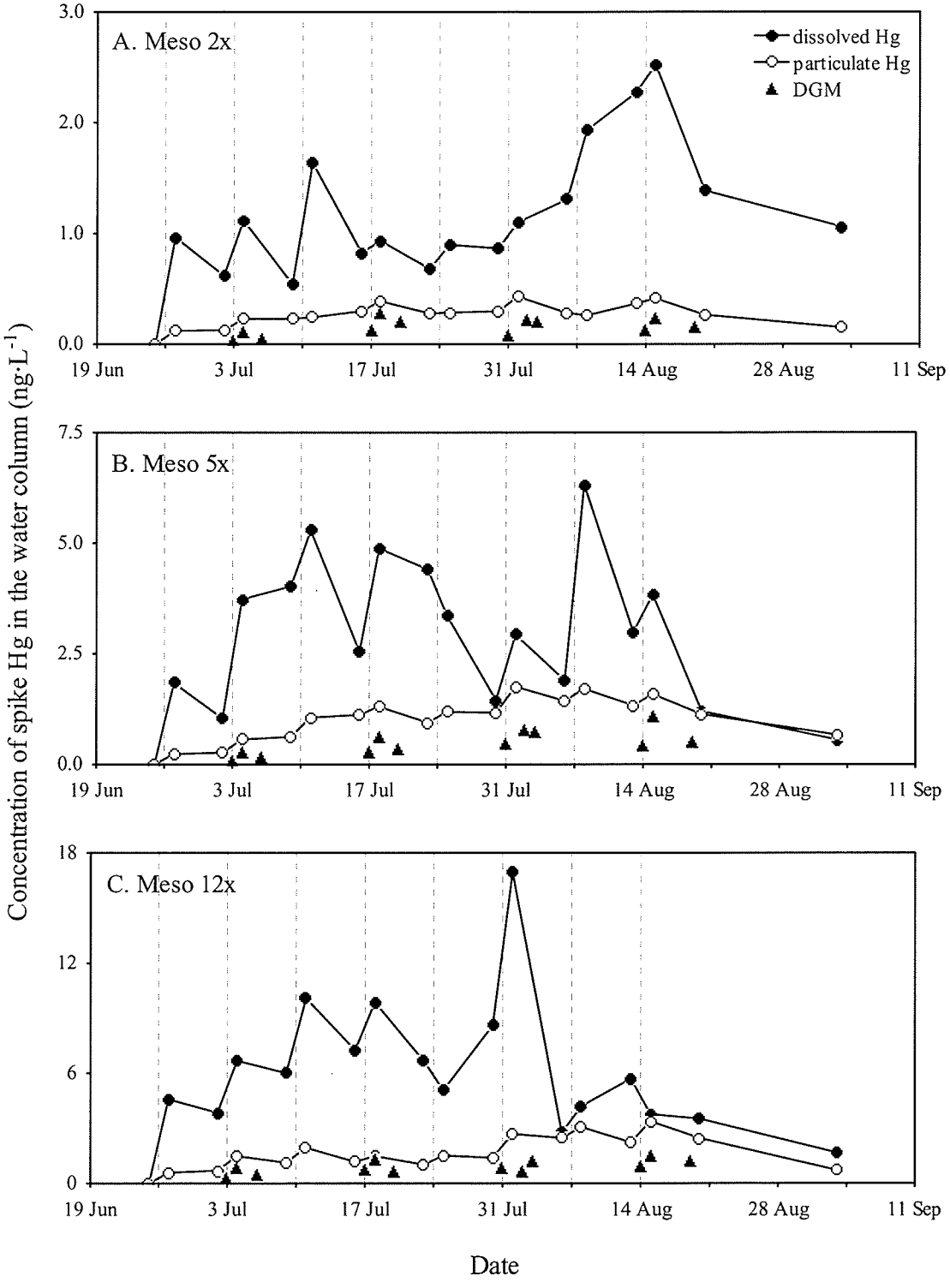

Figure 2-2. Temporal changes in the concentration of spike Hg that was dissolved in the water column ("dissolved Hg"), associated with suspended particles ("particulate Hg"), and in the dissolved gaseous form ("DGM"), shown for each intensive mesocosm (A – C). Vertical lines denote dates when mesocosms received stable Hg isotope additions. Y-axis scales are proportional to Hg loading rates.

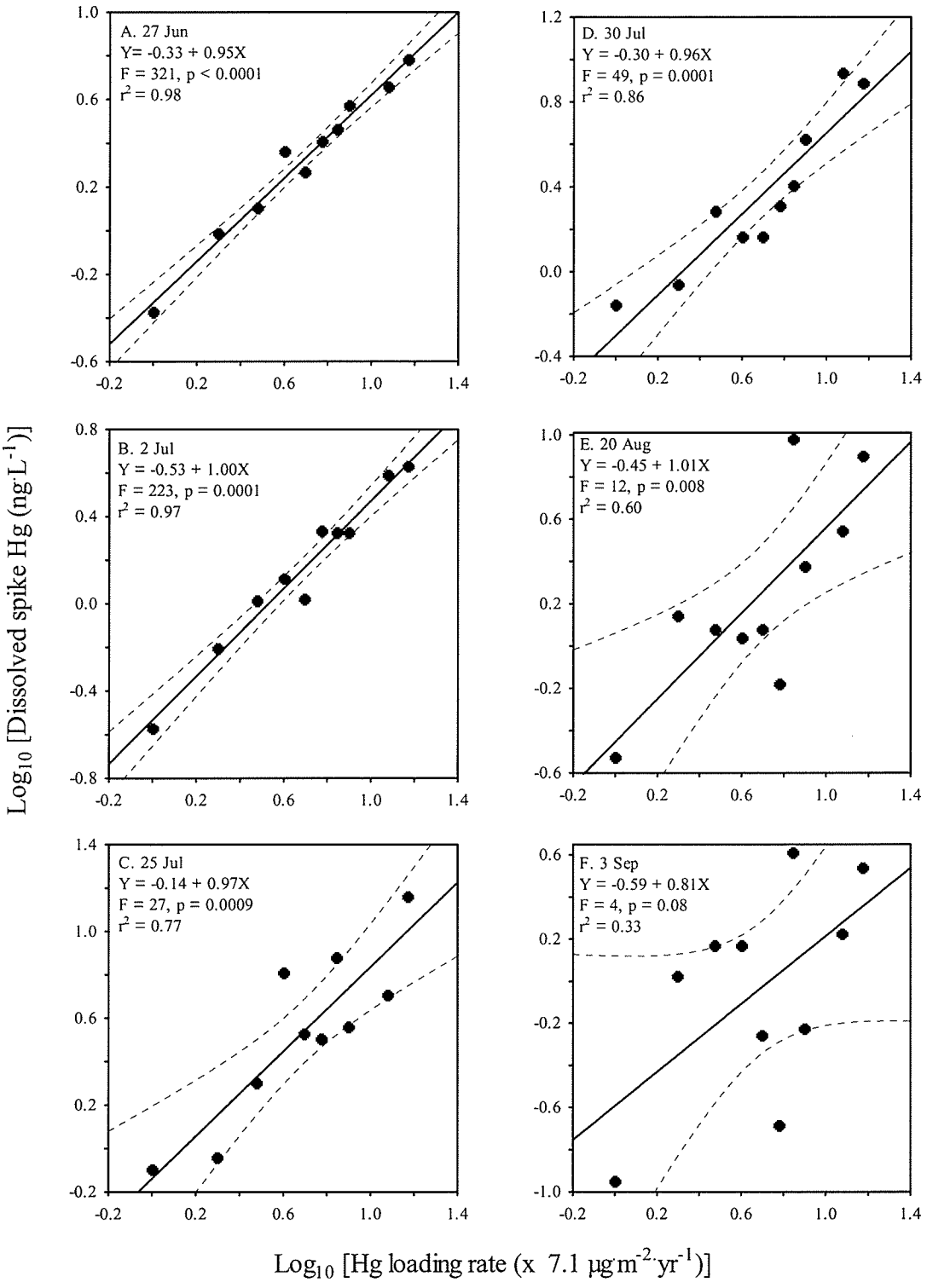

Figure 2-3. Dissolved spike Hg concentrations as a function of Hg loading rate on different sampling dates, during Hg loading (A-D) and after Hg loading had stopped (E-F). Shown in each panel is the regression line (solid line) and 95% confidence bands (dashed line), as well as the regression equation and associated statistics.

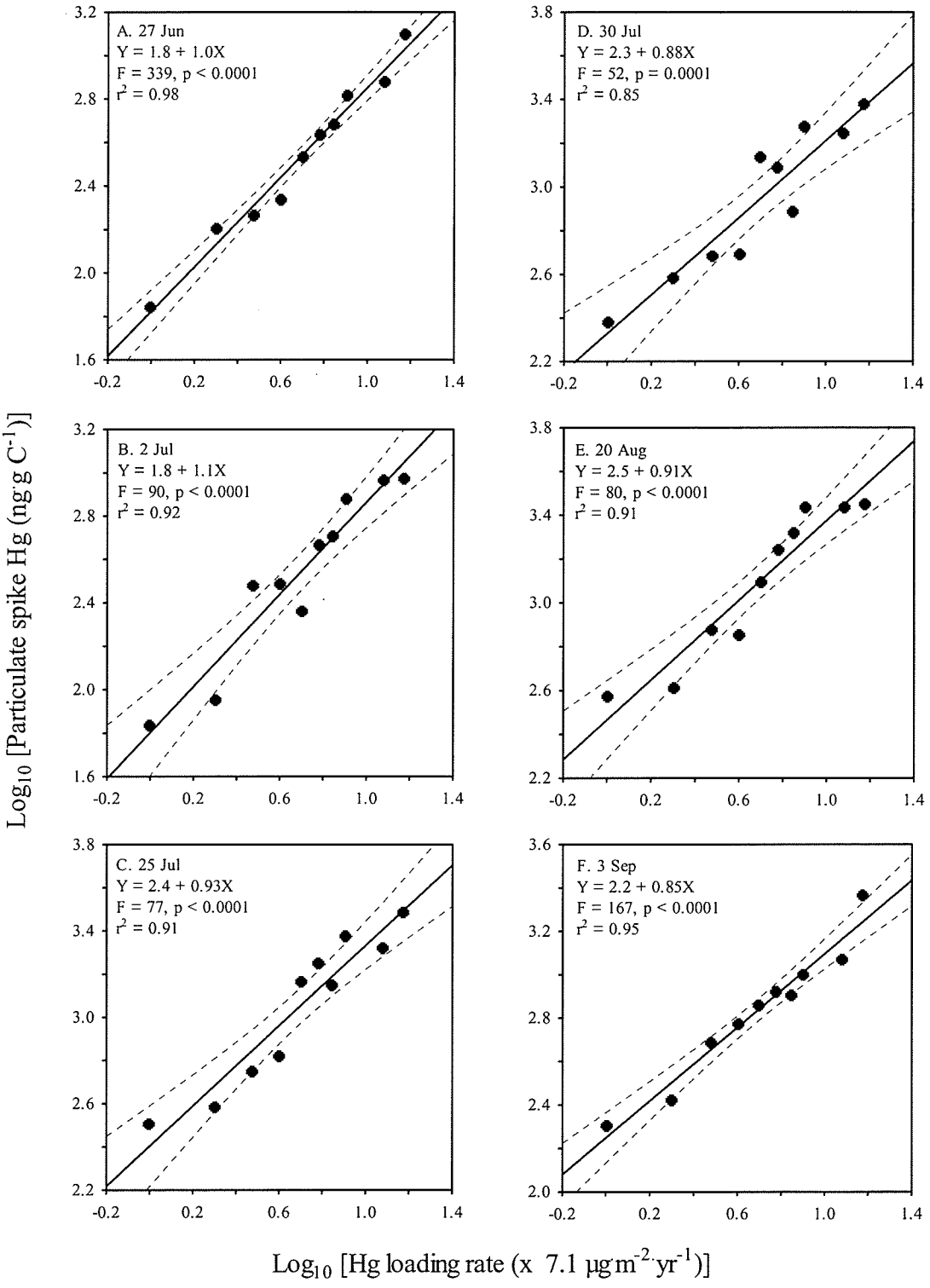

Figure 2-4. Particulate spike Hg concentrations as a function of Hg loading rate on different sampling dates, during Hg loading (A-D) and after Hg loading had stopped (E-F). Shown in each panel is the regression line (solid line) and 95% confidence bands (dashed line), as well as the regression equation and associated statistics.

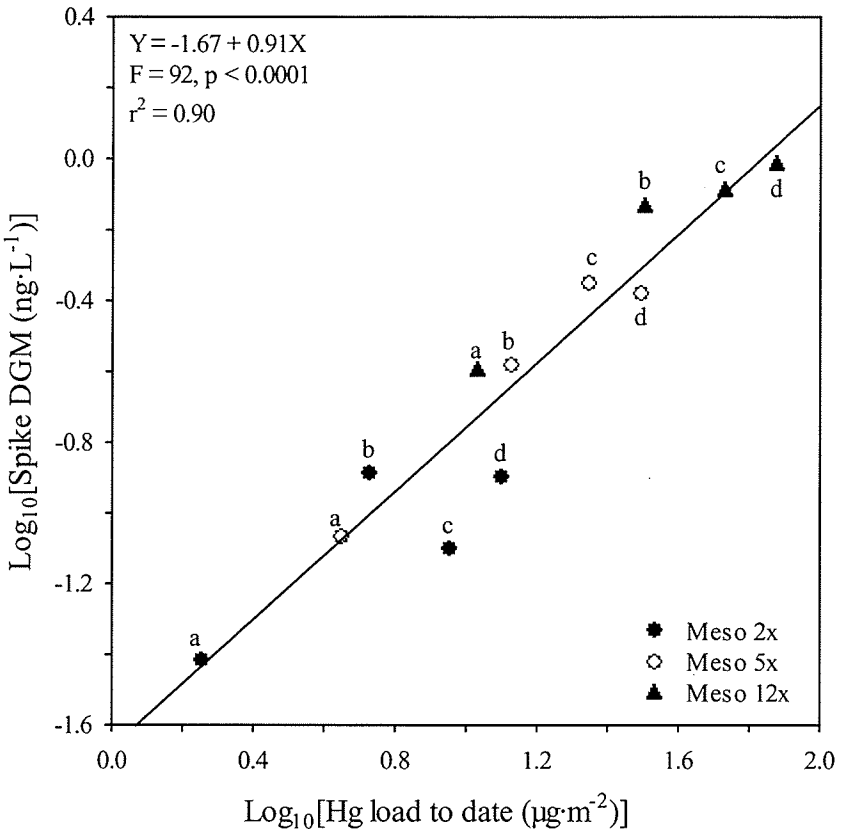

Figure 2-5. Spike DGM as a function of Hg load received to date in Mesocosms 2x, 5x, and 12x. DGM concentrations for this model were collected in the afternoons preceding each of the four Hg additions monitored (a = 3 July; b = 17 July; c = 31 July; d = 14 August). Shown is the regression line (solid line), regression equation, and associated statistics.

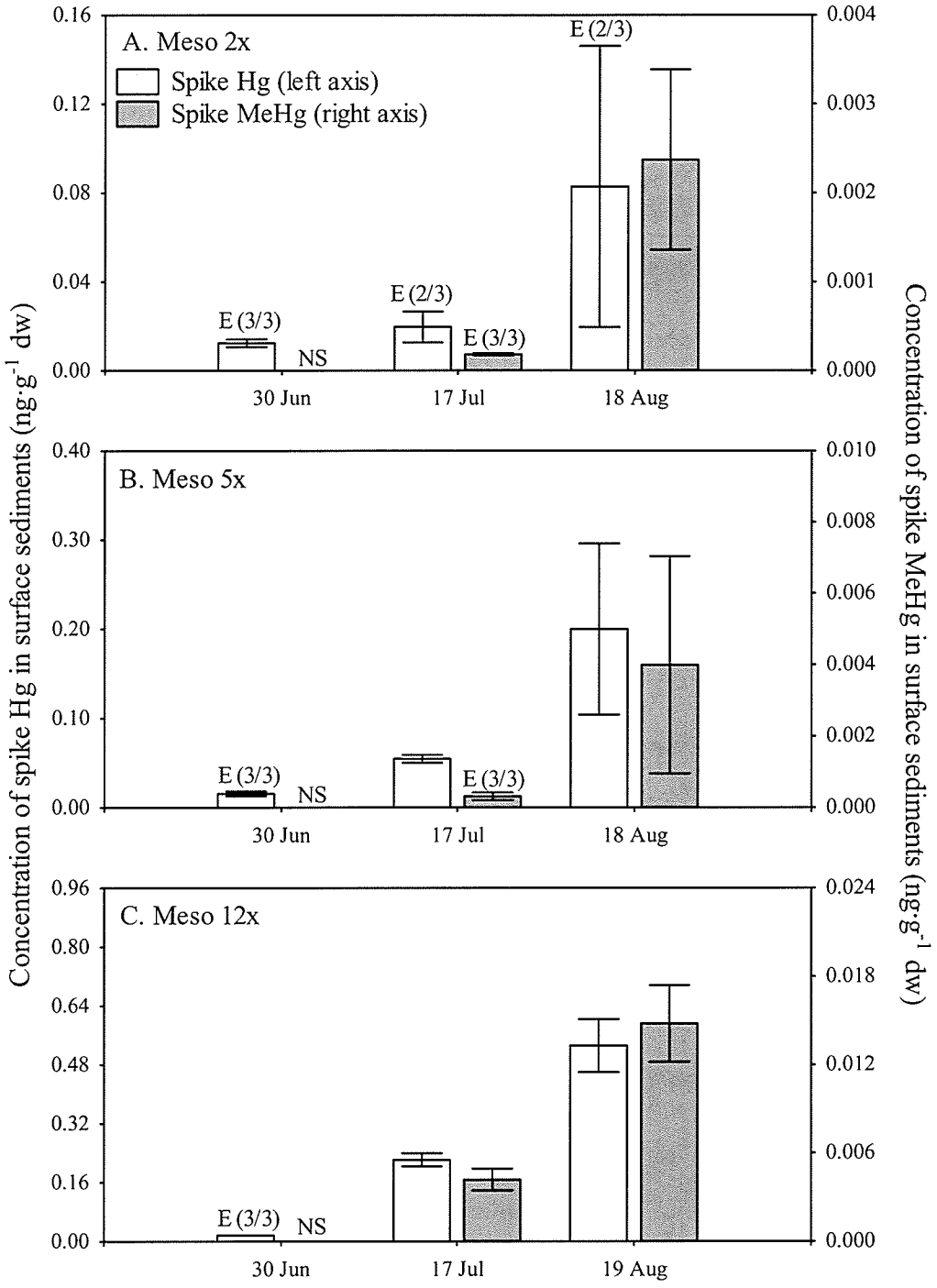

Figure 2-6. Concentrations of spike Hg (open bars; left axis) and spike MeHg (solid bars; right axis) over time in surface sediments, shown for each intensive mesocosm (A-C). Each bar is the mean (±SE) of three sediment samples (0 – 2 cm). "NS" indicates no sample is available, and "E" indicates that one or more samples was below the limit of detection (LOD) and was estimated as LOD/2. Following the "E" is (number of samples with estimated concentrations/total number of samples). Y-axis scales are proportional to Hg loading rates.

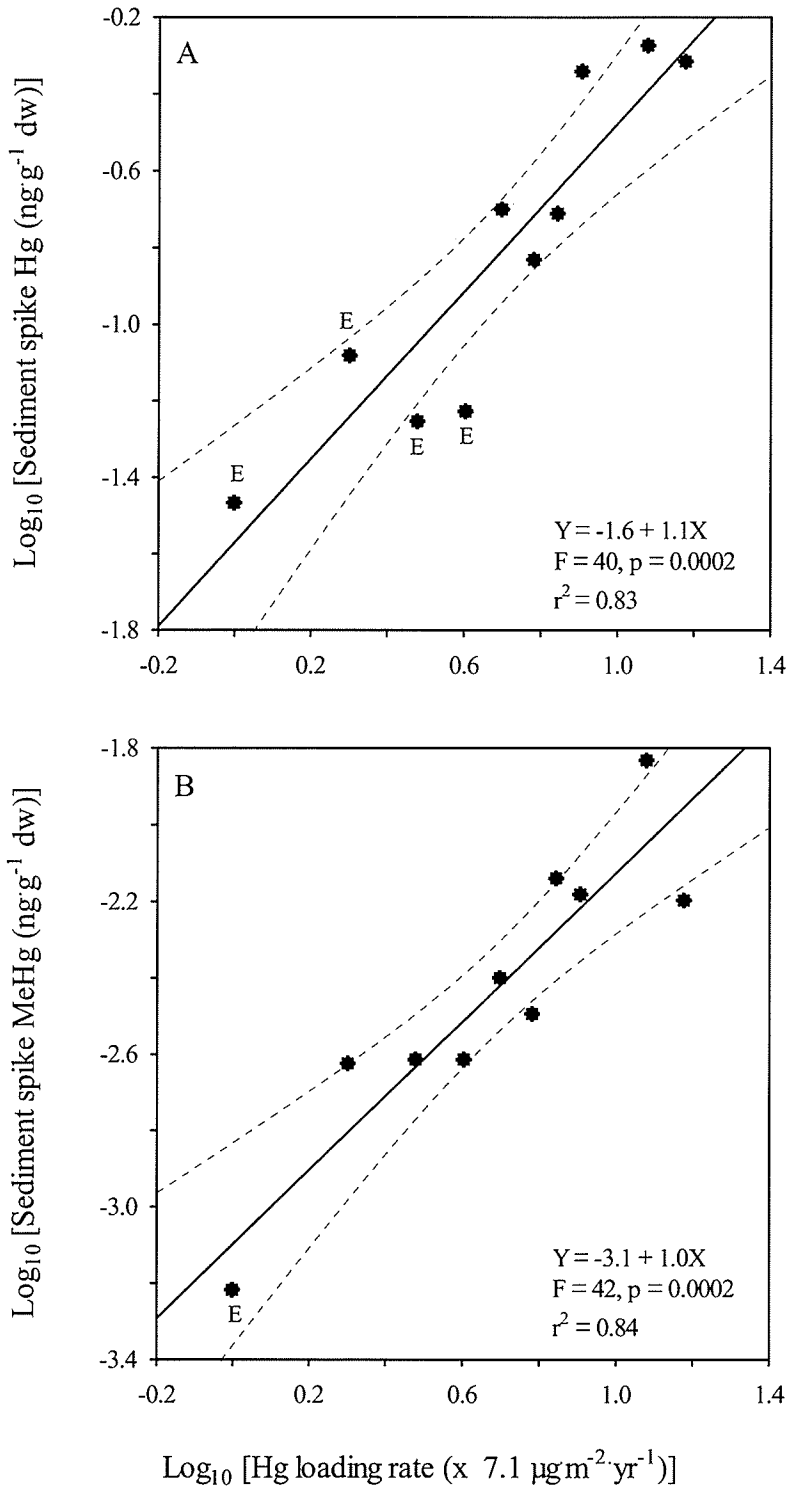

Figure 2-7. Sediment spike Hg (A) and spike MeHg (B) as a function of Hg loading rate. Sediment samples were collected on 18 – 19 August. Each point represents an average of three sediment samples (0 – 2 cm). See Figure 2-6 for explanation of symbols. Shown in each panel is the regression line (solid line) and 95% confidence bands (dashed line), as well as the regression equation and associated statistics

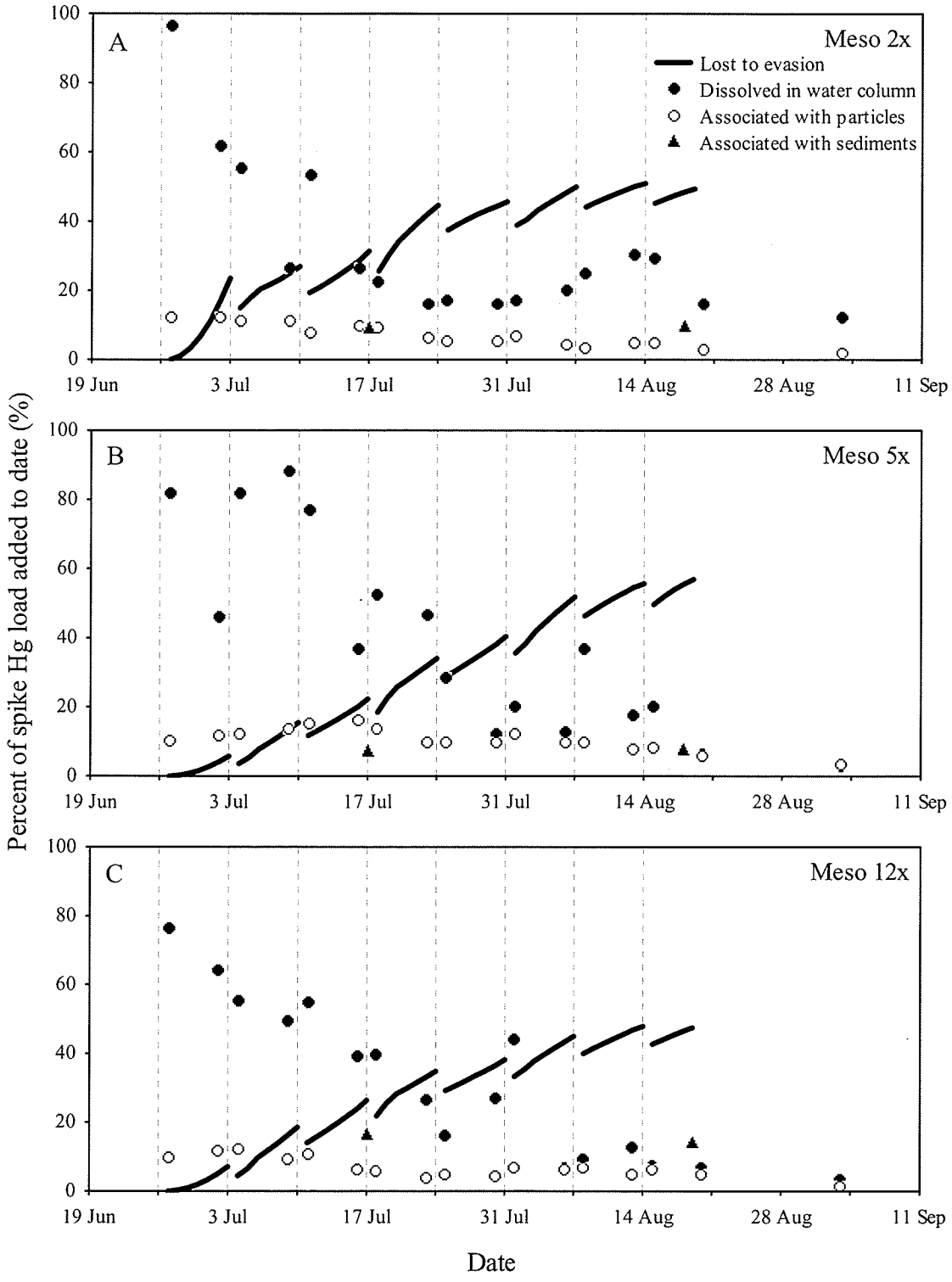

Figure 2-8. Changes in the mass balance of spike Hg over time, shown for each intensive mesocosm (A-C). Each panel illustrates the percent of spike Hg load added to date that was lost to evasion, dissolved in the water column, associated with suspended particles, or associated with surface sediments. Vertical lines denote dates when mesocosms received stable Hg isotope additions.

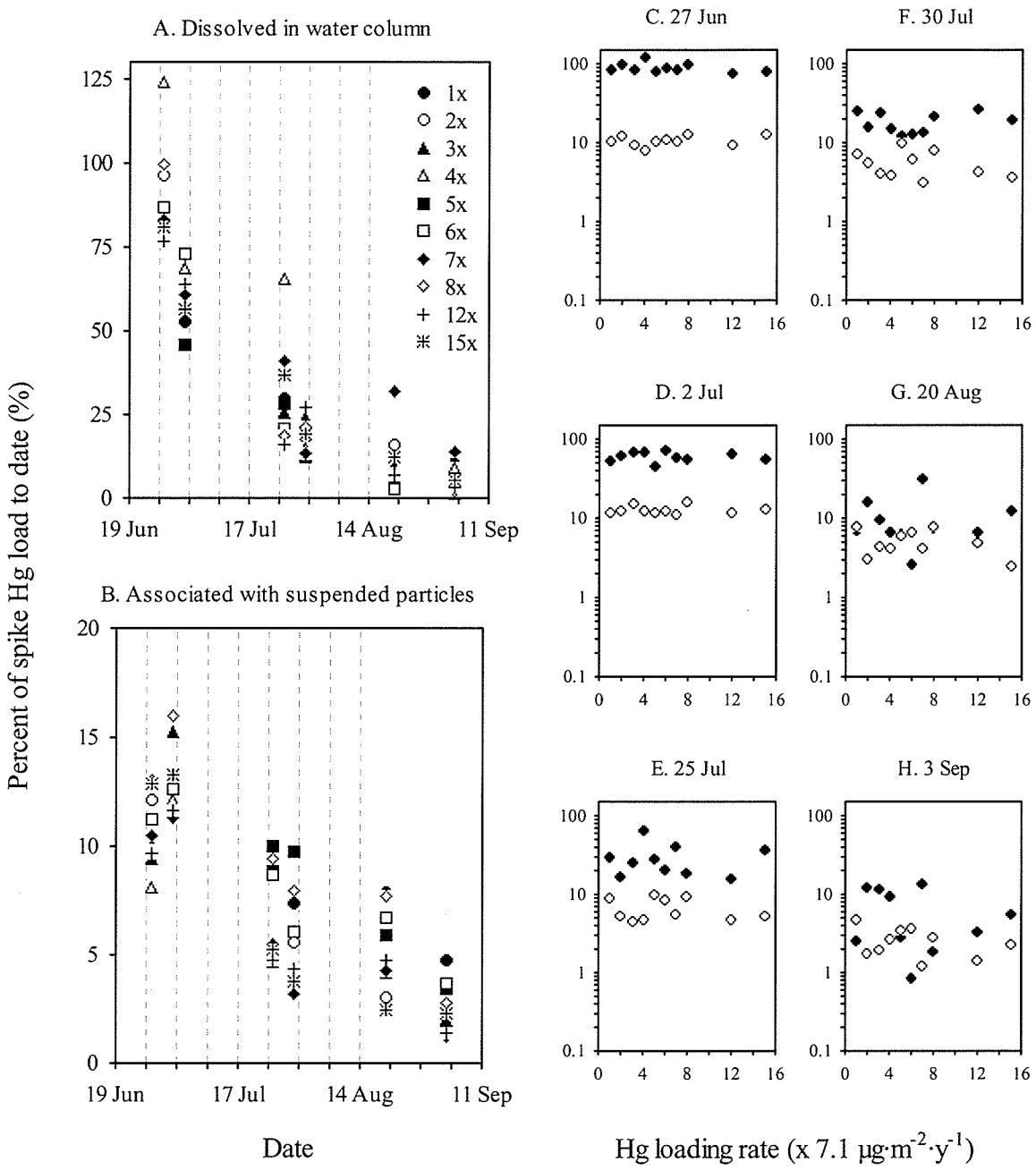

Figure 2-9. Temporal changes in the percent of spike Hg load to date in each mesocosm that was dissolved in the water column (A) or associated with suspended particles (B). Each mesocosm is represented by a different symbol, as indicated in the legend in panel A. Note the Y-axes have different scales. The variation among mesocosm on a given sampling day in panels A – B is shown as function of Hg loading rate in panels C – H, where solid circles represent the percent of spike Hg load dissolved in the water column, and open circles represent the percent of the spike Hg load associated suspended particles.

CHAPTER 3. Bioaccumulation of mercury in an aquatic food web as a function of mercury deposition rate

3.1 Introduction

Elevated levels of the toxin methylmercury (MeHg) have been reported in wild fish from many locations around the world (United Nations Environment Programme 2002). High concentrations of MeHg can potentially reduce the fitness of fish, and cause adverse health effects in fish-eating birds and mammals, including humans (Chapter 1). In North America, many water bodies are under advisory for Hg, and pregnant and nursing women have been advised to restrict their consumption of fish (Chapter 1). Furthermore, high concentrations of MeHg in wild fish have reduced the economic and cultural value of many freshwater and marine fisheries (Wiener et al. 2003).

MeHg levels are elevated in wild fish because humans have modified the cycling of mercury (Hg) in the environment. Coal combustion, metal smelting, and other industrial practices have released large amounts of inorganic Hg to the atmosphere, thereby increasing the amount of Hg cycling in the atmosphere by 3-fold (Mason et al. 1994). Volatile forms of Hg can reside in the atmosphere for over a year and undergo long-range transport in air currents (Lindqvist 1994). Consequently, even remote areas far from point sources are subjected to Hg pollution (Fitzgerald 1998). The atmosphere represents an important source of Hg that may be deposited directly to the surface of waterbodies or indirectly via runoff from the watershed (Mierle 1990; Sorenson et al. 1990; Glass et al. 1991). Because inorganic Hg is converted to MeHg by natural

processes in lakes and their watersheds (Gilmour et al. 1992; Eckley et al. 2005), atmospheric deposition of inorganic Hg potentially increases the amount of MeHg available to aquatic food webs. However, there is little evidence linking rates of atmospheric Hg deposition to concentrations of MeHg in fish and their food web.

The obvious solution to the Hg problem is to reduce the pollution at its source, i.e. decrease atmospheric Hg emissions from coal-fired utilities and other industries, but the implementation of this solution is complex. The question policy makers are faced with is how much do atmospheric Hg emissions need to be reduced to lower Hg levels in fish. Control technologies are costly and the growing demand for energy has led to proposals for even more coal-based power plants. In order to make sound decisions, policy makers need to understand the effects of different Hg emission strategies on MeHg levels in fish. Predictive models of Hg cycling can provide insights on when and how much Hg levels in fish will respond to different Hg emissions strategies. Hg cycling models are currently constrained by a number of knowledge gaps, one of which is the relationship between the rate of atmospheric Hg deposition and Hg concentrations in fish.

Previous studies have examined relationships between atmospheric Hg deposition rates and Hg concentrations in fish among a number of waterbodies and have found no significant correlation (e.g. Sorenson et al. 1990). This result may seem surprising at first, but when all chemical, physical, and biological factors that potentially modify this relationship are considered, it makes sense that any relationship between atmospheric Hg deposition and MeHg in fish would obscured when compared across different waterbodies. Concentrations of Hg in fish may be affected by a complex suite of variables, including the percentage of surrounding wetlands (Greenfield et al. 2001), lake

surface area (Bodaly et al. 1993), lake depth (Wren and MacCrimmon 1983), pH (Grieb et al. 1990), dissolved organic carbon (Wren et al. 1991), phytoplankton biomass (Lange et al. 1994), fish trophic status (Vander Zander and Rasmussen 1996), and fish growth rates (Verta 1990) . Because the relationship between atmospheric Hg deposition and Hg in fish is not readily apparent across water bodies, this does not preclude that this relationship does not exist for a given water body.

The objective of this study was to experimentally determine the relationship between atmospheric Hg deposition and concentrations of this contaminant in an aquatic food web by manipulating inorganic Hg loading within a single waterbody. This was achieved by isolating sections of a lake with large mesocosms and simulating different rates of atmospheric Hg deposition in each system. Atmospheric Hg deposition was simulated by multiple additions of inorganic Hg enriched with a stable Hg isotope (^{202}Hg). The use of stable Hg isotopes allowed the experimentally-added Hg to be traced through the aquatic food web of the mesocosms. In this chapter, concentrations of the experimentally-added Hg in aquatic organisms are related to the rate of Hg loading to the mesocosms. This is the first experimental test of the null hypothesis that the rate of Hg loading has no effect on the concentration of "new" Hg in fish and their food web.

3.2 Methods

3.2.1 Experimental design

Eleven littoral mesocosms were installed in Lake 240 at the Experimental Lakes Area (ELA), northwestern Ontario. A description of the mesocosms and the study site is provided in Chapter 2. Atmospheric deposition of Hg was simulated in the mesocosms

by eight weekly additions of stable Hg isotopes (91% ^{202}Hg) between 26 June and 14 August 2002. Hg loading rates to the mesocosms ranged from 1 – 15x the average annual rate of wet deposition to the ELA (7.1 $\mu g \cdot m^{-2} \cdot yr^{-1}$; St. Louis et al. 2001). The addition of stable Hg isotopes to the mesocosms is described in more detail in Chapter 2.

Between 24 – 26 June 2002, the mesocosms were stocked with native yellow perch (*Perca flavescens*) to achieve a target density of 40 fish per mesocosm. Prior to stocking, the mesocosms were intensively fished to remove any fish inadvertently trapped during installation of the mesocosms. Age 0+ yellow perch trapped during installation were not removed. To stock the mesocosms, yellow perch were captured from Lake 240 using a beach seine, marked with a caudal clip, and quickly transported in coolers of lake water to the mesocosms. Only fish with fork lengths between 50 – 60 mm were added to the mesocosms. This size range is typical for age 1+ yellow perch in Lake 240 in early summer (P. Blanchfield, pers. comm.). During the three days of stocking, mesocosms were monitored for mortalities, and any dead fish were removed and replaced with live fish in order to achieve the target stocking density. To deter avian predation on yellow perch, all mesocosms were covered with plastic meshing.

Lower food web organisms were not stocked in the mesocosms, but rather, were trapped inside during the installation of the mesocosms. This approach ensured the species composition and abundance of the lower food web in the mesocosms was realistic of natural littoral communities.

3.2.2 Sample collection

Zooplankton, benthic invertebrates, and fish were sampled from all mesocosms for MeHg or Hg determinations. Clean techniques were followed during sample collection and handling to minimize contamination (see Chapter 2).

Zooplankton – Zooplankton were collected from all mesocosms every two weeks between 26 June and 4 September. Samples were collected by swirling a sweep net (150 µm mesh size) through the water column, and transferring the concentrate to a Whirl-pak bag. Because non-zooplankton material may have been inadvertently collected using this sampling method, the term "zooplankton" in this chapter refers to all particles in the water column greater than 150 µm. Samples were frozen upon return to the field station, and later freeze-dried. Dried samples were homogenized, weighed (to the nearest 0.001 mg), and transferred to Teflon digestion vials for MeHg analysis.

Benthic invertebrates – Benthic invertebrates were sampled in all mesocosms between 6 – 11 September. Benthic invertebrates were collected using a petit ponar dredge and light traps. To separate invertebrates from sediments in the dredge samples, samples were vigorously swirled in a plastic bucket by hand, and the suspension was decanted through a stack of sieves (0.25, 0.50, and 1.18 mm mesh size). This process was repeated several times by adding more mesocosm water to the bucket each time. Each light trap consisted of a black plastic bucket with four holes and contained a glow stick. Light traps were set on the sediment surface after dusk and collected at dawn. In the laboratory, benthic invertebrates were live-sorted into major taxonomic groups and frozen in glass vials. Samples were freeze-dried, homogenized, weighed (to the nearest 0.001 mg), and transferred to Teflon digestion vials for MeHg analysis. Three benthic

invertebrate groups (Amphipoda, Gomphidae, and Hydracarina) were analyzed for MeHg in all mesocosms. An additional five benthic invertebrate groups (Planorbidae, Oligochaeta, *Hexagenia*, non-predatory Chironomidae, and Tanypodinae) were analyzed in Mesocosms 2x, 5x, and 12x, which are referred to as the "intensive mesocosms". See Table 3-1 for common names and diet of each invertebrate group.

Fish – Yellow perch were collected from the all mesocosms after five weeks (31 July – 2 August) and ten weeks (4 – 16 September). Fish were captured using minnow traps, gill nets, and seines. Fish were transported live to the field station in plastic buckets filled with water from their respective mesocosm, and then sacrificed by a lethal dose of clove oil. The fork length and fresh weight of each fish was measured (to the nearest 1 mm and 0.1 g, respectively), and viscera were removed. Fish were stored frozen in individual plastic bags. A skinless section of muscle tissue (ca. 0.2 g) was dissected from each fish, weighed to the nearest 0.0001 g, and transferred to a 20 mL glass vial. Muscle tissue samples were kept frozen until analysis. Ages of yellow perch were determined by examining saggital otolith sections. Otoliths were air-dried, embedded in an epoxy resin, and sectioned through the dorsal-ventral plane of the nucleus. Sections were examined at 5x magnification under transmitted light.

3.2.3 Hg analyses

All samples were analyzed by inductively coupled plasma mass spectrometry (ICP/MS) to determine individual Hg isotope concentrations (Hintelmann and Ogrinc 2003). Analyses were performed by H. Hintelmann (Trent University, Peterborough, Ontario).

Zooplankton samples for MeHg analysis were digested by adding 5 mL of KOH/MeOH (20% w,v) and heating overnight at 50 °C. Sample aliquots (50 µL) were added to Milli-Q water in gas-wash bottles, and then 0.2 mL of 2 M acetate buffer was added to obtain a pH of 4.9. Benthic invertebrate samples for MeHg analysis were digested by adding 5 mL of 4 M HNO_3 and heating at 55°C for 24 hours (Hintelmann and Nguyen 2005). Sample aliquots (50 – 5000 mL) were added to 100 mL Milli-Q water in gas-wash bottles, and the solution was neutralized with 20% KOH after adding 0.2 mL of 2 M acetate buffer to obtain a pH of 4.9. MeHg in zooplankton and benthic invertebrate samples was ethylated using tetraethyl borate (1%, w/v in 1% KOH, w,v), purged and concentrated on Tenax traps, thermodesorbed, and determined by GC-ICP/MS (Micromass Platform) as described in Hintelmann and Ogrinc (2003).

Individual fish muscle samples were digested by adding 10 mL HNO_3/H_2SO_4 (7:3 v/v) and heating at 80°C until formation of brown NOx gases had ceased. Total Hg contents of digests were analyzed by a continuous flow cold vapor generation technique, using $SnCl_2$ as a reductant. Generated Hg(0) was continuously purged into the ICP/MS (Thermo-Finnigan Element2). Fish samples were analyzed for total Hg because virtually all Hg in fish muscle is MeHg (Bloom 1992). Furthermore, previous studies adding inorganic ^{203}Hg to large enclosures stocked with yellow perch have verified that the majority of the isotope in fish muscle was present as MeHg. Hecky et al. (1991) reported that 85 – 100% of radioactive Hg in yellow perch muscle was MeHg. Rudd and Turner (1983) reported that, on average, over 80% of radioactive Hg in yellow perch muscle was MeHg after eight weeks of exposure.

Typical procedural detection limits were 0.02 to 1.0 $ng \cdot g^{-1}$ for MeHg in zooplankton and benthos (depending on available sample mass) and 0.2 $ng \cdot g^{-1}$ for Hg in fish. For each batch of samples, method blanks and certified reference materials were measured as well. Results for MeHg in oyster tissue (measured: 13.5 ± 1.7 $ng \cdot g^{-1}$, certified: 13.2 ± 0.7 $ng \cdot g^{-1}$) and Hg in DORM-3 (measured: 4680 ± 240 $ng \cdot g^{-1}$, certified: 4640 ± 260 $ng \cdot g^{-1}$) were not statistically different from certified values. No isotope enrichment was detected in samples collected from the control mesocosm.

All total Hg or MeHg in a sample derived from the stable Hg isotope additions is collectively referred to as "spike Hg" or "spike MeHg", respectively. The derivation of this parameter is described in Chapter 2. All total Hg or MeHg in a sample not derived from the stable Hg isotope additions is collectively referred to as "ambient Hg" or "ambient MeHg", respectively. If the concentration of spike Hg or MeHg in a sample was below the limit of detection (LOD), the concentrations was estimated as half of the LOD and marked with an "E". The LOD for spike Hg or spike MeHg for each sample was estimated as 0.5% of the ambient Hg or ambient MeHg concentration in the sample, respectively, which is the long-term average LOD for the Trent laboratory (H. Hintelmann, pers. comm.).

3.2.4 Data analysis

All data analyses were performed with STATISTICA 6.1 (StatSoft, Inc.). Simple linear regression was used to model the relationship between inorganic Hg loading rates and spike MeHg or Hg concentrations of zooplankton, benthic invertebrates, and yellow perch. All variables were $\log_{10}$-transformed. Residuals were examined for linearity, homoskedasticity, and normality. F-tests were performed to determine the significance

of each regression model. Two-tailed t-tests were used to test whether the slope of each model was significantly different from 1. A slope of 1 in a simple linear regression model, where both variables are log transformed, indicates the relationship between the variables is both linear and proportional. Principal components analysis (PCA) was performed to examine spike concentrations of different trophic groups in each mesocosm. Variables included in the PCA were: spike MeHg concentrations of zooplankton, Amphipoda, Gomphidae, and Hydracarina, and spike Hg concentrations of age 1+ yellow perch. Variables were $\log_{10}$-transformed and a correlation matrix was used. PCA scores of the mesocosms were then correlated with inorganic Hg loading rates and various limnological variables.

3.3 Results

3.3.1 Zooplankton

Spike MeHg was detected in zooplankton from all mesocosms within 2 – 4 weeks of the first stable Hg isotope addition. Concentrations of spike MeHg in zooplankton tended to increase over time, but the temporal pattern was not consistent among mesocosms (Figure 3-1).

Zooplankton spike MeHg concentrations were significantly related to the rate of inorganic Hg loading to the mesocosms on some, but not all, sampling dates (Figure 3-2). This relationship was statistically significant on 10 July and 4 September, explaining approximately half the variation in spike MeHg concentrations in zooplankton. The relationship on 10 July (Figure 3-2A) was significant both with and without the estimated data points. Zooplankton spike MeHg concentrations from Mesocosms 5x and 6x were

identified as outliers in the relationship on 4 September (Figure 3-2E), but the relationship was still significant after removing these two data points. While the relationship between Hg loading rate and zooplankton spike MeHg concentrations was not statistically significant on 24 July and 21 August (Figure 3-2B,D), the general trend on these dates was positive. Excluding 7 August, the slope of the log-log relationship between inorganic Hg loading and spike MeHg concentrations in zooplankton was not significantly different than 1 on all sampling dates (Table 3-2A).

3.3.2 Benthic invertebrates

Spike MeHg was detected in nearly all benthic invertebrate samples collected at the end of the experiment (Figure 3-3). In the intensive mesocosms, spike MeHg concentrations of the eight invertebrate groups sampled ranged from 0.049 – 2.44 $ng \cdot g^{-1}$ dw in Mesocosm 2x, 0.10 – 2.61 $ng \cdot g^{-1}$ dw in Mesocosm 5x, and 0.36 – 19.9 $ng \cdot g^{-1}$ dw in Mesocosm 12x. The invertebrate groups in the intensive mesocosms with the lowest concentrations were Planorbidae and Oligochaeta, while the highest concentrations were observed in Hydracarina in Mesocosm 2x and 12x and in Amphipoda in Mesocosm 5x.

In the three benthic invertebrate groups sampled in all mesocosms (Amphipoda, Gomphidae, and Hydracarina), spike MeHg concentrations were related to the rate of inorganic Hg loading (Figure 3-4). For Amphipoda and Gomphidae, this relationship was highly significant, with inorganic Hg loading explaining between 70 – 80% of the variation in spike MeHg concentrations among mesocosms (Figure 3-4A-B). The relationship between Hg loading and spike MeHg concentrations in Hydracarina was more variable (Figure 3-4C). If the estimated data point for Hydracarina was removed, the relationship became weaker ($F = 4.5$; $p = 0.07$; $r^2 = 0.39$). The slope of the

relationship between inorganic Hg loading and spike MeHg concentrations in all three benthic invertebrates groups was not significantly different from 1 (Table 3-2B), suggesting these relationships were linear and proportional.

3.3.3 Fish

Spike Hg was detected in the muscle tissue of 54% of yellow perch collected five weeks after the first stable Hg isotope addition, and 97% of yellow perch collected after ten weeks. Fish with spike Hg concentrations below the limit of detection were more common in mesocosms receiving lower Hg loading rates (Figure 3-5). Age 1+ yellow perch with detectable levels of spike Hg had muscle tissue concentrations between 0.59 – 4.9 $ng \cdot g^{-1}$ after five weeks, and 0.65 – 10.4 $ng \cdot g^{-1}$ after ten weeks. The average spike Hg concentration of age 1+ yellow perch in a mesocosm after ten weeks was approximately 2x higher than after five weeks in the same mesocosm (Figure 3-5).

Age 0+ yellow perch were captured from four mesocosms (2x, 7x, 12x and 15x) during the final sampling period. Concentrations of spike Hg in the muscle tissue of age 0+ yellow perch were all above the limit of detection and ranged from 1.1 – 12.7 $ng \cdot g^{-1}$. Age 0+ yellow perch had spike Hg concentrations that were similar, if not higher, than those of age 1+ yellow perch from the same mesocosm (Figure 3-5).

Spike Hg concentrations in the muscle tissue of yellow perch were strongly related to the rate of inorganic Hg loading to the mesocosms (Figure 3-6). The relationship between inorganic Hg loading and spike Hg in age 1+ yellow perch was more variable at the 5-week sampling period (Figure 3-6A) because of the number of fish with spike Hg concentrations below the limit of detection. This relationship was still highly significant after the exclusion of mesocosms with one or more fish below

detection limits. At the 10-week sampling period, inorganic Hg loading rate explained 97% of the variation of spike Hg concentrations of age 1+ yellow perch (Figure 3-6B). Despite the small sample size of age 0+ yellow perch, spike Hg concentrations of these fish were significantly related to the rate of inorganic Hg loading (Figure 3-6B). At the 10-week sampling period, the slope of the dose-response relationship was similar for age 0+ (0.96) and age 1+ (0.91). In all cases, the slope of the relationship between inorganic Hg loading and spike Hg concentrations in yellow perch was not significantly different than 1 (Table 3-2C), supporting that spike Hg concentration in yellow perch were directly proportional to the rate of inorganic Hg loading to their environment.

3.3.4 Food web

Spike MeHg or Hg concentrations at different levels of the food web at the end of the experiment are presented together in Figure 3-7. In all mesocosms, spike Hg concentrations of yellow perch (Figure 3-7, black bars) were consistently higher than spike MeHg concentrations in the lower food web (Figure 3-7, white and grey bars). On average, concentrations of age 1+ yellow perch were 7.5 times higher than zooplankton, 4.7 times higher than Amphipoda, 4.4 times higher than Gomphidae, and 7.0 times higher than Hydracarina. Relative concentrations of spike MeHg in zooplankton and benthic invertebrate groups were not consistent among all mesocosms.

In the principal components analysis of spike MeHg concentrations in zooplankton, Amphipoda, Gomphidae and Hydracarina, and spike Hg concentrations in age 1+ yellow perch in the mesocosms during the final sampling period, the first axis explained 79% of the variation (eigenvalue = 3.9). In all five trophic groups, concentrations were highly correlated with the first axis (Figure 3-8A; Table 3-3).

Mesocosms with lower Hg loading rates had higher scores on the first axis, while mesocosms with higher Hg loading rates had lower scores on this axis (Figure 3-8B). To examine this trend quantitatively, the scores of the mesocosms on the first axis were plotted against the rate of inorganic Hg loading to each mesocosm, which yielded a strong negative correlation (Figure 3-8B).

The second PCA axis explained 16% of the variation in spike MeHg or Hg concentrations in the food web (eigenvalue = 0.8). Spike MeHg concentrations in zooplankton and Hydracarina were positively correlated with the second axis, spike MeHg concentrations of Amphipoda and Gomphidae were negatively correlated with the second axis, and spike Hg concentrations in age 1+ yellow perch showed little correlation with the second axis (Figure 3-8A; Table 3-3). Mesocosm 2x had the highest score on the second axis, while Mesocosms 1x, 6x and 8x had the lowest scores on the second axis (Figure 3-8B). When the scores of the mesocosms on the second axis were plotted against various limnological variables, scores were negatively correlated with chlorophyll *a* (r = -0.69), suspended carbon (r = -0.76), and suspended nitrogen (r = -0.77) – all indicators of phytoplankton biomass.

In summary, most of the variation in spike MeHg or Hg concentrations in the food web was explained by the first PCA axis. The rate of inorganic Hg loading to the mesocosms was highly correlated with the first axis, such that higher inorganic Hg loading resulted in higher concentrations of spike MeHg or Hg in all five trophic groups. The second PCA axis explained 16% of the variation and was correlated with limnological variables associated with higher phytoplankton biomass, such that higher

phytoplankton biomass resulted in lower spike MeHg concentrations in zooplankton and Hydracarina, and higher concentrations in Gomphidae and Amphipoda.

3.4 Discussion

3.4.1 Timing

The response of Hg concentrations in fish to changes in atmospheric Hg deposition will depend, in part, on how quickly newly-deposited Hg is methylated, incorporated into the lower food web and transferred to fish. Using stable Hg isotope technology, this study determined that Hg added to the littoral area of a natural lake was bioaccumulated by all levels of the aquatic food web, including fish, in a matter of weeks. In the lower food web, spike MeHg was detected in zooplankton in all mesocosms within 2 – 4 weeks of the first Hg addition, and in almost all benthic invertebrates collected after ten weeks. In yellow perch, an important forage and game fish in many North American lakes, spike Hg was detected in muscle tissue as early as 35 days after the first stable Hg addition. Previous studies adding radioactive or stable Hg isotopes to natural systems have also detected the experimentally-added Hg in aquatic biota within a number of weeks (Rudd et al. 1983; Harrison et al. 1990; Hecky et al. 1991; Harris et al. 2004; Paterson et al. in prep.). Together, these studies support the hypothesis that new Hg in aquatic systems is quickly available for bioaccumulation in aquatic food webs.

Because the findings of this study suggest atmospheric deposition of inorganic Hg contributes to burdens of MeHg in aquatic organisms on short time scales, reductions in atmospheric Hg deposition could result in timely decreases in MeHg in aquatic food webs. However, the extent of the decrease will depend on the bioavailability of

previously-deposited Hg stored in sediments and terrestrial soils. If previously-deposited Hg continues to be available for uptake by biota, the effects of decreases in atmospheric Hg deposition may not appear to be effective, at least initially. The findings of at least one previous study do not support this – Hrabik and Watras (2002) attributed decreases in Hg concentrations in yellow perch over a 6-year period to reductions in atmospheric Hg deposition. Furthermore, after pulp and paper mills and chlor-alkali plants drastically reduced or stopped discharges of inorganic Hg to aquatic systems in the 1970s, many studies reported significant declines in Hg in fish and other biota within a few years (Olsson 1976; Armstrong and Scott 1979; Herut et al. 1996; Francesconi et al. 1997). Commonly, Hg concentrations in fish drop rapidly for the first few years after cessation of inorganic Hg discharges, then gradually decline for many years (e.g. Herut et al. 1996; Francesconi et al. 1997; Latif et al. 2001).

3.4.2 Magnitude

The addition of stable Hg isotopes to a series of littoral mesocosms to simulate different rates of atmospheric Hg deposition allowed for the first experimental determination of the relationship between the supply of inorganic Hg to an aquatic ecosystem and Hg bioaccumulation in fish. In all levels of the food web, a positive, linear relationship was observed between inorganic Hg loading and concentrations of the experimentally-added Hg in biota. At the end of the experiment, inorganic Hg loading rate explained 97% of the variation in spike Hg in age 1+ yellow perch among mesocosms. The relationship between Hg loading and spike MeHg in the food web was linear, despite the wide range of Hg loading rates manipulated in the mesocosms. Furthermore, this relationship was directly proportional over the time period of the

experiment, implying that a 50% increase in inorganic Hg loading resulted in a 50% increase in spike MeHg in biota.

Positive correlations between the supply of Hg to aquatic systems and Hg levels in fish have been reported in previous studies. Hg concentrations in several fish species were found to be positively correlated to the rate of Hg loading rate to sediments in 14 Ontario lakes (Johnson 1987). In Sweden, levels of Hg in pike were significantly correlated with Hg concentrations in the mor soil horizon, which are considered to be an indirect measure of atmospheric Hg deposition (Hakanson et al. 1990). Similarly, Hg levels in fish were modestly related to concentrations in terrestrial mosses (a relative measure of atmospheric Hg deposition) in 25 lakes in Norway (Fjeld and Rognerud 1993). A linear relationship has recently been reported between atmospheric Hg deposition and MeHg concentrations in mosquitoes (Hammerschmidt and Fitzgerald 2005).

In the comprehensive study by Sorensen et al. (1990) of 80 lakes in northeast Minnesota, there was no significant correlation between atmospheric Hg deposition and Hg levels in fish among lakes. This result can be attributed to the narrow range in Hg deposition rates examined (10.4 – 15.4 $\mu g \cdot m^{-2} \cdot yr^{-1}$) and the fact that Hg deposition rates to individual lakes were extrapolated from three monitoring sites. Alternatively, the study by Sorensen et al. shows how variation in limnological parameters, such as pH and organic carbon, modifies the relationship between atmospheric Hg deposition and MeHg in fish among different lakes.

In fact, the present study demonstrated how even small changes in certain limnological parameters within a single lake can obscure the relationship between

inorganic Hg loading and MeHg in biota, particularly in the lower food web. On some sampling dates, spike MeHg concentrations in zooplankton were not significantly related to differences in inorganic Hg loading rates. Zooplankton are presumably more sensitive to short-term changes in MeHg availability because these animals have relatively short life spans and eliminate MeHg relatively quickly (Tsui and Wang 2004b). Analyses revealed that some of the variation in spike MeHg in the lower food web that could not be explained by differences in Hg loading rate may have been related to differences in phytoplankton biomass among mesocosms. Specifically, higher phytoplankton biomass was associated with lower spike MeHg in zooplankton and Hydracarina, and higher spike MeHg in Gomphidae and Amphipoda. Phytoplankton biomass has been inversely correlated with Hg levels of zooplankton in previous studies (Pickhardt et al. 2002; Chen and Folt 2005).

This study determined that the relationship between the loading rate of inorganic Hg and its accumulation in the aquatic food web of mesocosms situated within a boreal lake was linear and proportional across a broad range of loading rates. The extent to which this relationship can be extrapolated to other aquatic ecosystems is presently unclear. However, when Hg was added to *in situ* mesocosms at three different loading levels in a vastly different environment – the Florida Everglades – levels of the experimentally-added Hg in fish were also directly proportional to Hg loading rates (D. Krabbenhoft, pers. comm.). In addition, temporal patterns in spike MeHg concentrations in zooplankton and spike Hg in yellow perch in the mesocosms over the 10-week period were similar to those observed in the companion whole-ecosystem Hg loading experiment during the first summer of Hg additions (P. Blanchfield and M. Paterson,

unpubl. data). It is also unclear whether this relationship would be proportional over longer time scales.

The dose-response relationship observed in this study suggests that decreases in atmospheric Hg deposition to aquatic systems will result in proportional changes in the Hg content in fish that is derived from direct atmospheric deposition. The contributions of previously-deposited Hg stored in lake sediments and in watersheds to MeHg burdens in biota must also be considered when predicted the response of aquatic biota to changes in atmospheric deposition. The relative contribution of these different sources to Hg concentrations in fish is poorly understood and likely varies among ecosystems. However, the results of this study suggest that in aquatic ecosystems in which the delivery of Hg is predominantly from precipitation, decreases in atmospheric Hg deposition will likely lead to proportional reductions in fish Hg levels.

Table 3-1. Benthic invertebrate groups and their diets.

Benthic invertebrate group	Common name	Feeding strategy
Planorbidae	ramshorn snail	herbivore, detritivore
Oligochaeta	aquatic worm	detritivore
Amphipoda	scud	generalist
Hexagenia	mayfly nymph	collector-gatherer
Non-predatory Chironomidae	midge fly larva	herbivore, detritivore
Gomphidae	dragon fly larva	predator
Tanypodinae	midge fly larva	predator
Hydracarina	water mite	predator

Table 3-2. Proportionality of the relationship between Hg loading rate and spike Hg or MeHg concentrations in various levels of the food web (A-D). Simple linear regression models for these relationships are illustrated in Figures 3-2, 3-4, and 3-6. Both variables were $\log_{10}$-transformed. This table presents the slopes (b_1) of these relationships, with their standard errors (SE), and the results of t-tests (t, p) examining the null hypothesis that the slope is not significantly different from 1. A slope not significantly different than 1 suggests the relationship between the two variables in their untransformed state is linear and proportional.

	Food web group	Date	Slope		H_o: Slope = 1	
			b_1	SE	t	p
A	Zooplankton					
		10 Jul	1.4	0.44	1.00	0.35
		24 Jul	0.70	0.43	-0.70	0.50
		7 Aug[a]	0.07	0.25	-	-
		21 Aug	1.2	0.67	0.27	0.79
		4 Sep	1.2	0.48	0.31	0.76
B	Benthic invertebrates					
	Amphipoda	6 – 11 Sep	0.81	0.19	-1.00	0.35
	Gomphidae	6 – 11 Sep	0.98	0.18	-0.13	0.90
	Hydracarina	6 – 11 Sep	1.5	0.38	1.34	0.22
C	Fish					
	Yellow perch (age 1+)	31 Jul – 2 Aug	0.67	0.16	-2.06	0.07
	Yellow perch (age 1+)	4 – 16 Sep	0.91	0.05	-1.64	0.14
	Yellow perch (age 0+)	4 – 16 Sep	0.96	0.15	-0.26	0.82

[a] t-test not performed because regression model was highly non-significant (p = 0.8).

Table 3-3. Correlations between variables and PCA axes 1 and 2. See Figure 3-8 for explanation of analysis and variable codes.

Variable	PCA Axis 1	PCA Axis 2
Zoop	-0.79	0.54
Amph	-0.89	-0.42
Gomp	-0.91	-0.40
Hydr	-0.89	0.39
YP 1+	-0.96	-0.04

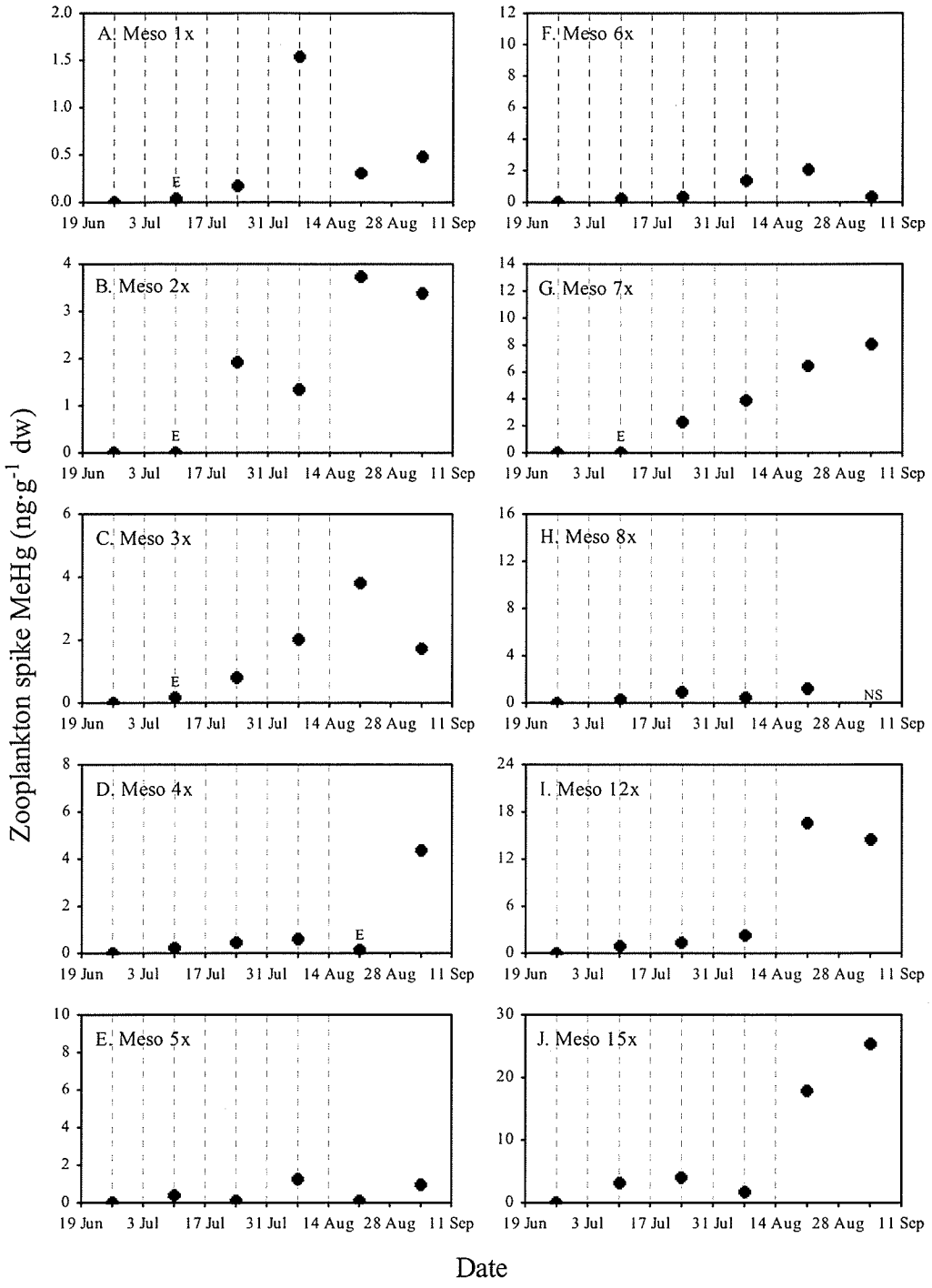

Figure 3-1. Concentration of spike MeHg in zooplankton over time, shown for each mesocosm (A-J). Each point represents one sample, or a mean of 2 – 3 subsamples. "NS" indicates no sample is available, and "E" indicates the concentration was below the limit of detection (LOD) and was estimated as LOD/2. Vertical lines denote dates when mesocosms received stable Hg isotope additions. Y-axis scales are proportional to Hg loading rates.

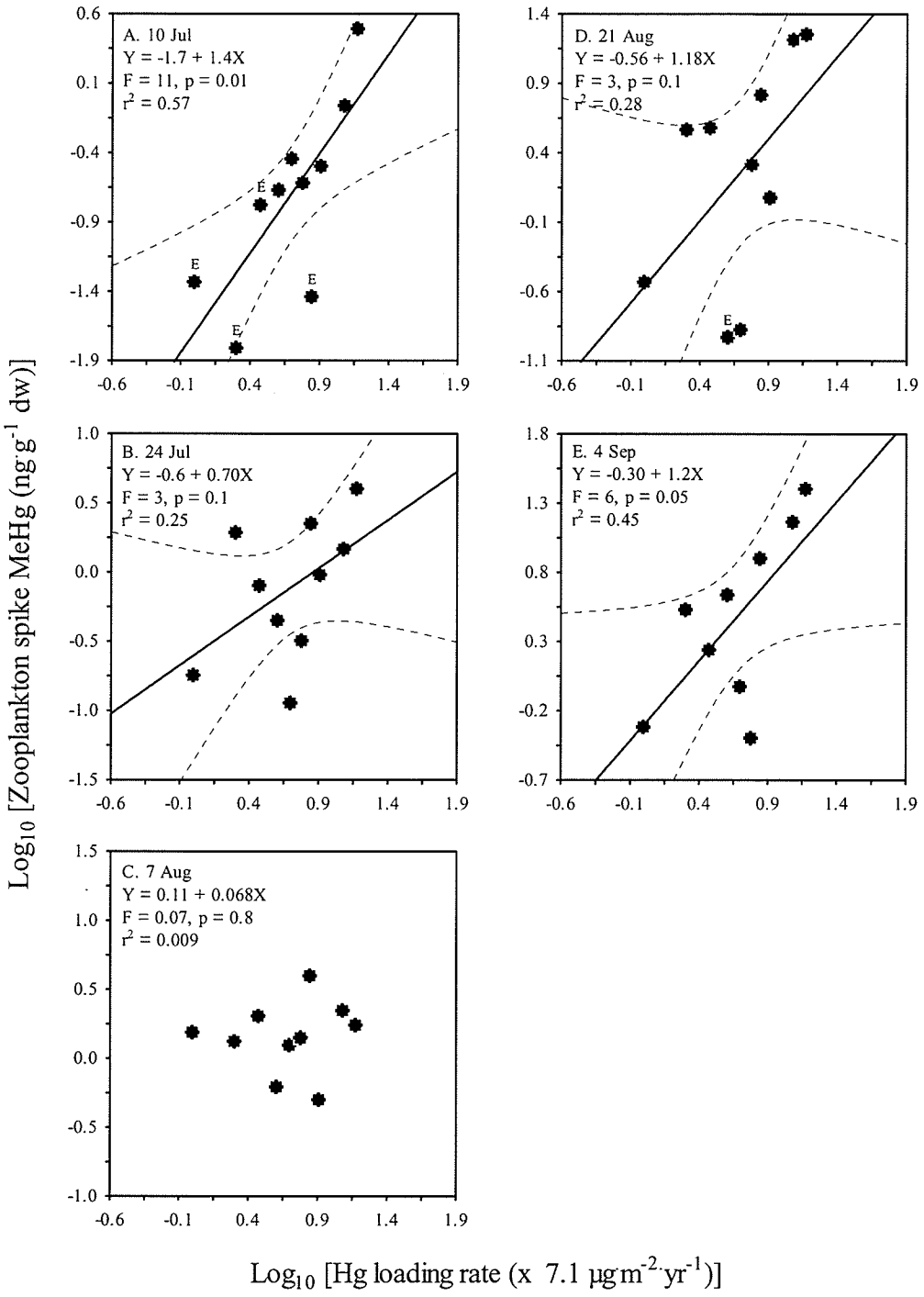

Figure 3-2. Spike MeHg concentrations of zooplankton as a function of Hg loading rate, shown for each sampling date (A-E). Each panel shows the regression line and 95% confidence bands, as well as the regression equation and associated statistics. A regression line is not shown in panel C because the model was highly non-significant. Symbols as in Figure 3-1.

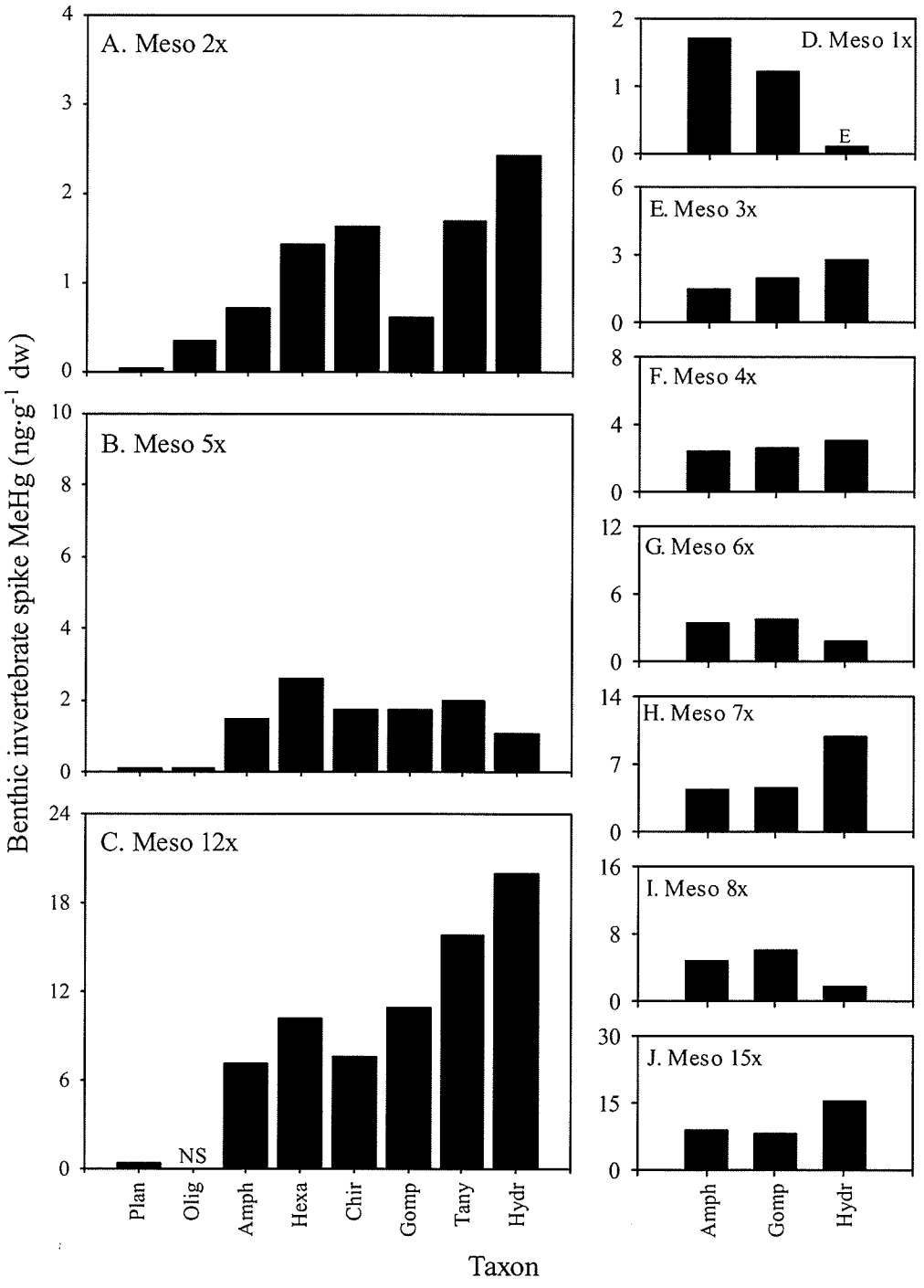

Figure 3-3. Spike MeHg concentrations of benthic invertebrates collected 6 – 11 September from each mesocosm. Eight invertebrate groups were collected from the intensive mesocosms (A-C), and three groups were collected from the non-intensive mesocosms (D-J). Individuals of each group were pooled for MeHg analyses. Group codes: Plan = Planorbidae; Olig = Oligochaeta; Amph = Amphipoda; Hexa = *Hexagenia*; Chir = Non-predatory Chironimidae; Tany = Tanypodinae; Hydr = Hydracarina. Concentrations represent one sample, or a mean of 1 – 3 subsamples. Y-axis scales are proportional to Hg loading rates. Symbols as in Figure 3-1.

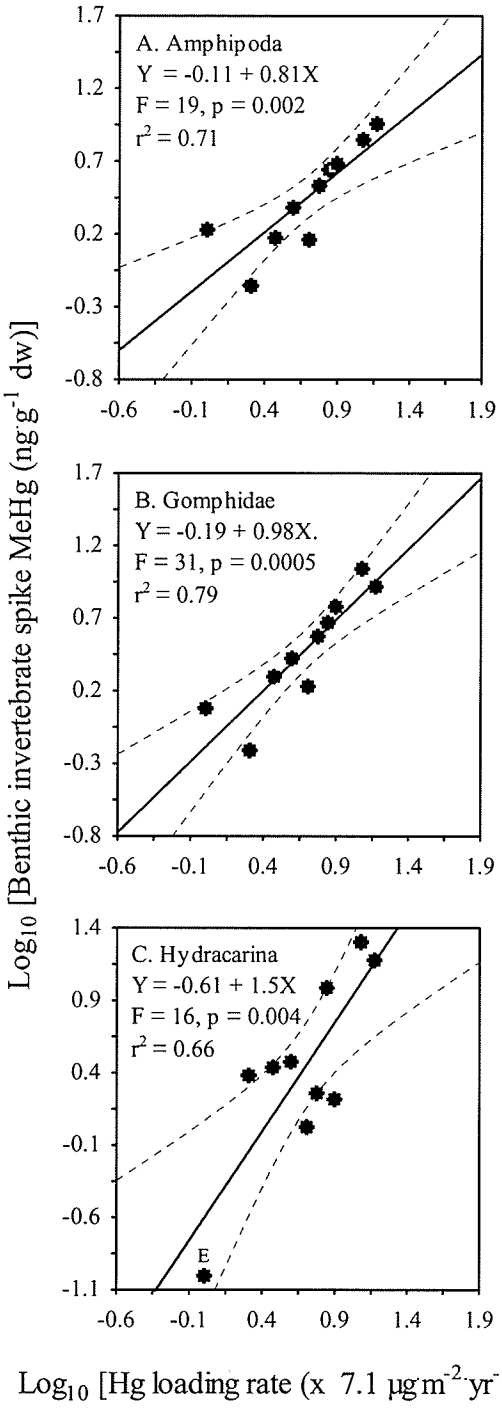

Figure 3-4. Spike MeHg concentrations of benthic invertebrates as a function of Hg loading rate, shown for each taxonomic group (A-E). Each panel shows the regression line and 95% confidence bands, as well as the regression equation and associated statistics. Symbols as in Figure 3-1

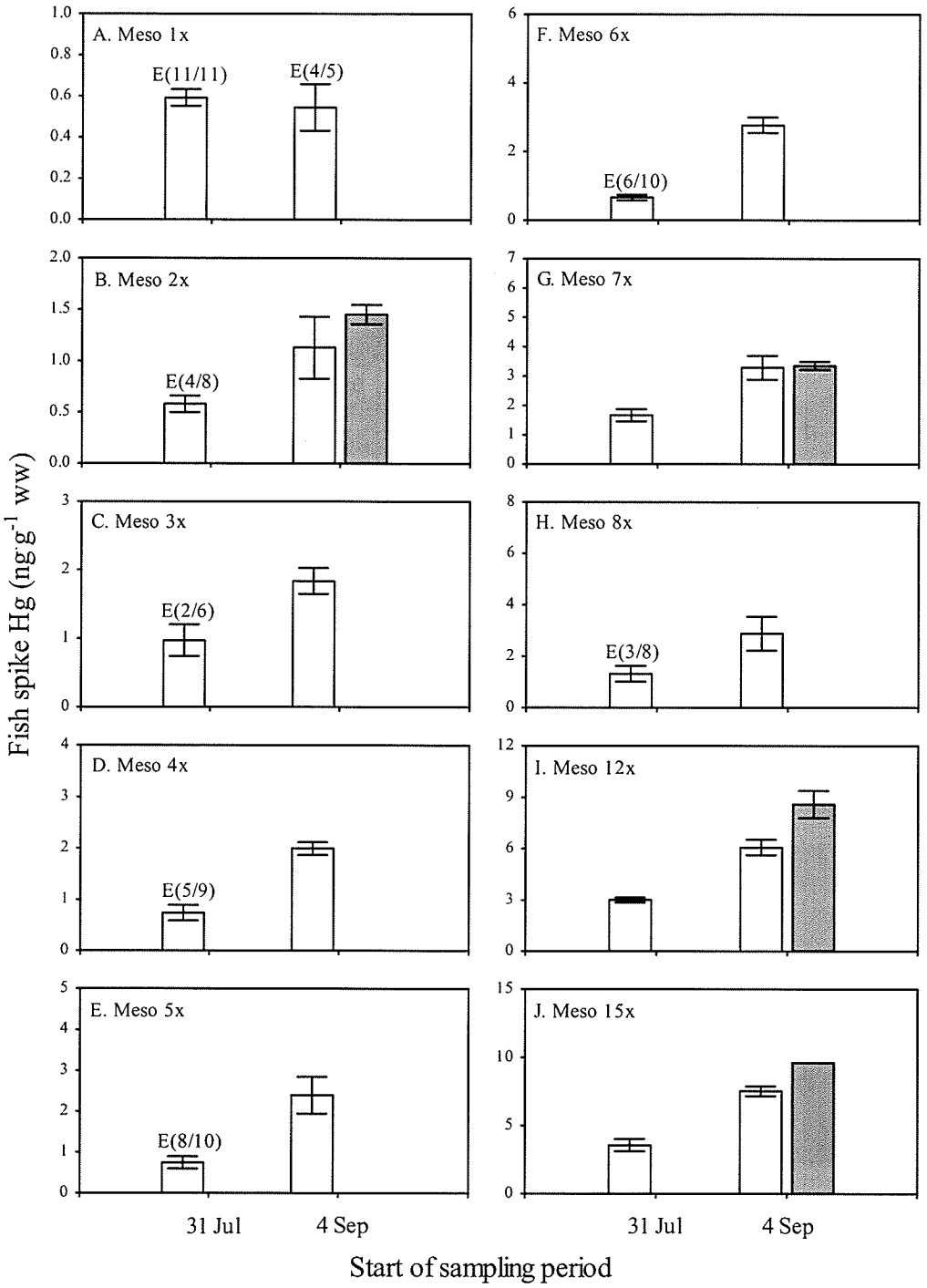

Figure 3-5. Concentrations of spike Hg in yellow perch muscle tissue at two sampling periods, shown for each mesocosm (A-J). The first sampling period occurred 31 July – 2 August, and the second sampling period occurred 4 – 16 September. Shown are the mean and standard error of spike Hg in age 1+ fish (open bars) and age 0+ fish (solid bars). Age 0+ fish were only captured in the second sampling period, and only in four mesocosms. "E" indicates the mean was calculated with one or more fish with estimated spike Hg concentrations because their measured concentrations were below the limit of detection. The bracket following the "E" indicates (number of fish with estimated concentrations/ total number of fish).

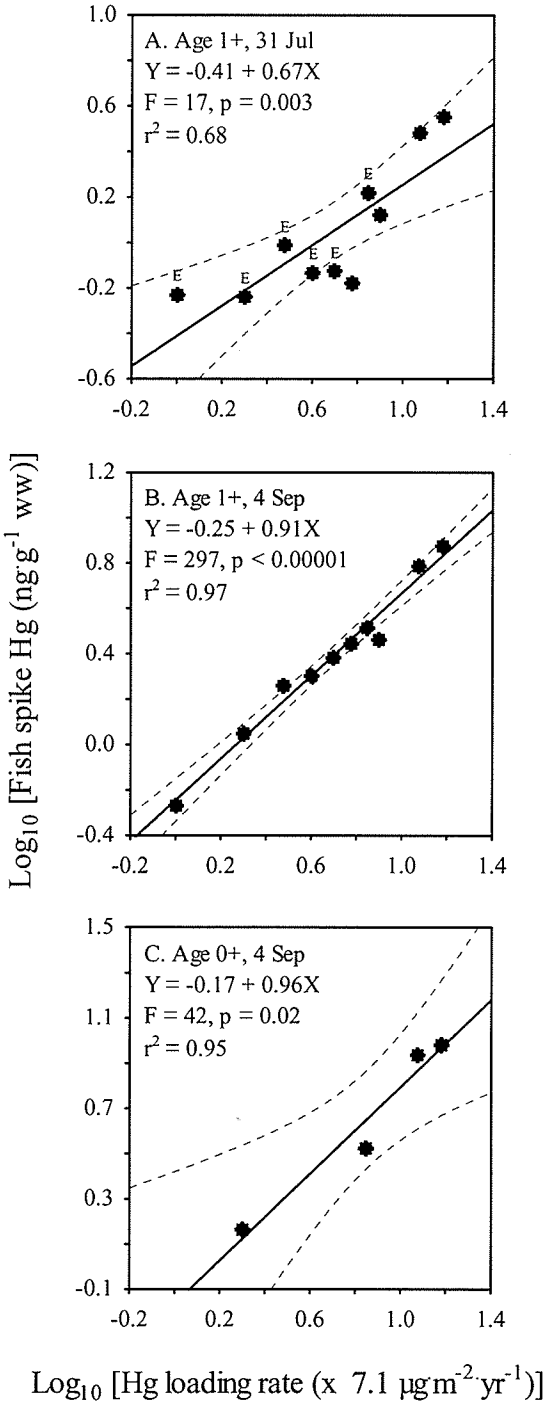

Figure 3-6. Spike Hg in yellow perch muscle as a function of Hg loading rate. Shown are mean concentrations of age 1+ fish collected 31 July – 2 August (A), age 1+ fish collected 4 – 16 September (B), and age 0+ fish collected 4 – 16 September. Age 0+ fish were only captured from four mesocosms. Symbols as in Figure 3-5. Refer to Figure 3-5 for number of estimated concentrations used to calculate means marked with an "E".

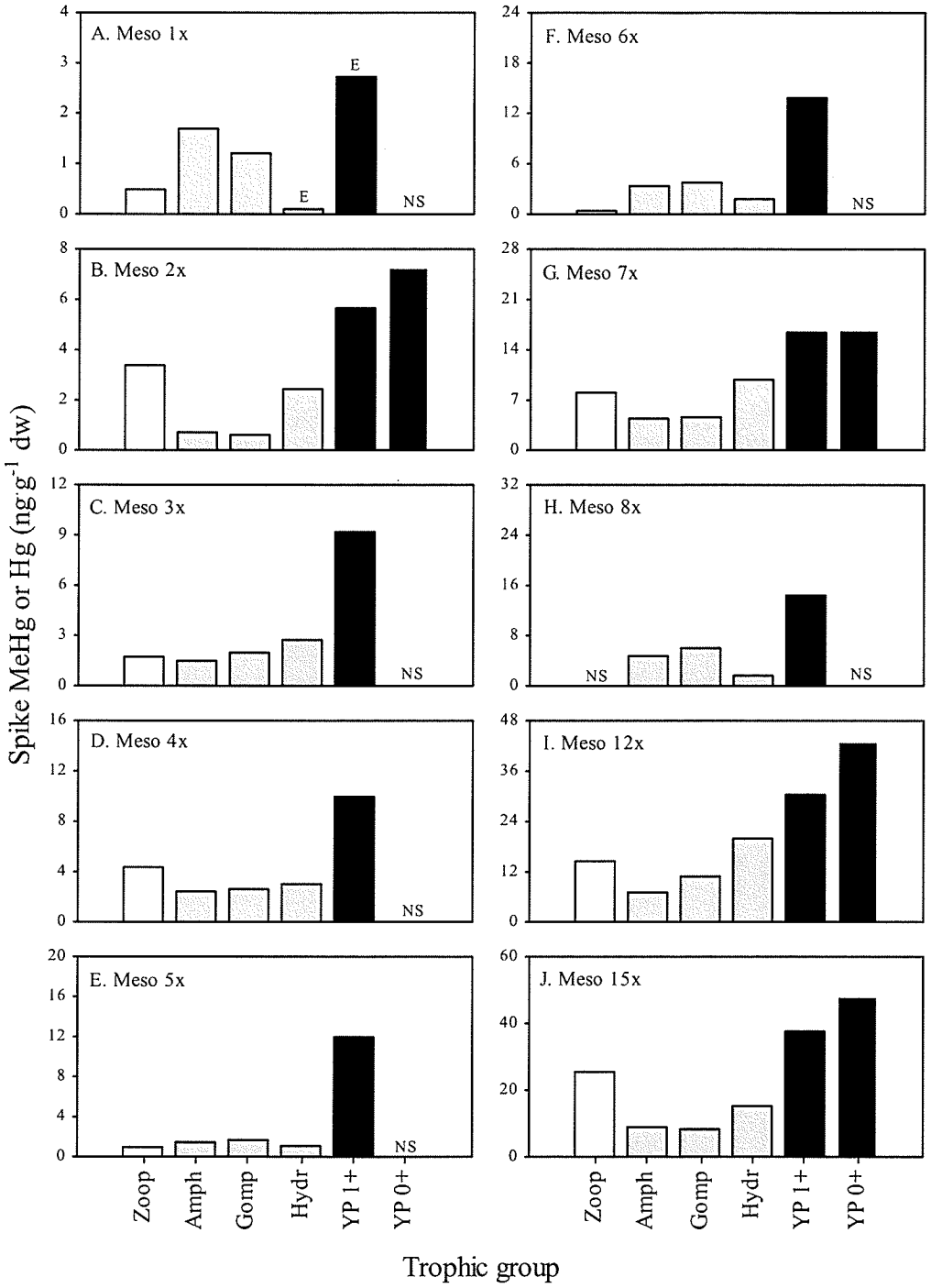

Figure 3-7. Spike MeHg or Hg levels in different levels of the aquatic food web in each mesocosm (A-J). Spike MeHg of zooplankton (Zoop) is shown in white, spike MeHg of benthic invertebrate groups Amphipoda (Amph), Gomphidae (Gomp), and Hydracarina (Hydr) are shown in grey, and spike Hg concentrations of age 1+ and age 0+ yellow perch (YP 1+ and YP 0+, respectively) are shown in black. All animals were collected during the final sampling period in September. The values represent the concentration of one sample, or the mean of several subsamples. Symbols as in Figure 3-1.

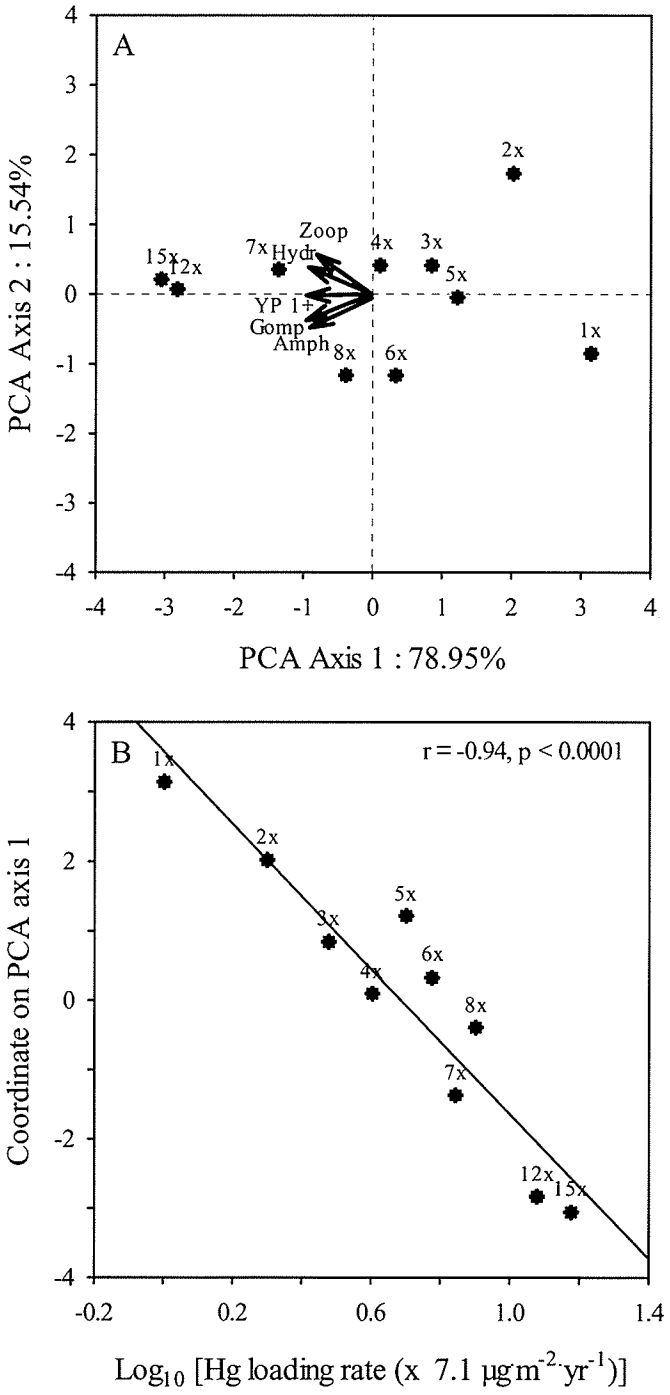

Figure 3-8. PCA of spike MeHg concentrations in the aquatic food web of the mesocosms during the final sampling period. Projection of variables (arrows) and objects (circles) on the first two PCA axes (A). The variables included were: spike MeHg of zooplankton (Zoop), Amphipoda (Hydr), Gomphidae (Gomp), Hydracarina (Hydr), and spike Hg of age 1+ yellow perch muscle tissue (YP 1+). The objects are the mesocosms (1x – 15x). Because the zooplankton sample collected from Meso 8x during this sampling period was lost, this missing value was assigned the spike MeHg concentration observed for zooplankton in Meso 8x on 21 Aug. Correlation between Hg loading rate of mesocosms and coordinates of mesocosms on PCA axis 1 (B).

CHAPTER 4. Synthesis

Mercury (Hg) pollution is a widespread problem that is potentially impacting the health of fish, wildlife, and humans. Inorganic Hg released to the environment is converted by natural processes to the neurotoxin methylmercury (MeHg), which biomagnifies in aquatic food webs resulting in high levels in fish tissues. Consumption of fish is the primary route by which humans are exposed to this neurotoxin. Today, Hg contamination of aquatic ecosystems largely originates from atmospheric waste emissions released from industries, particularly coal-fired electric utilities. Policies to reduce Hg emissions from coal-fired electric utilities have been issued or proposed by some countries to ameliorate Hg pollution. Unfortunately, it is poorly understood if these emission reductions will lead to significant decreases in Hg levels in fish. Policy-makers need to understand when and how much Hg levels in fish will decline in order to develop effective Hg regulations.

The purpose of this study was to examine the relationship between atmospheric deposition of Hg and its distribution in the environment, its conversion to MeHg, and its bioaccumulation in an aquatic food web. Different rates of atmospheric Hg deposition (1 – 15 times 7.1 μg $Hg \cdot m^{-2} \cdot yr^{-1}$) were simulated in large, in-lake mesocosms by adding multiple doses of inorganic Hg enriched with the stable isotope ^{202}Hg . The mesocosms were installed in Lake 240 of the Experimental Lakes Area (ELA) and stocked with native yellow perch (*Perca flavescens*). Over ten weeks, concentrations of Hg and MeHg were monitored in the environment (water and sediments) and in the food web (zooplankton, benthic invertebrates, and fish).

Because the mesocosms were loaded with Hg enriched with a stable isotope, the experimentally-added Hg (referred to as "spike Hg") could be traced through the environment and the food web. This new technology provided interesting observations on the timing of important biogeochemical processes in aquatic ecosystems:

i) Spike Hg had a short residence time (i.e. hours to days) in the dissolved phase of the water column;

ii) Spike Hg was detected on suspended particles 12 hours after the first Hg addition;

iii) Spike dissolved gaseous mercury (DGM) formation was stimulated by the addition of inorganic Hg, but only temporarily;

iv) Spike Hg accumulated in littoral sediments within three weeks;

v) Spike Hg was converted to its organic form – MeHg – in the mesocosms and observed in surface sediments as early as three weeks after the first Hg addition ;

vi) Spike MeHg was incorporated into zooplankton in all mesocosms within four weeks;

vii) Spike MeHg was observed in almost all benthic invertebrates sampled after ten weeks;

viii) Spike Hg was detected in the muscle tissue of about 50% of yellow perch sampled after five weeks and 97% of yellow perch sampled after ten weeks.

These observations suggest that atmospheric Hg deposited to aquatic ecosystems immediately enters the aquatic Hg biogeochemical cycle and is acted on by evasion, sedimentation, and methylation processes on short time-scales. Most importantly, these

observations suggest that atmospheric Hg is converted to MeHg, incorporated into the lower food web, and bioaccumulated by fish within weeks of deposition to an aquatic ecosystem. The implication of these findings is that decreases in atmospheric deposition will immediately remove a pool of Hg from aquatic systems that would otherwise be quickly methylated and bioaccumulated by the food web.

This experiment tested the following null hypotheses:

i) The fate of new Hg in aquatic ecosystems is not dependent on its loading rate to the ecosystem;

ii) The bioaccumulation of new Hg by fish and their food web is not dependent on the loading rate of inorganic Hg to the ecosystem.

The first hypothesis was examined by relating Hg loading rates to the mesocosms to concentrations of spike Hg dissolved in the water column, associated with suspended particles, present as DGM, and associated with surface sediments. Relationships between Hg loading and spike Hg concentrations in all ecosystem components were statistically significant. Furthermore, concentrations of spike MeHg in surface sediments were also significantly related to inorganic Hg loading rates. Analyses support that all relationships were linear and proportional across the range in Hg loading rates examined. Consequently, the relative partitioning of spike Hg among ecosystem components was found to be independent of loading rates to the mesocosms. This finding suggests that the relative fate of new Hg in aquatic ecosystems does not change under different Hg deposition regimes. Most importantly, this finding suggests that concentrations of new Hg in aquatic systems will decrease in direct proportion to changes in Hg deposition, and

the Hg emission reductions will be equally effective across a broad range of deposition rates.

The second hypothesis was examined by relating Hg loading rates to the mesocosms to spike MeHg concentrations in zooplankton and benthic invertebrates and spike Hg concentrations in fish muscle tissue. In all levels of the food web, a positive relationship was observed between inorganic Hg loading and spike MeHg or Hg concentrations in biota. Analyses strongly support that these relationships were both linear and proportional. After ten weeks, Hg loading rate explained 97% of the variability in spike Hg concentrations in age 1+ yellow perch among mesocosms. These findings suggest that decreases in atmospheric Hg deposition to aquatic systems will result in proportional changes in the MeHg content in biota that is derived from newly-deposited atmospheric Hg.

In summary, the main implications for Hg reductions suggested by this study are:

i) Decreases in atmospheric deposition will immediately remove a pool of Hg from aquatic systems that would otherwise be quickly methylated and bioaccumulated by the food web;

ii) Concentrations of new Hg in aquatic ecosystems will decrease in direct proportion to changes in atmospheric Hg deposition;

iii) Hg emission reductions will be equally effective across a broad range of atmospheric Hg deposition rates;

iv) Decreases in atmospheric Hg deposition to aquatic systems will result in proportional changes in the MeHg content in biota that is derived from newly-deposited atmospheric Hg.

The impact this will have on Hg concentrations in the aquatic environment and MeHg concentrations in aquatic food webs will depend, however, on the bioavailability of previously-deposited "old Hg" stored in sediments and soils. If the bioavailability of old Hg is sustained over long periods of time, the response to changes in atmospheric Hg deposition will take years, if not decades. Furthermore, if old Hg continues to be bioavailable, MeHg concentrations in fish will not be reduced in direct proportion to changes in Hg deposition, at least in the short-term. Unfortunately, we currently have little understanding of how long after deposition Hg continues to active in the aquatic Hg cycle. Further research should focus on the bioavailability of old Hg in lakes and their watersheds, and how this bioavailability may differ among ecosystems.

APPENDIX I. Estimating water volumes and leakage of aquatic mesocosms

I.1 Introduction

To construct a mass balance model for Hg in the mesocosms (Ch. 2), it was first necessary to obtain accurate estimates of water volume in each mesocosm, and to test the assumption that significant water leakage did not occur from the mesocosms during the period of the experiment. Water volumes could not be accurately determined from the dimensions of the mesocosms because of their non-rigid construction and the unevenness of the lake bottom. Water exchange between the mesocosms and the surrounding lake presumably could have occurred through holes in the wall material, waves splashing over the floating collars, or an incomplete seal between the walls and the sediments. To quantify water volumes and trace water movements, water labelled with tritium (^3H) was added to the mesocosms. The objectives of this chapter are:

i) to estimate the water volume of each mesocosm at the beginning of the experiment based on initial ^3H concentrations;

ii) to estimate subsequent water volumes over the period of the experiment based on daily inputs from precipitation and losses from evaporation;

iii) to develop a dynamic ^3H model (DTM) that predicts changes in ^3H concentrations from evaporation, sediment diffusion, and precipitation;

iv) to compare observed ^3H concentrations in the mesocosms to those predicted by the DTM in order to assess water losses from leakage.

I.2 Methods

I.2.1 Tritium additions and monitoring

On 14 June 2002, 9 mCi ^{3}H was added to each of the eleven mesocosms. An additional 4 mCi was distributed among Mesocosms 0x, 5x, 6x, and 8x, but inadvertently, the exact amount received by each was not measured (S. Page, pers. comm.). Each ^{3}H dose was diluted in 4 L of lake water, and then poured onto the water surface of the mesocosm. A trolling motor was used to mix the ^{3}H dose into the water column. To monitor tritium concentrations, duplicate water samples (250 mL) were collected from each mesocosm between 17 June – 3 September, using either an integrated sampler (prior to 15 July) or a surface grab (after 15 July). Water samples were collected every day for the first week, twice a week for the next two weeks, and once a week for the remaining eight weeks. A 5 mL aliquot was extracted from each water sample, mixed with 12 mL scintillation cocktail (Beckman Ready-Safe), and stored in darkness until analysis. Samples were analyzed at the Freshwater Institute (Winnipeg, MB) using a Packard Tri-Carb 2100TR liquid scintillation counter. Sample counts were corrected for background activity measured in blank samples. In this chapter, ^{3}H concentrations are expressed as either disintegrations per minute (dpm) or counts per minute (cpm) per unit volume of sample (mL).

I.2.2 Estimating water volumes

The initial water volumes of the seven mesocosms that received 9 mCi ^{3}H were each calculated based on the concentrations of ^{3}H in the mesocosm during the week following the ^{3}H addition:

$$V_0 = \frac{D \cdot k}{C_0}$$

where V_0 = water volume of mesocosm on day 0 (L)

D = ^{3}H dose (Ci)

k = unit conversion (2.22×10^{12} dpm· Ci $^{-1}$)

C_0 = average ^{3}H concentration in mesocosm on 17 – 21 June (dpm·L^{-1})

C_0 was set to the average concentration over the first five sampling dates rather than the first sampling date because some time is required for ^{3}H to be completely mixed in the water column. The initial water volumes of the four mesocosms that received an uncertain amount of ^{3}H were each estimated by:

$$V_0 = \frac{V_{nom}}{f}$$

where V_0 = water volume of mesocosm on day 0 (L)

V_{nom} = nominal water volume of mesocosm calculated from average depth (L)

f = ratio of the nominal water volume to the actual water volume

The parameter f was estimated by the mean f of the seven mesocosms that received 9 mCi ^{3}H. In these mesocosms, f was calculated by dividing the nominal water volume

calculated from average depth by the initial water volume determined from ^{3}H concentrations. The standard deviation of the mean *f* of the seven mesocosms was 0.02.

Subsequent changes in water volumes over the period of 14 June – 1 October 2002 were predicted based on daily water inputs from precipitation and daily water losses from evaporation:

$$V_t = V_{t-1} + R_{t-1} - E_{t-1}$$

where V_t = water volume of mesocosm on day t (L)

V_{t-1} = water volume of mesocosm on day t-1 (L)

R_{t-1} = volume of water deposited to mesocosm on day t-1 (L)

E_{t-1} = volume of water evaporated from mesocosm on day t-1 (L)

Precipitation was measured using a rain gauge at the ELA meteorological site, and evaporation was modeled for Lake 239 using a mass transfer approach (K. Beaty, unpubl. data). Precipitation and evaporation levels (mm) were converted to volumes (L) by multiplying by the surface area of a mesocosm (estimated using the formula for a decagon).

I.2.3 Dynamic Tritium Model (DTM)

A dynamic model of ^{3}H decline was developed for the mesocosms based on: i) losses to evaporation; ii) losses to sediment diffusion; and iii) dilution by precipitation.

i) Evaporation

Gross evaporation of ^3H from the mesocosms was estimated based on the loss rate of ^3H added to a Class A evaporation pan (122 cm diameter, 25 cm depth) at the ELA meteorological site. The evaporation pan was spiked with 500 µCi ^3H and on 10 July 2003 and ^3H concentrations were monitored daily (R. Hesslein, S. Page, K. Beaty, unpubl. data). The water level in the evaporation pan was maintained at 19 cm by adding or removing water on a daily basis. ^3H counts were corrected for the removal of water. The concentration of ^3H in the evaporation pan declined exponentially at rate of 5.5% per day (10 July – 22 August, 2003). Changes in ^3H concentrations in a mesocosm from evaporative losses were predicted by:

$$C_{E_t} = C_{E_{t-1}} \cdot e^{-k_{pan} \cdot (d_{pan} / d_{meso_t}) \cdot t}$$

where C_{E_t} = ^3H concentration as a result of evaporation on day t (cpm·mL^{-1})

$C_{E_{t-1}}$ = ^3H concentration as a result of evaporation on day t-1 (cpm·mL^{-1})

k_{pan} = ^3H evaporation coefficient of evaporation pan (day^{-1})

d_{pan} = water depth in evaporation pan (m)

d_{meso} = water depth in mesocosm on day t (m)

t = time (days)

Temporal changes in mesocosm water depth were estimated from daily measurements of water level in Lake 239 (K. Beaty, unpubl. data). Daily losses of ^3H from a mesocosm from evaporation were then predicted by:

$$L_{E_t} = C_{E_{t-1}} - C_{E_t}$$

where L_{E_t} = decline in ^3H as a result of evaporation on day t (cpm·mL^{-1})

$C_{E_{t-1}}$ = ^3H concentration as a result of evaporation on day t-1 (cpm·mL^{-1})

C_{E_t} = ^3H concentration as a result of evaporation on day t (cpm·mL^{-1})

ii) Sediment diffusion

The sediment depth to which ^3H diffused each day was estimated by:

$$z = \sqrt{d_s t}$$ (Carslaw and Jaeger 1959)

where z = mean depth of ^3H diffusion in sediments (cm)

d_s = ^3H diffusion coefficient for sediments (cm^2·s^{-1})

t = time (s)

The diffusion coefficient for tritium in pure water is described by:

$$d_o = (0.0525T + 1.099) \times b$$ (Sweerts et al. 1991)

where d_o = diffusion coefficient in pure water (cm^2·s^{-1})

T = temperature (°C)

b = 10^{-5} cm^2·s^{-1}

The average temperature of bottom waters in the mesocosms during 23 June – 5 September (21.6 °C) was assumed for this calculation. The diffusion coefficient for ^3H in whole sediments (d_s) was then estimated using a d_s/d_o ratio of 1.4 (Sweerts et al. 1991), which was empirically determined for Lake 302S. The type, porosity, and organic content of sediments in this lake is similar to Lake 240.

Daily losses in ^3H from a mesocosm from sediment diffusion were predicted by:

$$L_{S_t} = \left[\frac{A \cdot (z_t - z_{t-1}) \cdot p}{V_0} \right] \cdot C_0$$

where L_{S_t} = decline in ^3H as a result of sediment diffusion on day t (cpm·mL^{-1})

A = surface area of sediments in a mesocosm (cm^2)

z_t = mean depth of ^3H diffusion in sediments on day t (cm)

z_{t-1} = mean depth of ^3H diffusion in sediments on day t-1 (cm)

p = porosity of mesocosm sediments (L·cm^{-3})

V_0 = water volume of mesocosm on day 0 (L)

C_0 = ^3H concentration on day 0 (cpm·mL^{-1})

Sediment porosity was determined for each mesocosm from triplicate sediment cores (0 – 2 cm) collected on 18 – 19 August 2002. Sediments samples were weighed before and after drying at 60°C to quantify water content.

iii) Precipitation

Changes in ^3H concentrations in a mesocosm caused by dilution from rain were estimated by:

$$C_{R_t} = C_0 - \left[\frac{R_{0 \to t}}{V_0} \cdot C_0 \right]$$

where C_{R_t} = ^3H concentration as a result of precipitation on day t (cpm·mL^{-1})

$R_{0 \to t}$ = cumulative rainfall from day 0 to day t (L)

V_0 = mesocosm water volume on day 0 (L)

C_0 = ^3H concentration on day 0 (cpm·mL^{-1})

Precipitation data was collected daily at the ELA meteorological site (K. Beaty, unpubl. data). Precipitation levels (mm) were converted to volumes (L) by multiplying by the surface area of a mesocosm (estimated using the formula for a decagon). Daily declines in ^3H concentrations from rain dilution were then predicted by:

$$L_{R_t} = C_{R_{t-1}} - C_{R_t}$$

where L_{R_t} = decline in ^3H as a result of precipitation on day t (cpm·mL^{-1})

$C_{R_{t-1}}$ = ^3H concentration as a result of precipitation on day t-1 (cpm·mL^{-1})

C_{R_t} = ^3H concentration as a result of precipitation on day t (cpm·mL^{-1})

Whole model

The concentrations of ^3H in a mesocosm were predicted based on the daily decline in ^3H from evaporation, sediment diffusion, and precipitation:

$$C_t = C_{t-1} - (L_{E_{t-1}} + L_{S_{t-1}} + L_{R_{t-1}})$$

where C_t = ^3H concentration on day t (cpm·mL^{-1})

C_{t-1} = ^3H concentration on day t-1 (cpm·mL^{-1})

$L_{E_{t-1}}$ = decline in ^3H as a result of evaporation on day t-1 (cpm·mL^{-1})

$L_{S_{t-1}}$ = decline in ^3H as a result of sediment diffusion on day t-1 (cpm·mL^{-1})

$L_{R_{t-1}}$ = decline in ^3H as a result of precipitation on day t-1 (cpm·mL^{-1})

I.3 Results and Discussion

I.3.1 Water volumes

Initial water volumes of the mesocosms were determined to range from 129,779 – 146,605 L (Table I-1). These water volumes are reasonable considering the dimensions of the mesocosms (nominal volume of 157,000 L, assuming a perfect cylinder with 5 m radius and 2 m height). Initial water volumes did not differ between mesocosms by more than 10%. Changes in water volumes from precipitation and evaporation were relatively minimal over the period of 14 June – 1 October (Figure I-1). Maximum and minimum water volumes were observed on 25 June and 8 August, respectively, corresponding to the cool, wet conditions in June and hot, dry conditions throughout July and early

August. Overall, water volumes in the mesocosms varied by less than 10% during the period of the experiment.

I.3.2 Water exchange

Concentrations of ^{3}H declined by over 50% over the sampling period in all mesocosms (Table I-2). A similar pattern of ^{3}H decline over time was observed in all mesocosms (Figure I-2). As the extent and temporal pattern of ^{3}H decline were similar among mesocosms, either no water leakage occurred from any mesocosm, or water leakage occurred at the same rate in all mesocosms. To determine if the observed decline in ^{3}H could be accounted for by evaporation, sediment diffusion, and precipitation, the DTM was run for each mesocosm. The difference between the decline in ^{3}H concentrations predicted by the DTM and the observed concentrations is assumed to represent ^{3}H loss from water leakage. The change in ^{3}H concentration over the sampling period predicted by the DTM for each mesocosm generally agreed well with the observed declines (Table I-2). Leakage was estimated to be less than 20% from all mesocosms. In fact, in the mesocosms where the exact amount of ^{3}H added was known, leakage did not exceed 10%. The DTM predicted that most of the decline in ^{3}H was from evaporation (69 – 73%) and precipitation (23 – 25%), while sediment diffusion was of minor importance (3 – 7%). The DTM captured the overall time dynamics of ^{3}H in the mesocosms, but tended to overestimate ^{3}H decline in July and underestimate decline in August (Figure I-2). In conclusion, the similarity of ^{3}H decline among mesocosms and the good agreement between observed concentrations and those predicted by the DTM support the assumption that water leakage from the mesocosms was likely minor during the experiment.

Table I-1. Initial water volume of each mesocosm. See text for explanation of calculations.

Mesocosm	Initial water volume (L)
0x	142,043
1x	129,779
2x	131,787
3x	134,360
4x	141,448
5x	146,605
6x	135,528
7x	132,790
8x	142,043
12x	132,127
15x	132,640

Table I-2. Decline in tritium (^{3}H) concentration observed in each mesocosm over the sampling period, compared to the decline predicted by a dynamic tritium model based on evaporation, sediment diffusion, and precipitation. ^{3}H decline was calculated as the observed or predicted ^{3}H concentration on 3 September divided by the observed average ^{3}H concentration on 17 – 21 June. Estimated leakage is the difference between the observed and predicted decline.

Mesocosm	Observed ^{3}H decline (%)	Predicted ^{3}H decline (%)	Estimated leakage (%)
0x	58	50	8
1x	55	53	2
2x	56	52	4
3x	56	51	5
4x	54	50	4
5x	68	50	18
6x	59	51	8
7x	53	52	1
8x	58	50	8
12x	61	51	10
15x	56	51	5

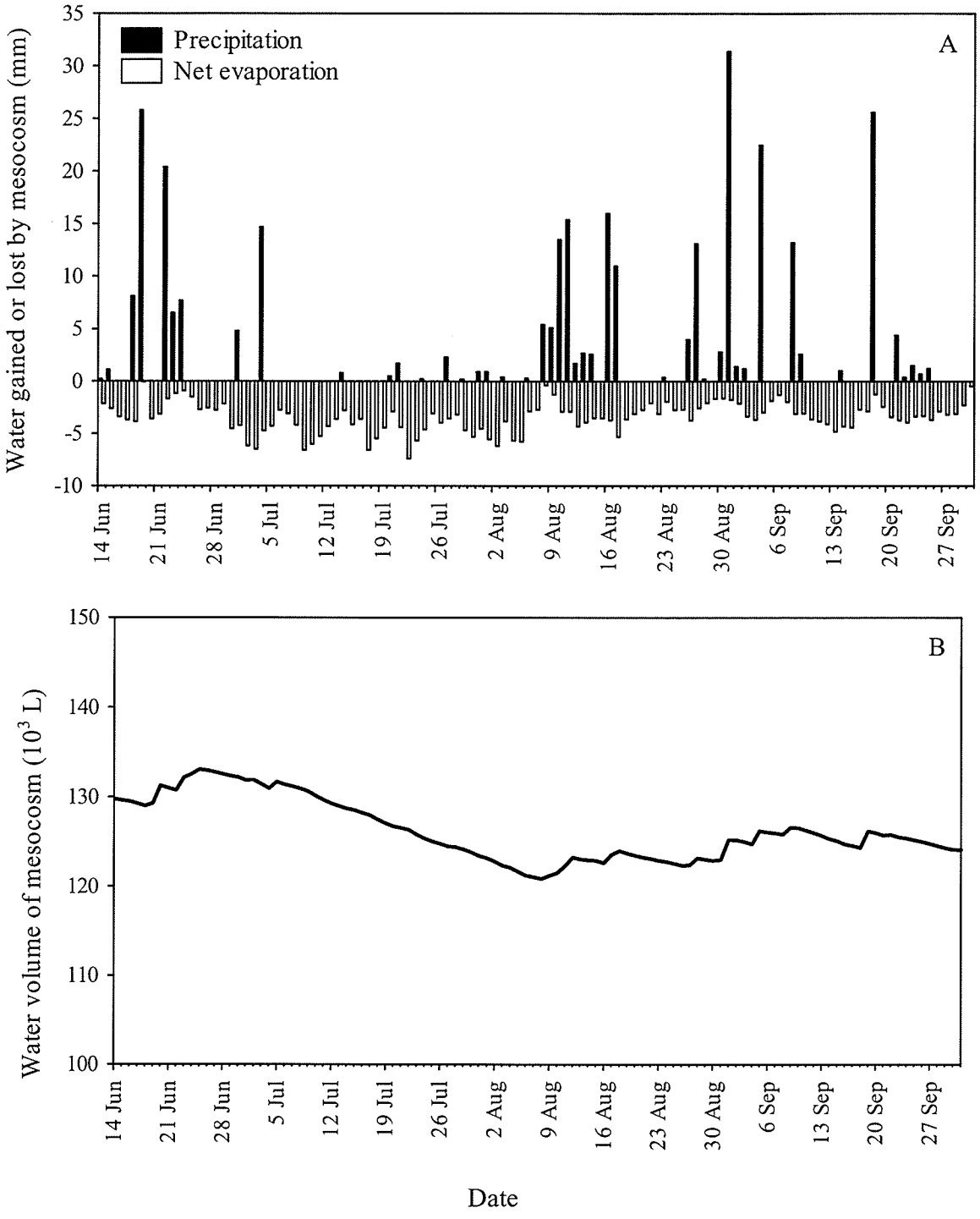

Figure I-1. Daily water inputs to the mesocosms from precipitation and losses from evaporation (A). Temporal changes in mesocosm water volume, shown for Mesocosm 1x, as an example (B). The temporal changes in water volumes of all mesocosms are assumed to be the same.

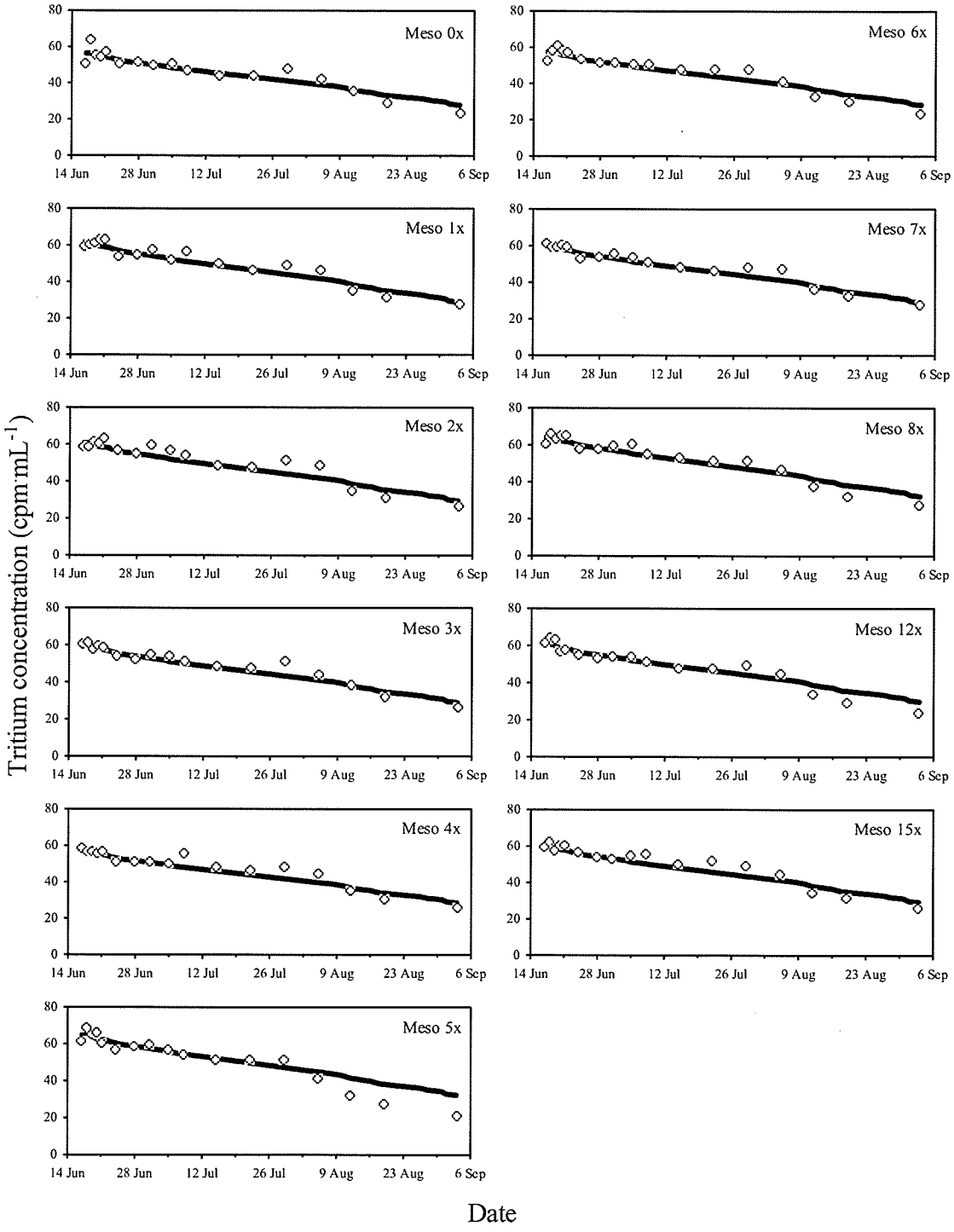

Figure I-2. Changes in observed (open circles) and predicted (solid line) tritium concentrations in each mesocosm over time. Observed values represent an average of duplicate samples. Predicted values were obtained from a dynamic tritium model based on evaporation, sediment diffusion, and precipitation.

APPENDIX II. Ancillary physical, chemical, and biological data

II.1 Introduction

This chapter describes the physical, chemical, and biological characteristics of the eleven mesocosms between June – September 2002. Where possible, characteristics are compared: i) within each mesocosm over time; ii) among mesocosms at given points in time; and iii) between the mesocosms and the surrounding lake at given points in time. The purpose of these comparisons is to understand how the physical, chemical, or biological environment in the mesocosms may have deviated from each other and/or the surrounding lake. Furthermore, these comparisons help identify potential variables confounding the Hg dose-response relationship.

II.2 Methods

II.2.1 Temperature

Vertical profiles of water temperature were conducted in the mesocosms and Lake 240 on seven occasions between 23 June – 4 September (YSI 95 probe). The Lake 240 profiles were performed in a location adjacent to the mesocosms. Temperature measurements were taken at every meter in the water column. Underwater temperature loggers (Onset StowAway TidbiT) were installed in Mesocosm 2x and Lake 240 (0.5 m from Mesocosm 2x) to record surface water temperatures every 30 min between 19 July –

16 September 2002. Temperature dynamics in Mesocosm 2x were assumed to be representative of the other mesocosms.

II.2.2 Dissolved oxygen

Depth profiles of dissolved oxygen ($mg \cdot L^{-1}$) were conducted in the mesocosms and Lake 240 on seven occasions between 23 June – 4 September (YSI 95 probe). Dissolved oxygen measurements were taken at every meter in the water column in conjunction with temperature measurements. Percent saturation of dissolved oxygen was calculated as described in WOW (2004).

II.2.3 Light penetration

Vertical profiles of light intensity were performed in the mesocosms and Lake 240 between 24 July – 4 September. Using an Li-Cor Photometer, light intensity was measured above the water surface and in the water column at every 0.5 m. Duplicate readings were obtained at each depth. A correction factor of $(1.32)^{-1}$ was applied to light intensity measurements above the water surface. Light extinction coefficients were calculated for each light profile by the slope of the relationship of depth vs. ln(light intensity).

Unfiltered water was collected at a depth of 1 m from each mesocosm on 25 June, 23 July, and 20 August for spectral analysis. Absorbance of light through 10 cm of sample water was determined at 1 nm increments between 190 – 1,100 nm (Shimadzu 1601-PC spectrophotometer). Spectral analyses were performed by the Freshwater Institute chemistry laboratory.

II.2.4 Water chemistry

Every two weeks between 25 June – 3 September, water in the mesocosms was sampled at a depth of 1 m (CanSun Electronics pump) for chemical analyses. Chemical parameters measured include: alkalinity, pH, conductivity, sodium (Na^+), potassium (K^+), magnesium (Mg^{2+}), calcium (Ca^{2+}), chloride (Cl^-), sulphate (SO_4^{2-}), nitrate (NO_3^-), ammonia (NH_4^+), nitrite (NO_2^-), suspended nitrogen, dissolved nitrogen, suspended phosphorus, dissolved phosphorus, suspended carbon, dissolved organic carbon (DOC), and dissolved inorganic carbon (DIC). Concentrations of major ions were only determined once a month. Samples were analyzed at the Freshwater Institute using methods described in Stainton et al. (1977). Water chemistry of integrated epilimnion samples from Lake 240 was provided by M. Stainton (unpubl. data).

II.2.5 Sediment properties

Sediment samples were collected from three random locations in each of the intensive mesocosms (i.e. Mesocosms 2x, 5x, and 12x) on 30 June and 17 July, and in all mesocosms on 18-19 August. Sediments samples were also collected from a reference site in Lake 240 (situated 50 m north of the mesocosms) on 23 June, 17 July, and 20 August. Intact sediment cores were manually collected in clear polycarbonate tubes (4.8 cm diameter). In the laboratory, water above the sediment surface was siphoned off and the top 2 cm of the sediment core was transferred into a 120 mL polypropylene container and stored frozen. At the Academy of Natural Sciences, dry weight and ash weight of each sediment sample was determined by drying sample aliquots at 60°C to constant weight and then ashing at 450°C (C. Gilmour, pers. comm.).

Porosity of each sample was calculated by:

$$P = \frac{(D_{wet} - D_{dry})}{D_{wet}}$$

where P = porosity ($mL \cdot cm^{-3}$)

D_{wet} = wet weight density ($g \cdot cm^{-3}$)

D_{dry} = dry weight density ($g \cdot cm^{-3}$)

Loss on ignition (a surrogate measure for organic matter) was calculated by:

$$LOI = \frac{(D_{dry} - D_{ash})}{D_{dry}} \cdot 100$$

where LOI = loss on ignition (%)

D_{dry} = dry weight density ($g \cdot cm^{-3}$)

D_{ash} = ash weight density ($g \cdot cm^{-3}$)

II.2.6 Phytoplankton

Water samples for determination of chlorophyll *a* concentration (an indicator of phytoplankton biomass) were collected from the mesocosms every two weeks between 25 June – 3 September. Water samples were collected from the mesocosms from a depth of 1 m (CanSun Electronics pump). Samples were analyzed at the Freshwater Institute using methods described in Stainton et al. (1977). Chlorophyll *a* data of integrated epilimnion samples from Lake 240 were provided by M. Stainton (unpubl. data).

II.2.7 Zooplankton

Zooplankton samples for determination of community composition and biomass were collected from the mesocosms between 29 – 30 September. Zooplankton were sampled from a depth of 1 m using a Schindler-Patalus trap (50 L). Two hauls were

performed in each mesocosm. Samples were narcotized with methanol and preserved in 4% sugar-formalin. Counts of zooplankton species were performed by the Freshwater Institute (M. Paterson, unpubl. data.). Zooplankton biomass was estimated by multiplying species counts by the nominal weight of each species (M. Paterson, pers. comm.).

II.2.8 Fish

The mesocosms were stocked with 50 – 60 mm yellow perch (*Perca flavescens*) from Lake 240 between 24 – 26 June. A subsample of 10 fish was collected from the pool of fish from Lake 240 used to stock the mesocosms. Fish were sampled from the mesocosms after five weeks (31 July – 2 August) and ten weeks (4 – 16 September). The fork length and wet weight of each fish was measured (to the nearest 1 mm and 0.1 g, respectively). Fish condition factor was calculated as 100000[weight]/[fork length]^3. Fish captured from Lake 240 between 24 – 26 June and from the mesocosms between 31 July – 2 August were assumed to be age 1+ based on their fork lengths. Some perch captured in the mesocosms between 4 – 16 September were suspected to be young-of-year, so fish caught during this period were aged by examining saggital otolith sections.

II.3 Results

II.3.1 Water temperature

Vertical profiles – Water temperatures in the mesocosms ranged from 18 – 26 °C on the seven dates vertical profiles were performed. Water temperatures in the mesocosms were usually observed to increase toward the surface, particularly on warmer days (Figure

II-1). Surface water temperatures in the mesocosms were, on average, 1 °C warmer than bottom waters on the dates sampled. The greatest thermal differences between surface and bottom waters were observed on 28 June, which was the sampling date with the highest maximum air temperature. The mesocosms were isothermal on 7 August, following a decrease in air temperature (Figure II-2A). Differences in water temperature among mesocosms on a given sampling date were small (Figure II-1) and were presumed to be a sampling artifact, as sampling took approximately 3 h to complete (during which time air temperatures would have changed).

Profiles of water temperature in the mesocosms usually showed greater changes with depth than in Lake 240 (Figure II-1). While temperatures at the surface of the mesocosms were observed to be up to 2 – 5 °C higher than bottom waters (i.e. 28 June), the difference in temperature between 0 – 2 m in Lake 240 did not exceed 0.7 °C. On the dates sampled, surface water temperatures in the mesocosms were usually warmer than in Lake 240, while bottom water temperatures in the mesocosms tended to be cooler than in Lake 240. Consequently, the mean water column temperatures of the mesocosms were similar to Lake 240 on a given sampling date (< 0.8 °C difference).

Surface temperature loggers – Between 19 July – 18 September, surface water temperatures in Mesocosm 2x ranged from 17.2 – 28.0 °C (Figure II-2B). The difference between the daily minimum and maximum temperature in Mesocosm 2x was on average 2.2 °C (range: 0.6 – 4.9 °C). Mesocosm 2x and Lake 240 exhibited similar diel and seasonal patterns in surface water temperatures, but Mesocosm 2x experienced greater warming and cooling than Lake 240 in response to changes in air temperatures (Figure II-2). Surface temperatures in Mesocosm 2x were as much as 1.2 °C colder than Lake

240 (1:00 on 19 August) following a decrease in air temperature, and 2.9 °C warmer than Lake 240 (17:30 on 8 August) following an increase in air temperature. The mean temperatures of Mesocosm 2x and Lake 240 were similar across the sampling period (28.0 and 27.4 °C, respectively).

II.3.2 Dissolved oxygen

Dissolved oxygen concentrations in the water column of the mesocosms ranged from 7.3 – 10.6 $mg \cdot L^{-1}$ on the seven dates vertical profiles were performed. Dissolved oxygen concentrations were usually fairly similar at different depths in the water column, although surface concentrations were sometimes slightly lower than those deeper in the water column (Figure II-3). This small decrease in dissolved oxygen was presumably related to the higher temperature of surface waters (Figure II-1). The water column of the mesocosms was nearly saturated or supersaturated with oxygen on all sampling dates (range: 84 – 129 %), even on days when air temperatures were near 30 °C. The similarity among vertical profiles and the high levels of saturation on all sampling dates strongly suggests that dissolved oxygen was not depleted in the mesocosms during the experiment.

Small differences in dissolved oxygen concentrations among mesocosms on a given sampling date are assumed to be a sampling artifact, as water temperatures changed over the 3-hr sampling period. After Hg additions began on 26 June, all sampling was conducted in sequence of Hg loading (i.e. from Mesocosm 0x to Mesocosm 15x) to avoid contaminating lower Hg mesocosms with equipment from higher Hg mesocosms. Any apparent increases in dissolved oxygen with Hg loading (e.g. 28 June) are presumably as a result of decreasing water temperature during the sampling period (Figure II-2B).

Dissolved oxygen concentrations in the mesocosms were generally within ± 1 $mg \cdot L^{-1}$ of concentrations observed in Lake 240 at the same depth (Figure II-3). Dissolved oxygen concentrations in Lake 240 tended to be more uniform with depth than in the mesocosms, as expected based on temperature profiles.

II.3.3 Light penetration

Light extinction coefficients in the mesocosms ranged from 0.6 – 1.8 on the dates sampled. Differences in light extinction coefficients among mesocosms were not consistent across sampling dates (Figure II-4). No consistent change in light extinction coefficients was apparent over time in the mesocosms. Light extinction coefficients in the mesocosms were similar or higher than those observed in Lake 240 (Figure II-4). Taken together, these observations do not suggest water in the mesocosms changed during the 10-week experiment.

Spectral scans of unfiltered water on three sampling dates are presented in Figure II-5. On 25 June, spectral scans were similar among mesocosms, with the exception of Mesocosm 3x where percent transmittance was somewhat lower at wavelengths between 450 - 950 nm. Percent transmittance was also considerably decreased in this region in five mesocosms (2x < 1x < 4x < 3x < 6x) on 23 July. Spectral scans on 20 August were very similar among all mesocosms. A small increase in percent transmittance in the ultraviolet region was observed over time in all mesocosms.

II.3.4 Water chemistry

Alkalinity and pH – Alkalinity of the mesocosms ranged from 123 – 170 $\mu eq \cdot L^{-1}$ on the dates sampled. A small increase in alkalinity was observed over time in the mesocosms,

but not in Lake 240 (Figure II-6). The difference in alkalinity between Lake 240 and the mesocosms was usually within 20% on a given sampling date (Figure II-7). Differences in alkalinity among mesocosms may be related to their position in the lake, as alkalinity generally decreased from north to south (data not shown).

The range in pH of the mesocosms was 6.9 – 7.2 on 25 June, but increased to 7.2 – 7.5 by 3 September (Figure II-6). As expected, smaller changes in pH were observed in mesocosms with higher alkalinity. A similar increase in pH was also observed in Lake 240 in early summer, but pH levels in the lake began to decrease in August. Differences in pH among mesocosms on a given date are presented in Figure II-7. The greatest variation in pH among mesocosms was observed at the beginning of the experiment, and became smaller over time.

Conductivity and major ion concentrations – Conductivity of the mesocosms ranged between 22 – 29 $\mu S \cdot cm^{-1}$ during the sampling period. In both the mesocosms and Lake 240, conductivity was relatively stable over time (Figure II-8). Conductivity among mesocosms and between the mesocosms and Lake 240 was similar on all sampling dates (Figure II-9). Temporal changes in major ion concentrations in the mesocosms and Lake 240 are presented in Figure II-10. Calcium and sulphate were the most abundant ions, with concentrations of ca. 2 $mg \cdot L^{-1}$. Concentrations of sodium, magnesium, potassium, and chloride were below 1 $mg \cdot L^{-1}$. Differences in major ion concentrations among mesocosms and the surrounding lake are presented in Figure II-11.

Carbon – On all sampling dates, the majority of carbon in the water column of the mesocosms and Lake 240 was in the dissolved phase, largely as DOC. Specifically, DOC concentrations were about 8 $mg \cdot L^{-1}$ while DIC and suspended carbon

concentrations did not exceed 2 $mg \cdot L^{-1}$. There was no evidence of a significant change in the quantity of DOC or DIC over time in any of the mesocosms, however, a temporary increase in suspended carbon was observed in Mesocosms 2x, 5x, and 15x on 10 July (Figure II-12). In general, DOC and DIC concentrations among the mesocosms were similar to each other and to Lake 240, but considerable differences in suspended carbon were observed among mesocosms later in the experiment (Figure II-13).

Nitrogen – Concentrations of dissolved nitrogen in the mesocosms were three or more times higher than concentrations of suspended nitrogen (Figure II-14). Dissolved nitrogen concentrations tended to be more variable over time in the mesocosms than in Lake 240 (Figure II-14). Suspended and dissolved nitrogen concentrations were similar among mesocosms at the beginning of the experiment, but differences emerged over time (Figure II-15). Notably, the mesocosms with the highest suspended nitrogen also had the highest suspended carbon (Figure II-13, Figure II-15).

On all sampling dates, ammonia concentrations in the mesocosms were above 6 $\mu g \cdot L^{-1}$, nitrate concentrations did not exceed 10 $\mu g \cdot L^{-1}$, and nitrite concentrations were usually below detection limits (Figure II-16). Particularly high ammonia concentrations were observed in Lake 240 and some mesocosms on 23 July. Differences in ammonia and nitrate among mesocosms neither increased nor decreased over time and were not consistent across sampling dates (Figure II-17).

Phosphorus – Levels of suspended phosphorus in the mesocosms ranged between 3 – 7 $ug \cdot L^{-1}$, while levels of dissolved phosphorus ranged from 1 – 5 $ug \cdot L^{-1}$. These ranges are similar to those observed in Lake 240 over the same period. Changes over time in suspended and dissolved phosphorus were not consistent among all mesocosms (Figure

II-18). Differences in suspended and dissolved phosphorus among mesocosms became greater over time (Figure II-19).

II.3.5 Sediment properties

In the area where the mesocosms were situated in Lake 240, the sediments were mostly composed of sand. The porosity of surface sediments in the mesocosms ranged from 0.2 – 0.6 $mL \cdot cm^{-3}$ (Figure II-20). Sediments at the Lake 240 reference site had a similar porosity (0.3 – 0.4 $mL \cdot cm^{-3}$). Based on sediment samples collected 18 – 20 August, the rank order of the mesocosms, from lowest to highest porosity, was 8x < 4x < 12x < 6x < 15x < 0x < 2x < 3x < 7x < 5x < 1x. Loss on ignition of samples ranged from 1 – 3%, indicating that surface sediments in the mesocosms had low levels of organic matter (Figure II-20). The Lake 240 reference site had a similar loss on ignition (1 – 2%). Porosity and loss on ignition of sediment samples were highly correlated ($r^2 = 0.70$, $p < 0.001$), so the rank order of the mesocosms based on loss on ignition (15x < 0x < 12x < 2x < 8x < 4x < 6x < 7x < 5x < 3x < 1x) was similar to the order based on porosity. Porosity and loss on ignition of surface sediments tended to increase from north to south along the line of mesocosms (data not shown).

II.3.6 Phytoplankton

Concentrations of chlorophyll *a*, a surrogate measure for phytoplankton biomass, ranged from 1.3 – 4.7 $\mu g \cdot L^{-1}$ in the mesocosms. Chlorophyll *a* in Lake 240 was within the range in concentrations observed in the mesocosms on all sampling dates except 3 September. Changes in chlorophyll *a* over time were not consistent among all mesocosms (Figure II-21). Mesocosm 2x and 5x experienced a brief increase in

chlorophyll *a* in July. In late summer, a large increase in chlorophyll *a* was observed in Lake 240, and to a lesser extent, in Mesocosms 0x, 1x, 5x, 6x, and 8x. Differences in chlorophyll *a* among mesocosms were more apparent later in the experiment than at the beginning (Figure II-22). On the last two sampling dates, the highest chlorophyll *a* concentrations tended to be in the mesocosms situated at either end of the series of mesocosms.

II.3.7 Zooplankton

Zooplankton abundance and diversity on 29 – 30 September varied greatly among mesocosms (Figure II-23). Less than 2 organisms·L^{-1} were present in Mesocosms 0x, 1x, 5x, 6x, and 8x, between 23 – 52 organisms·L^{-1} were present in Mesocosms 2x, 3x, 7x, 12x, and 15x, and 233 organisms·L^{-1} were present in Mesocosm 4x. The lowest diversity of zooplankton was observed in Mesocosm 0x and 1x, and the highest diversity was observed in Mesocosm 12x.

The estimated dry weight biomass of zooplankton ranged from 0.003 ug·L^{-1} in Mesocosm 1x to 98 ug·L^{-1} in Mesocosm 15x (Figure II-24A). Mesocosms with greater zooplankton biomass had lower phytoplankton biomass (as indicated by chlorophyll *a* concentrations) (Figure II-24B).

II.3.8 Fish

While the average size of age 1+ perch in the mesocosms increased during the experiment (Table II-1), differences in fish growth were apparent among mesocosms (Figure II-25). In particular, age 1+ perch in Mesocosms 0x, 1x, 5x, 6x, and 8x tended to be shorter and thinner than fish in the other mesocosms, and showed little or no increase

in size between week 5 and 10 (Figure II-25A,B). The mean condition of fish caught from each of these five mesocosms was less than 1.0 during both sampling periods, while the mean condition of fish caught from the other mesocosms were all above 1.0 during both sampling periods (Figure II-25C). Condition of age 1+ perch during the final sampling period tended to be higher in mesocosms with lower phytoplankton biomass and higher zooplankton biomass (Figure II-26).

Age 0+ perch captured from four mesocosms during the final sampling period tended to be smaller than age 1+ fish, but the ranges in fork lengths and weights of these two age classes overlapped in a given mesocosm (Figure II-25A,B). Nearly all age 0+ fish had condition factors above 1.0, and the mean condition factor of age 0+ fish were higher than that of age 1+ fish in the same mesocosm (Figure II-25C).

II.4 Summary

i) The mesocosms experienced greater warming and cooling than the surrounding lake in response to changing air temperatures, but the average temperature in the mesocosms was similar to that of Lake 240.

ii) There was no evidence of oxygen depletion in the water column of the mesocosms.

iii) Light profiles did not show a change in light penetration over time, but spectral scans suggested a small increase in UV transmission later in the experiment.

iv) An increase in pH was observed over time in all mesocosms.

v) Differences in carbon, nitrogen, and phosphorus among mesocosms emerged over the period of the experiment.

vi) All mesocosms contained sandy sediments with low organic content.

vii) Differences in phytoplankton abundance among mesocosms emerged over time.

viii) The abundance and diversity of zooplankton varied greatly among mesocosms at the end of the experiment.

ix) The average size of yellow perch increased over time in the mesocosms, but differences in growth rates were observed among mesocosms.

x) Mesocosms situated at either end of the line of mesocosms tended to have higher phytoplankton biomass, lower zooplankton biomass, and poorer fish growth than mesocosms situated near the center.

Because Hg loading rates were randomly assigned to the mesocosms, differences in physical, chemical or biological variables among mesocosms do not bias the Hg dose-response relationship, but may increase the variability around the regression line.

Table II-1. Mean (±SD) length and weight of age 1+ perch in the mesocosms at the beginning, middle, and end of the experiment. The first sampling period represents a random subsample from the pool of fish captured from Lake 240 to stock the mesocosms. The second and third sampling periods represent age 1+ fish captured from all mesocosms.

Sampling period	n	Fork length (mm)	Wet weight (g)
24 – 26 Jun	10	58 (± 2)	2.1 (± 0.2)
31 Jul – 2 Aug	95	69 (± 6)	3.5 (± 1.2)
4 – 16 Sep	90	76 (± 9)	4.6 (± 2.2)

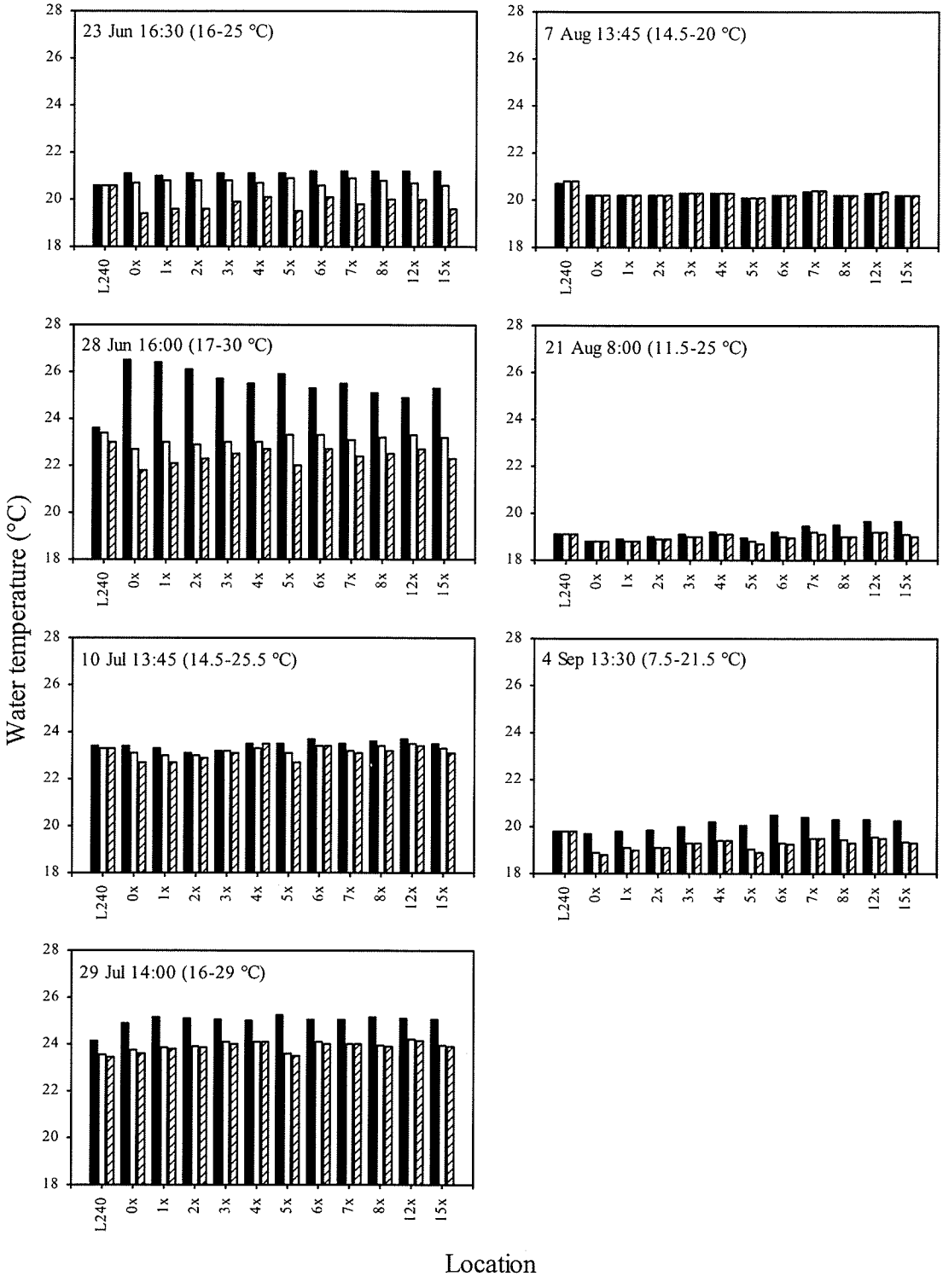

Figure II-1. Water temperatures of the mesocosms and Lake 240 at a depth of 0 m (solid bars), 1 m (open bars), and 2 m (striped bars), shown for each sampling date. The start time of sampling and the range in air temperatures on the sample day are indicated on each panel. Because water levels in Mesocosms 2x, 3x, 4x, 6x, 7x, 8x, 12x, 15x were less than 2 m on 21 August and 4 September, the 2 m measurement was taken just above the sediment surface.

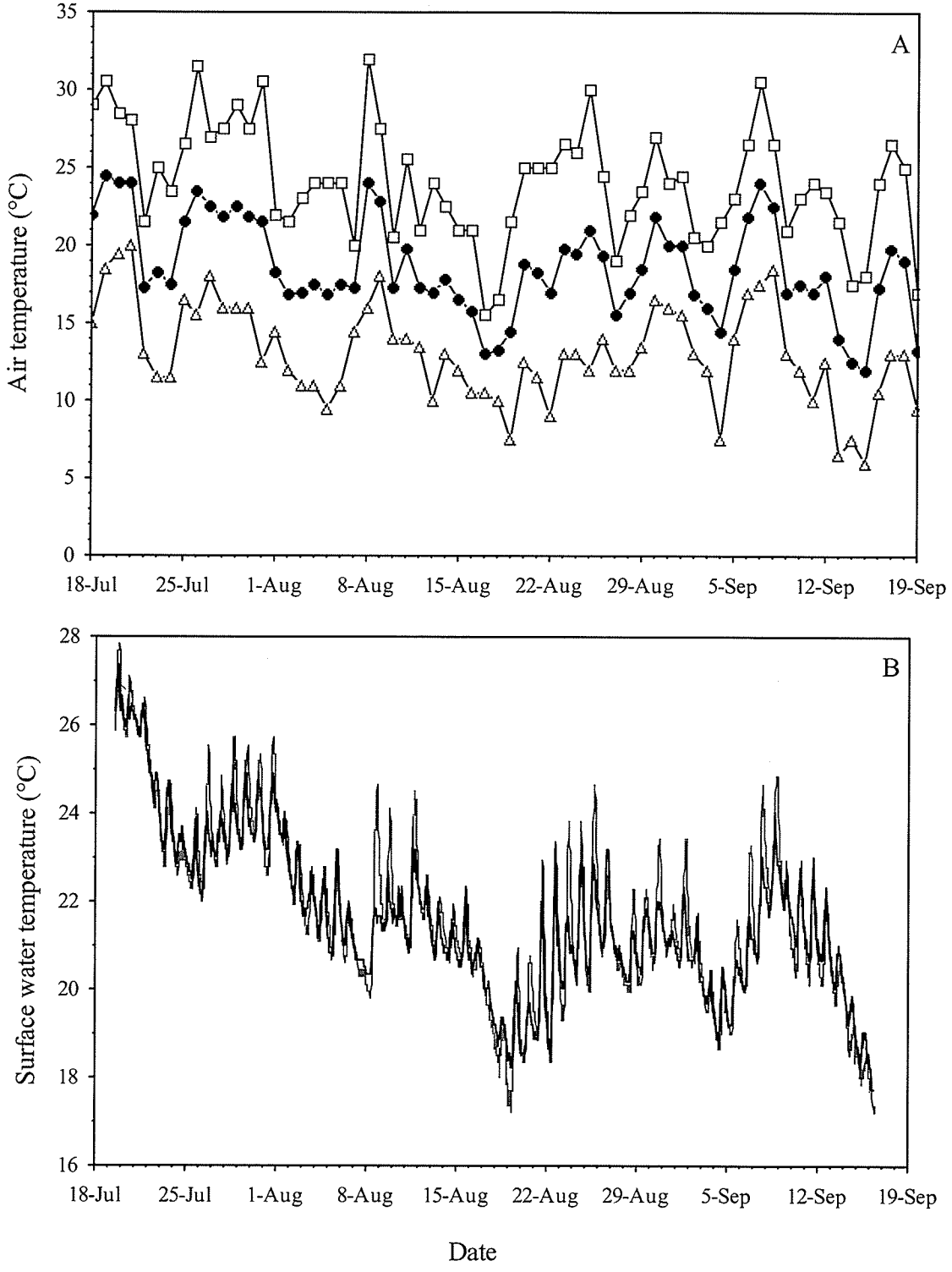

Figure II-2. Daily minimum (open triangles), maximum (open squares), and mean (solid circles) air temperatures at the Lake 239 meteorological station (K. Beaty, unpubl. data.) (A); surface water temperatures in Mesocosm 2x (striped line) and Lake 240 (solid line) every 30 min (B).

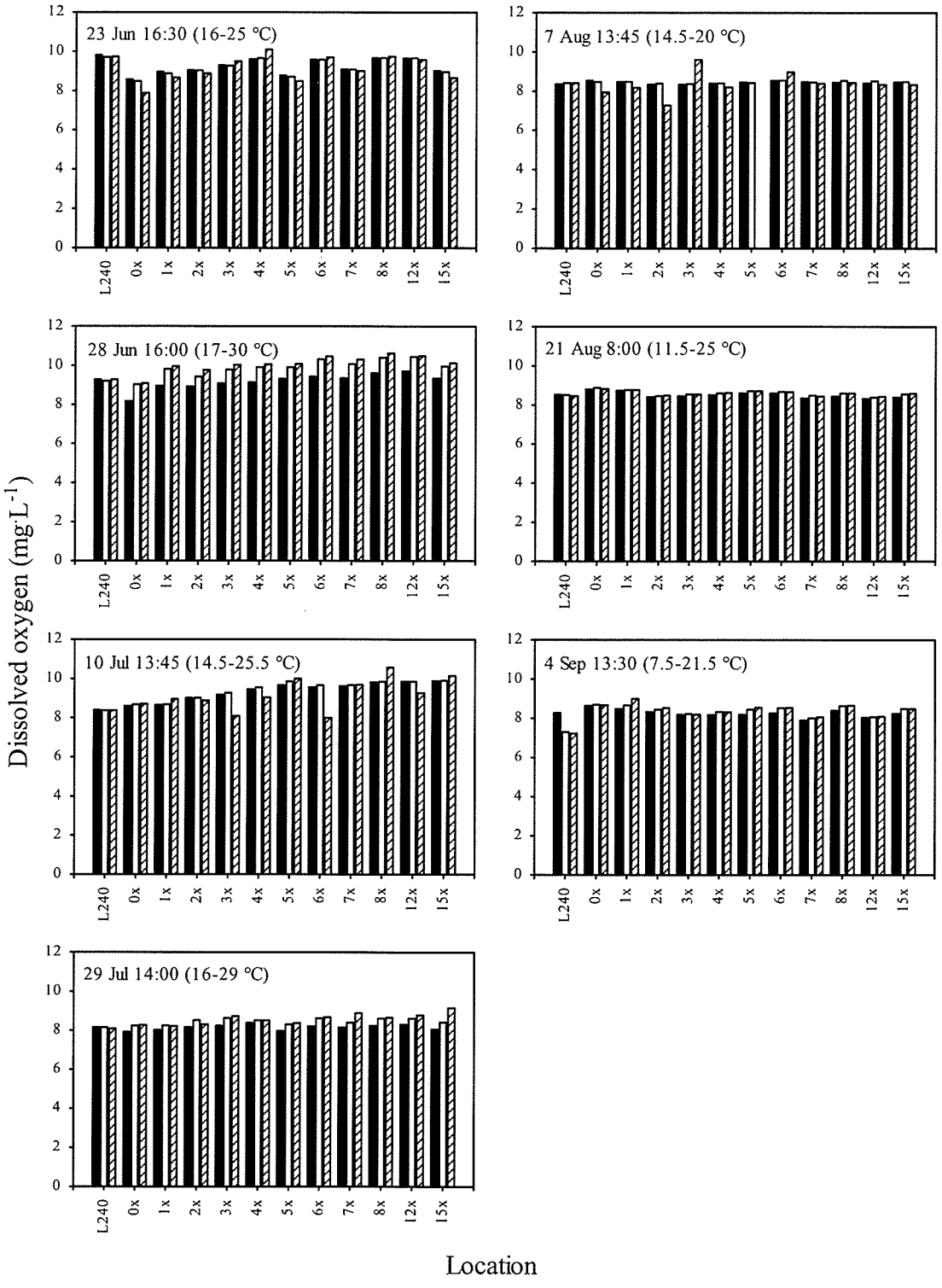

Figure II-3. Dissolved oxygen concentration in the mesocosms and Lake 240 at a depth of 0 m (solid bars), 1 m (open bars), and 2 m (striped bars), shown for each sampling date. The start time of sampling and the range in air temperatures on the sampling day are indicated on each panel. Because water levels in Mesocosms 2x, 3x, 4x, 6x, 7x, 8x, 12x, 15x were less than 2 m on 21 August and 4 September, the 2 m measurement was taken just above the sediment surface.

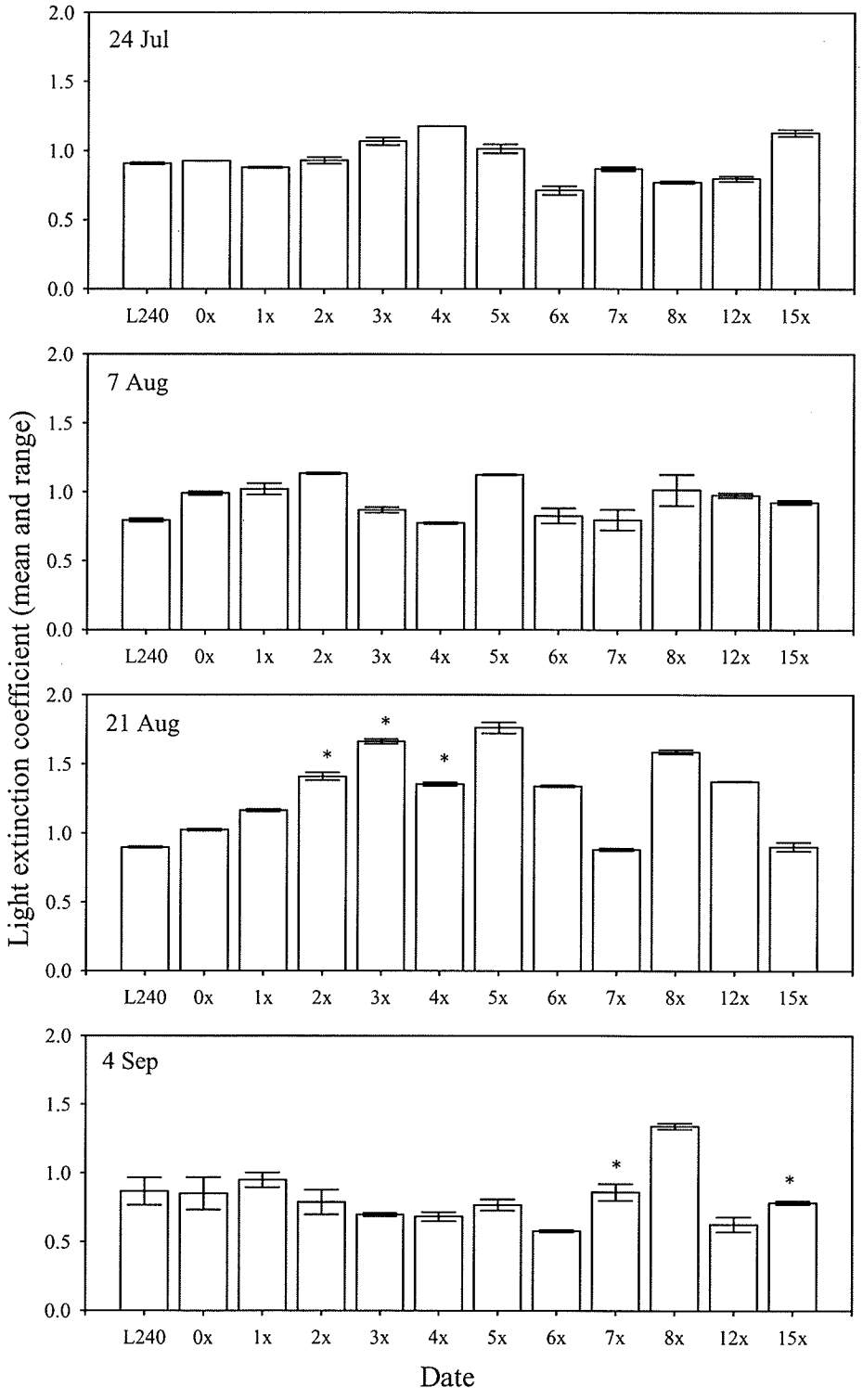

Figure II-4. Light extinction coefficients (mean and range) in the mesocosms and Lake 240 on each sampling date. Two profiles were conducted in each mesocosm on every sampling date. An asterisk indicates that the slope of the relationship of depth vs. ln(light intensity) was not significant (i.e. $p > 0.05$).

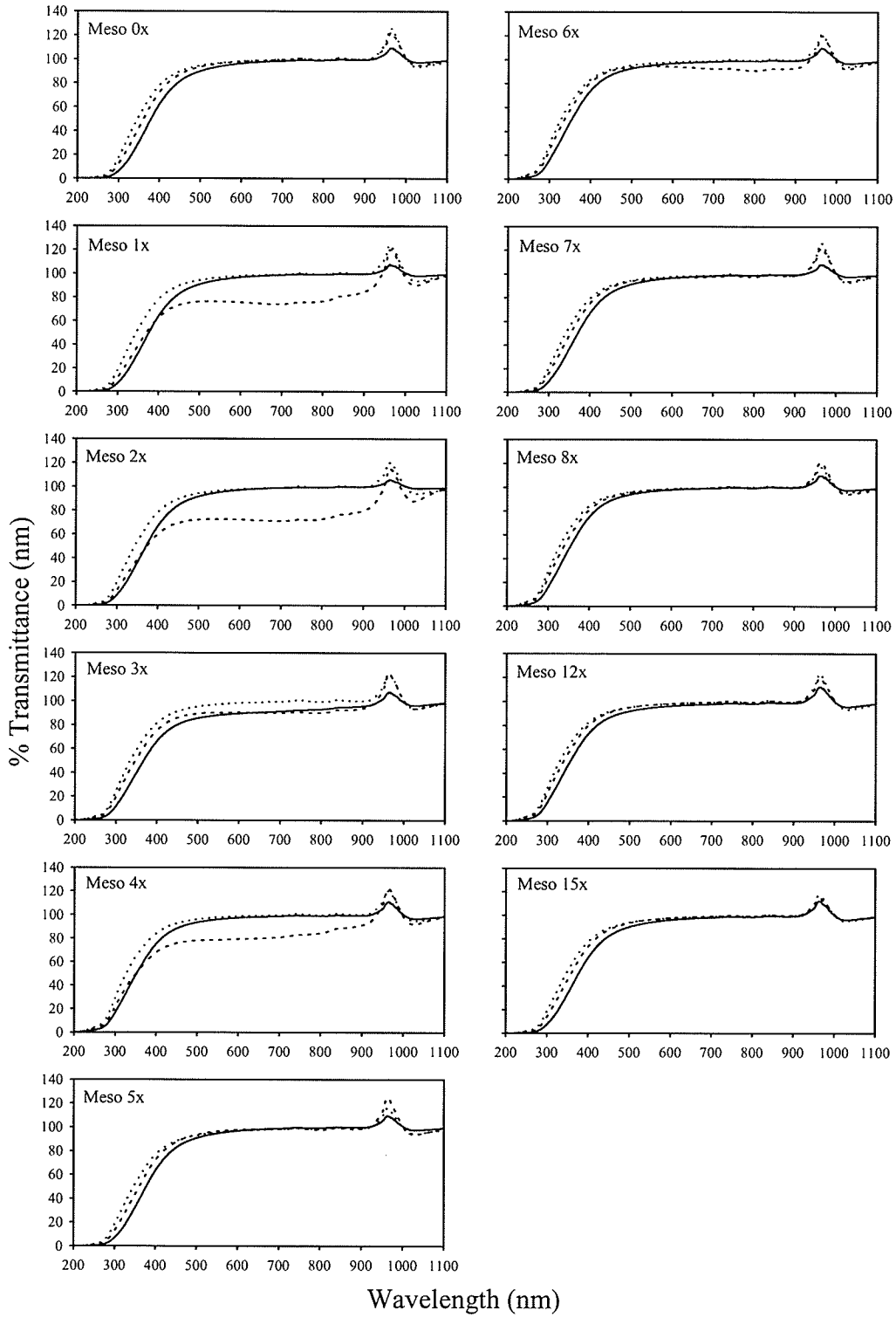

Figure II-5. Spectral scans of unfiltered water collected from the mesocosms on 25 June (solid line), 23 July (dashed line), and 20 August (dotted line).

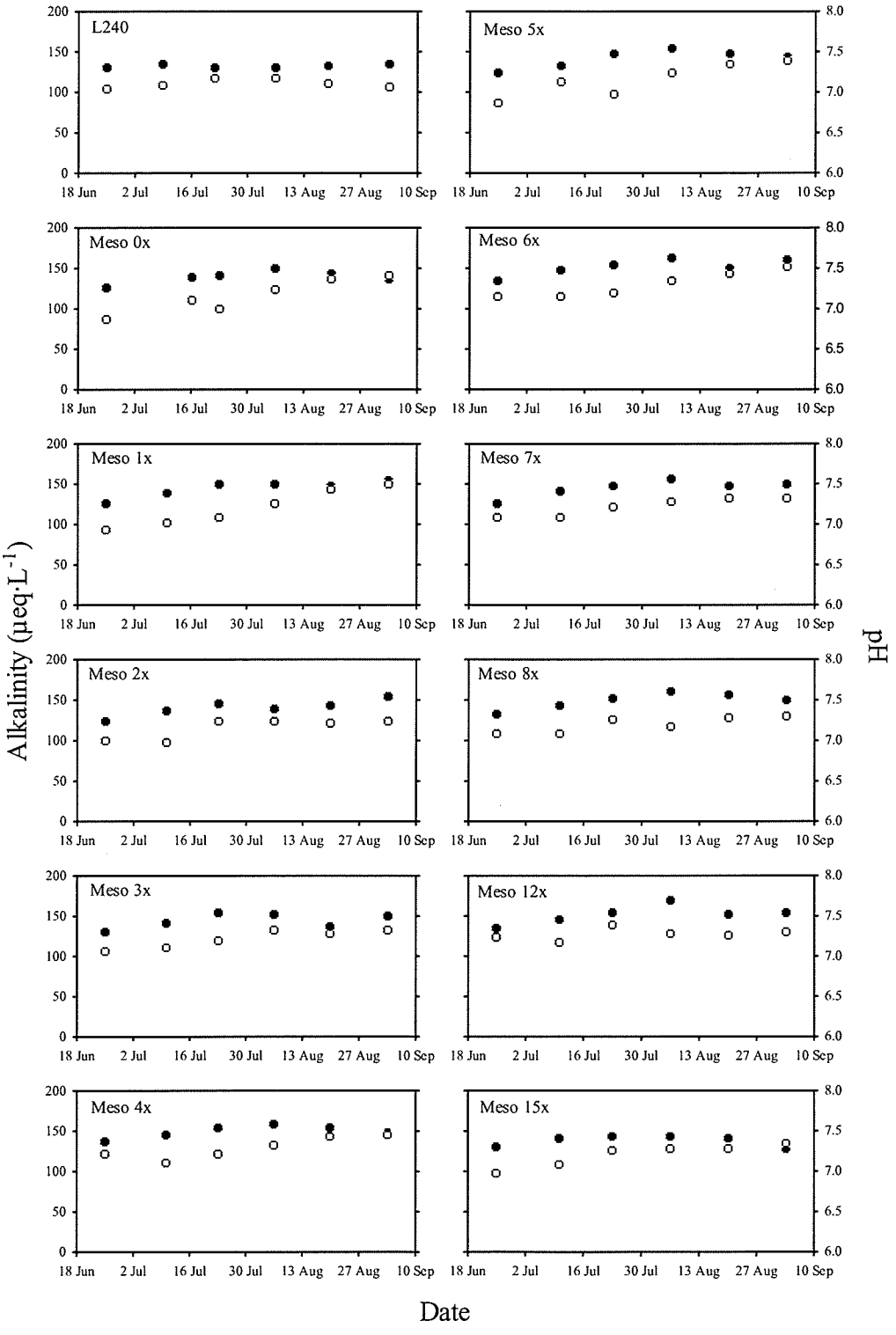

Figure II-6. Temporal changes in alkalinity (solid circles; left axis) and pH (open circles; right axis) in each mesocosm and Lake 240.

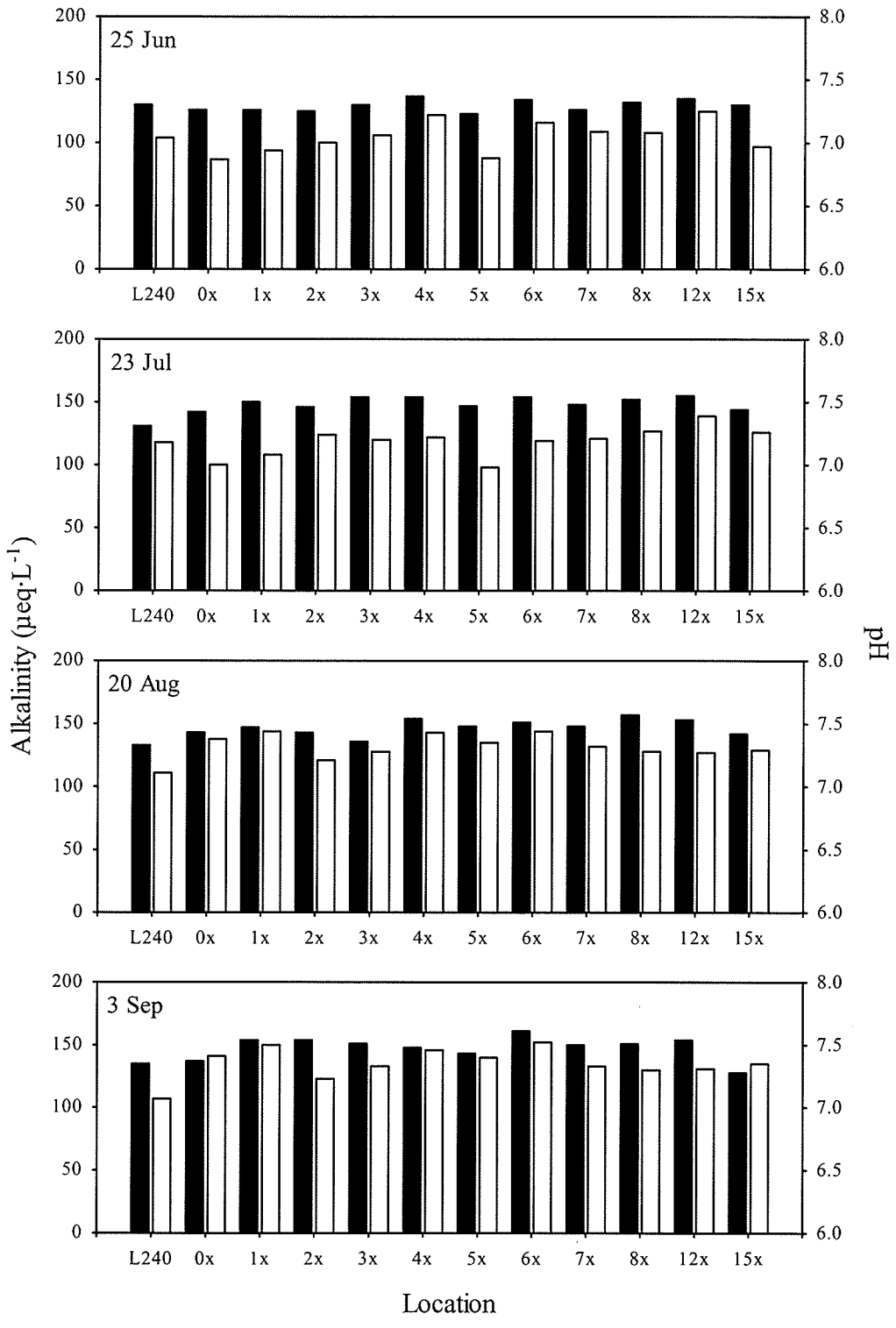

Figure II-7. Comparison of alkalinity (solid bars; left axis) and pH (open bars; right axis) among the mesocosms and Lake 240 on four sampling dates.

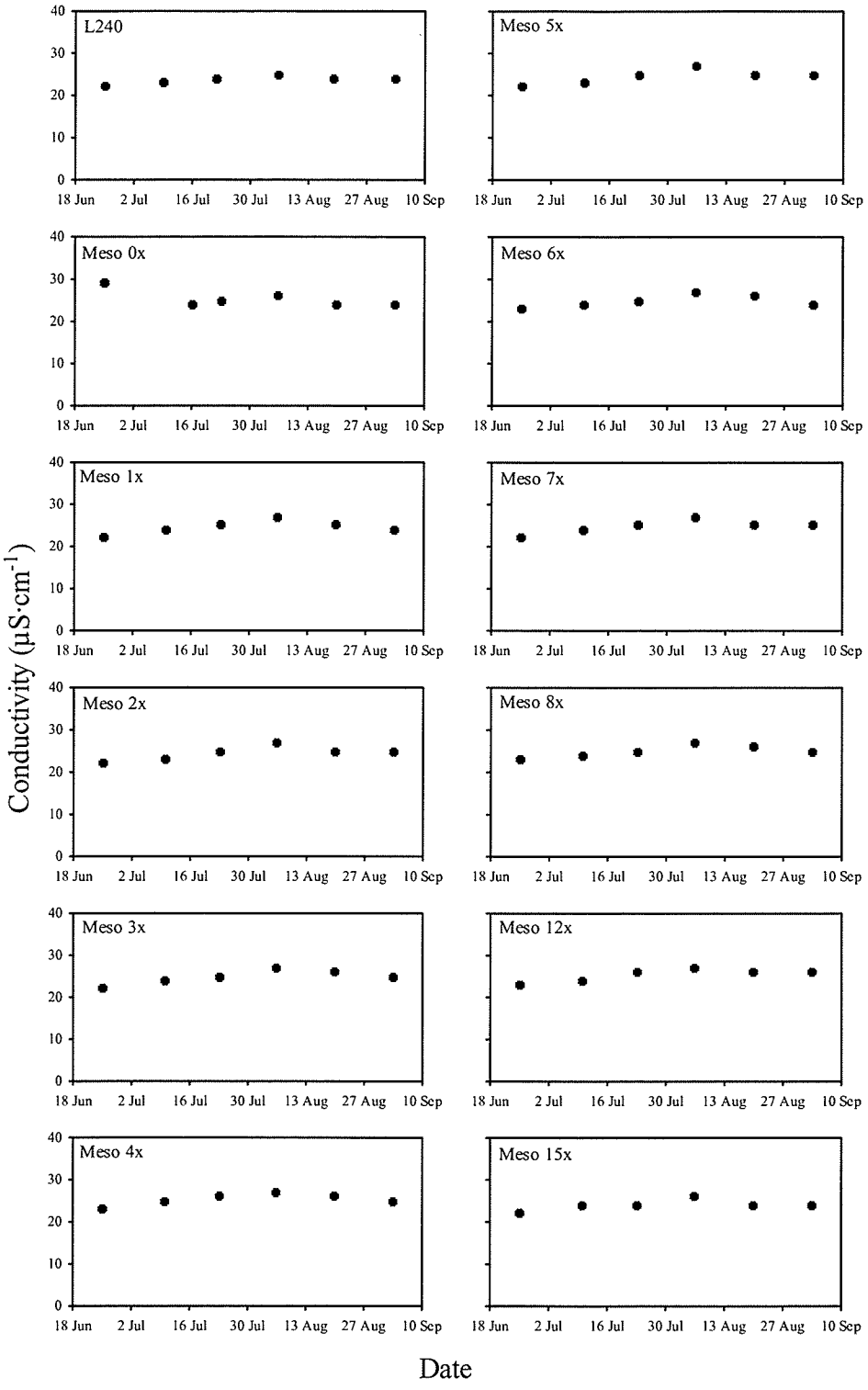

Figure II-8. Temporal changes in conductivity in each mesocosm and Lake 240.

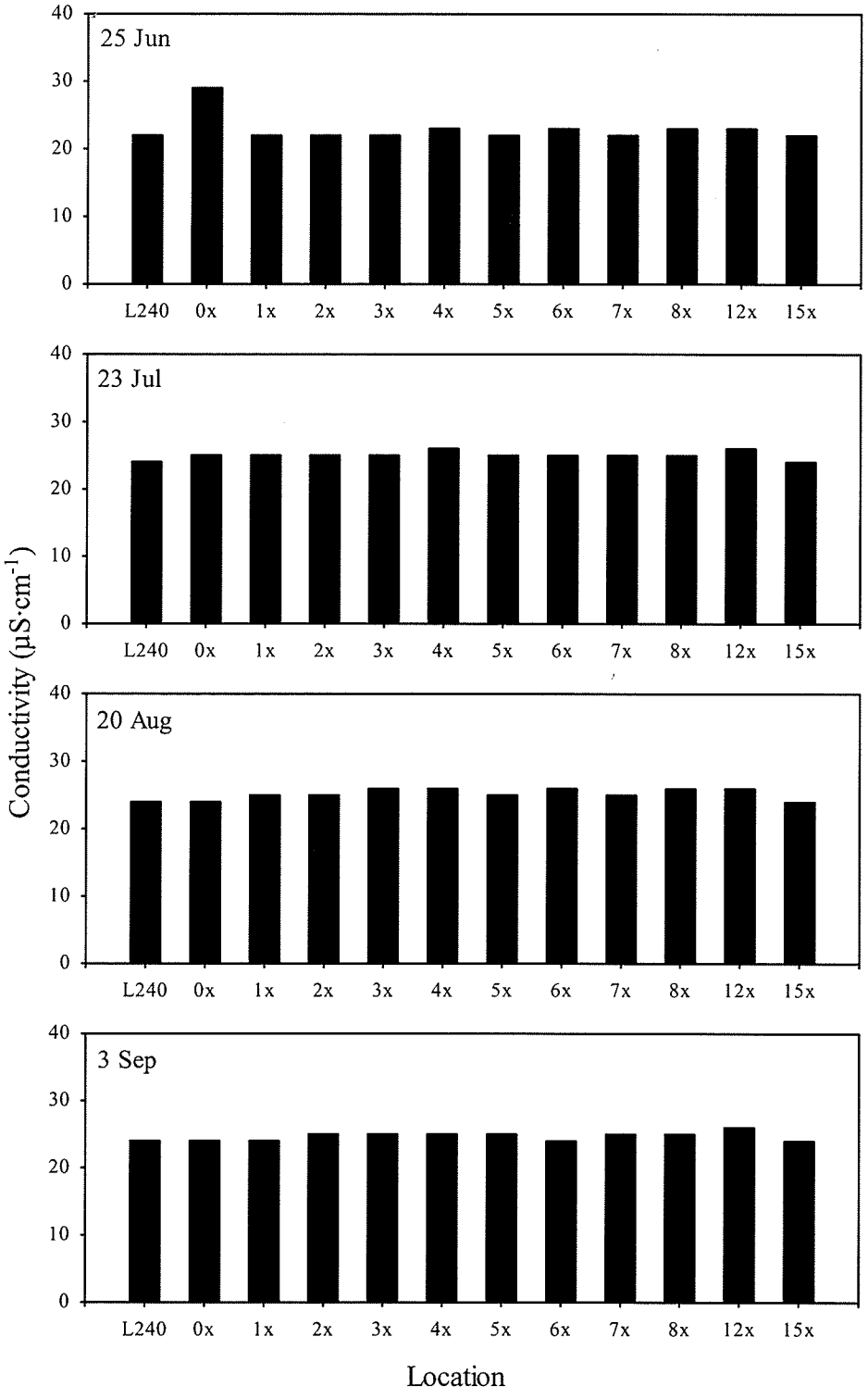

Figure II-9. Comparison of conductivity among the mesocosms and Lake 240 on four sampling dates.

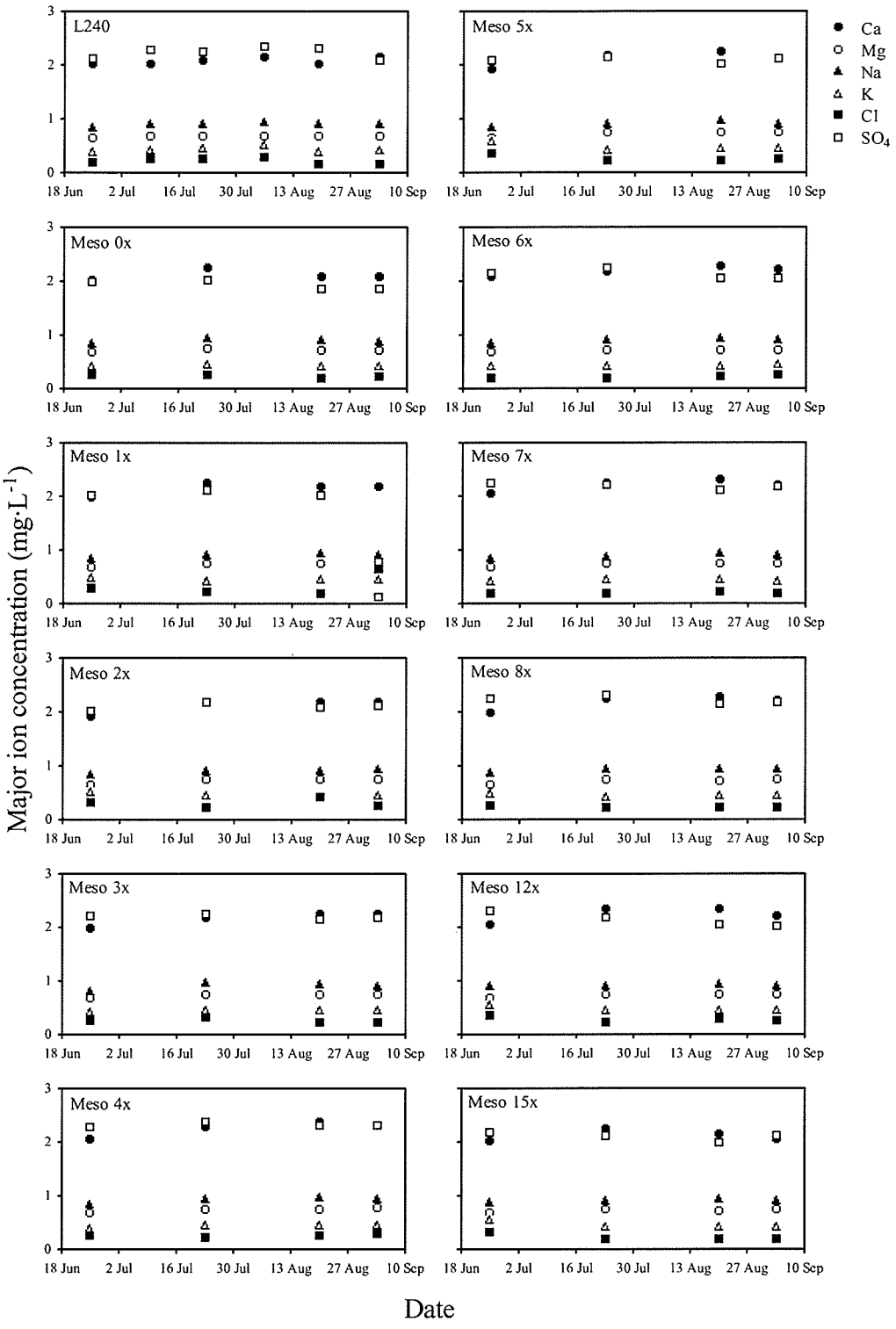

Figure II-10. Temporal changes in major ions in each mesocosm and Lake 240.

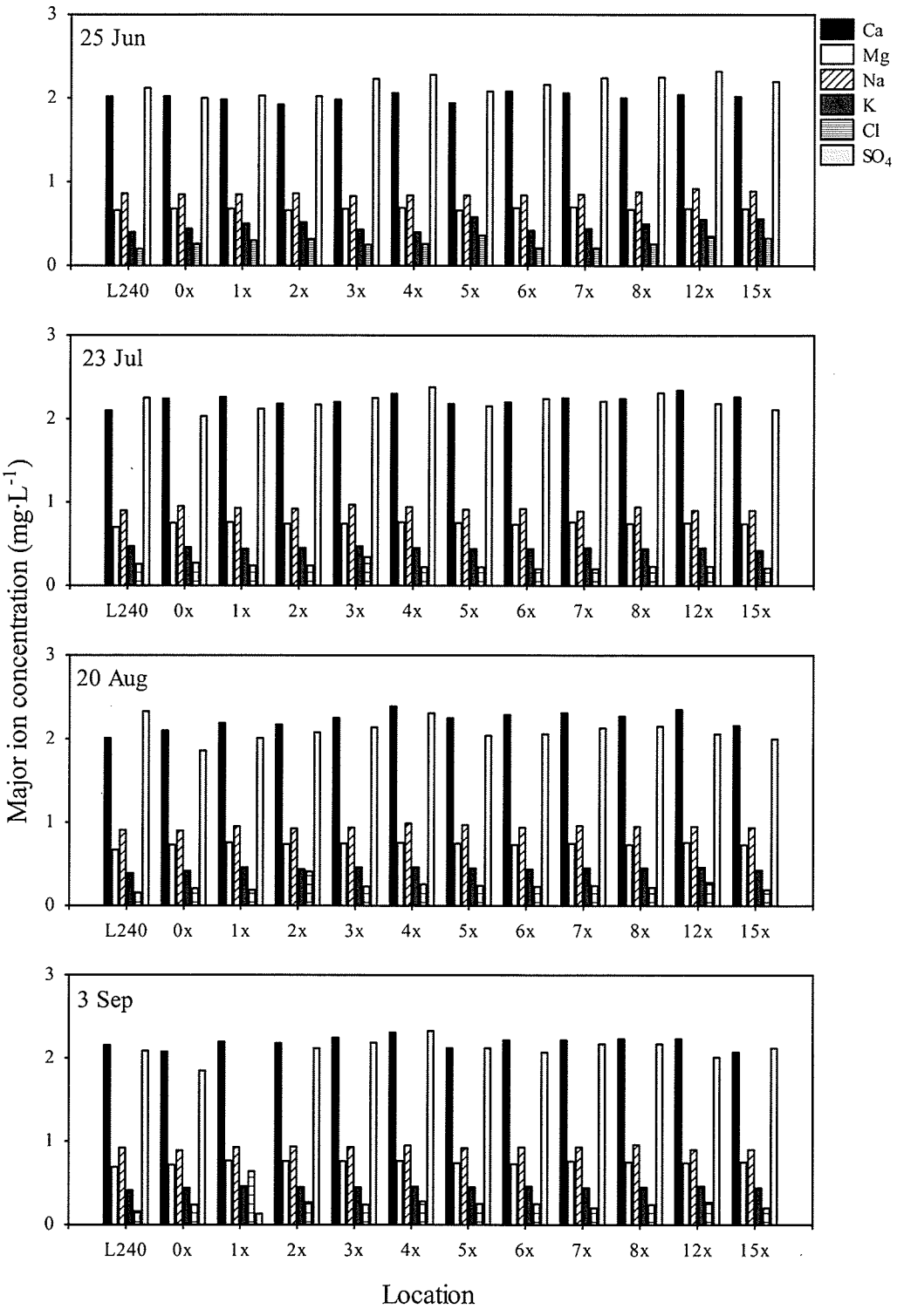

Figure II-11. Comparison of major ions among the mesocosms and Lake 240 on four sampling dates.

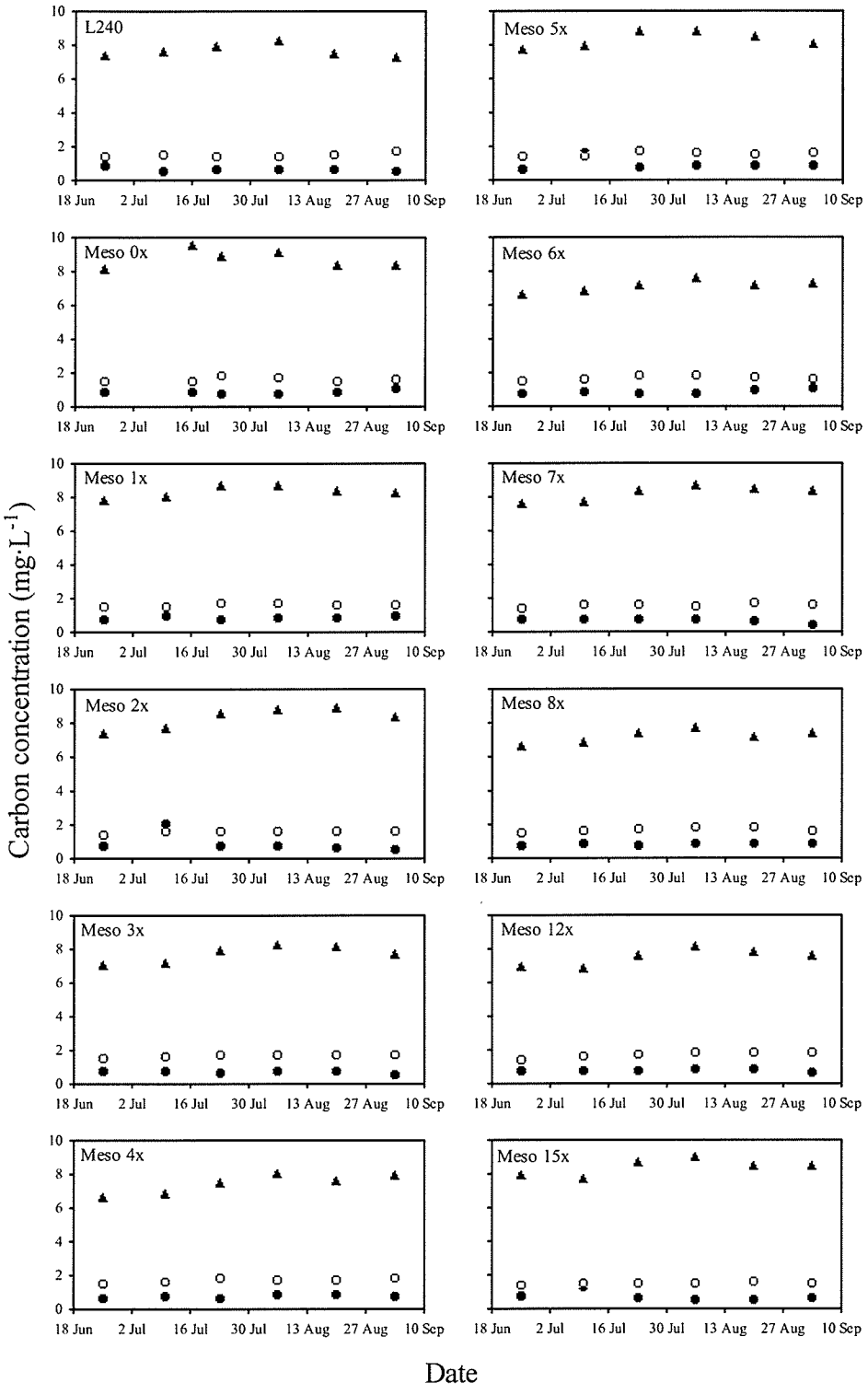

Figure II-12. Temporal changes in suspended carbon (solid circles), dissolved inorganic carbon (open circles), and dissolved organic carbon (solid triangles) in each mesocosm and Lake 240.

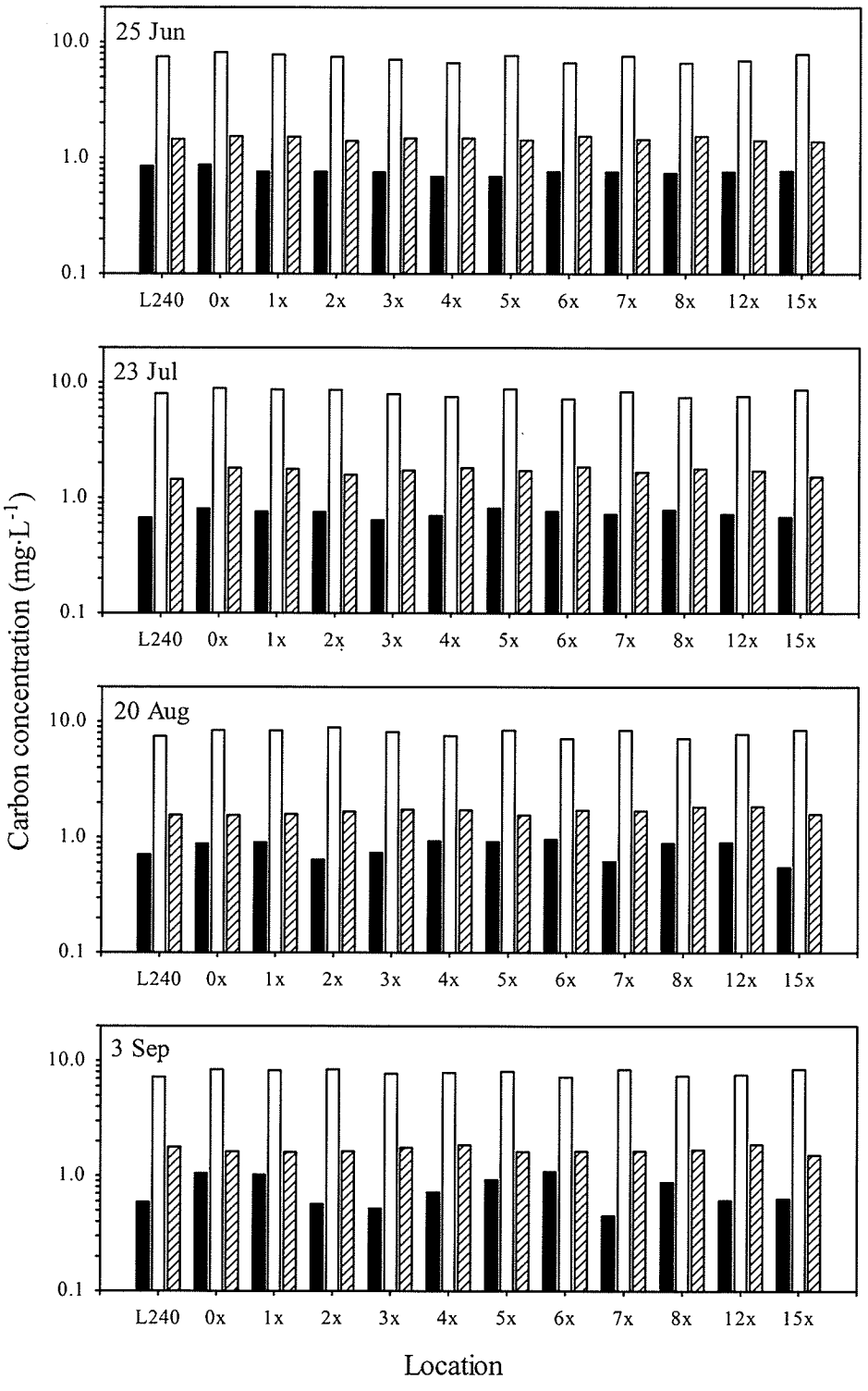

Figure II-13. Comparison of suspended carbon (solid bars), dissolved organic carbon (open bars), and dissolved inorganic carbon (striped bars) among the mesocosms and Lake 240 on four sampling dates. Note that Y-axes are on a log scale.

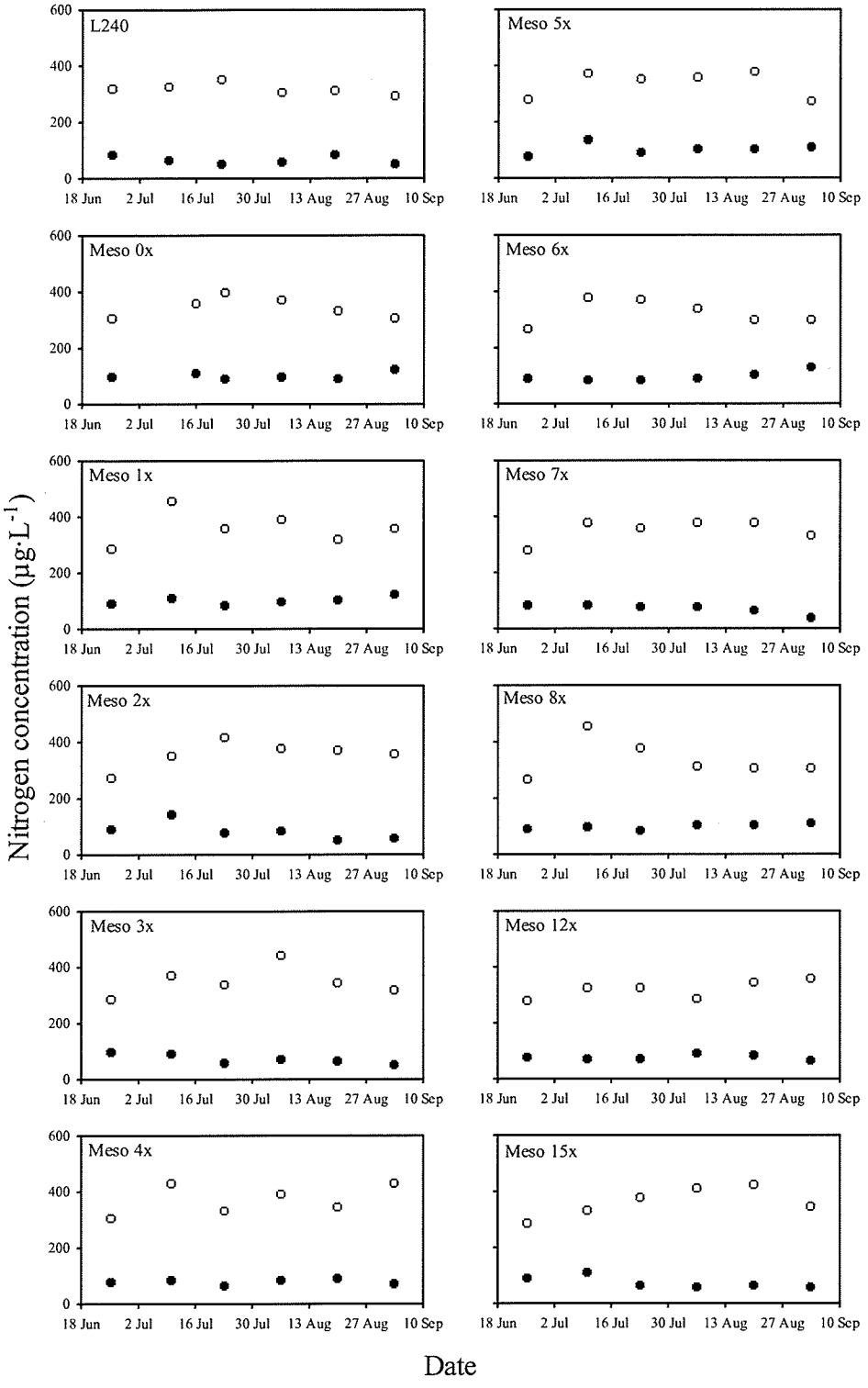

Figure II-14. Temporal changes in suspended nitrogen (solid circles) and dissolved nitrogen (open circles) in each mesocosm and Lake 240.

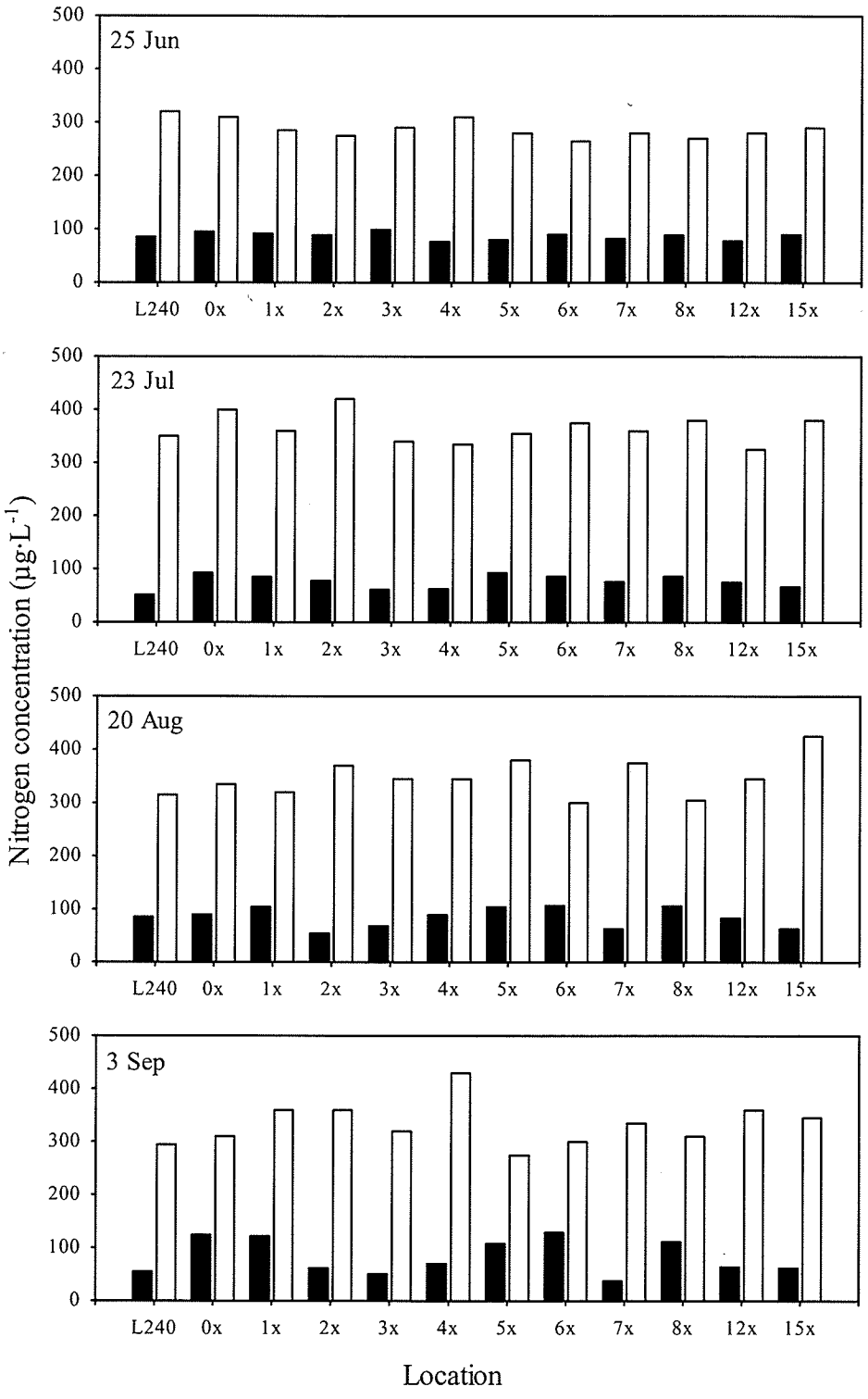

Figure II-15. Comparison of suspended nitrogen (solid bars) and dissolved nitrogen (open bars) among the mesocosms and Lake 240 on four sampling dates.

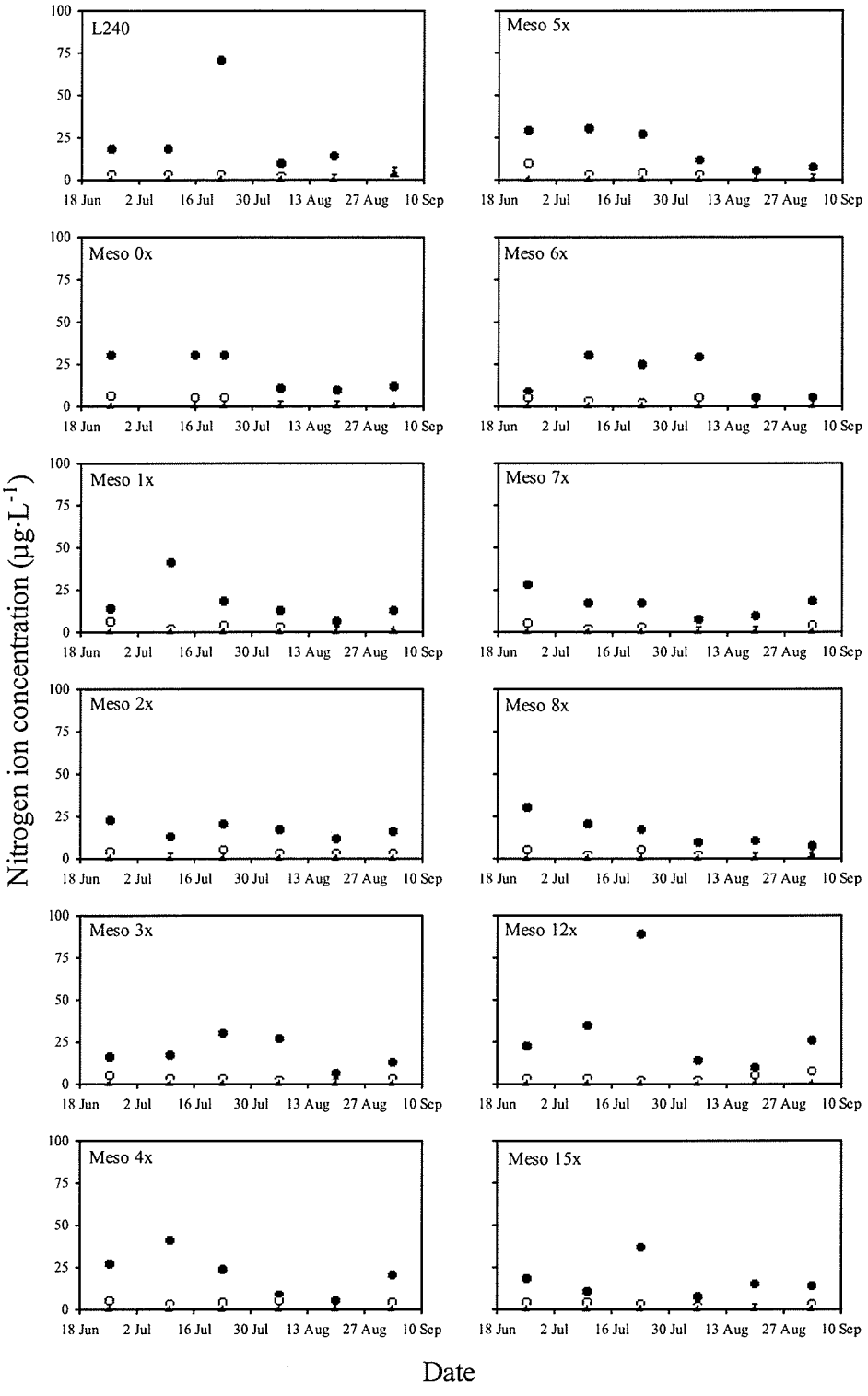

Figure II-16. Temporal changes ammonia (solid circles), nitrate (open circles), and nitrite (solid triangles) in each mesocosm and Lake 240.

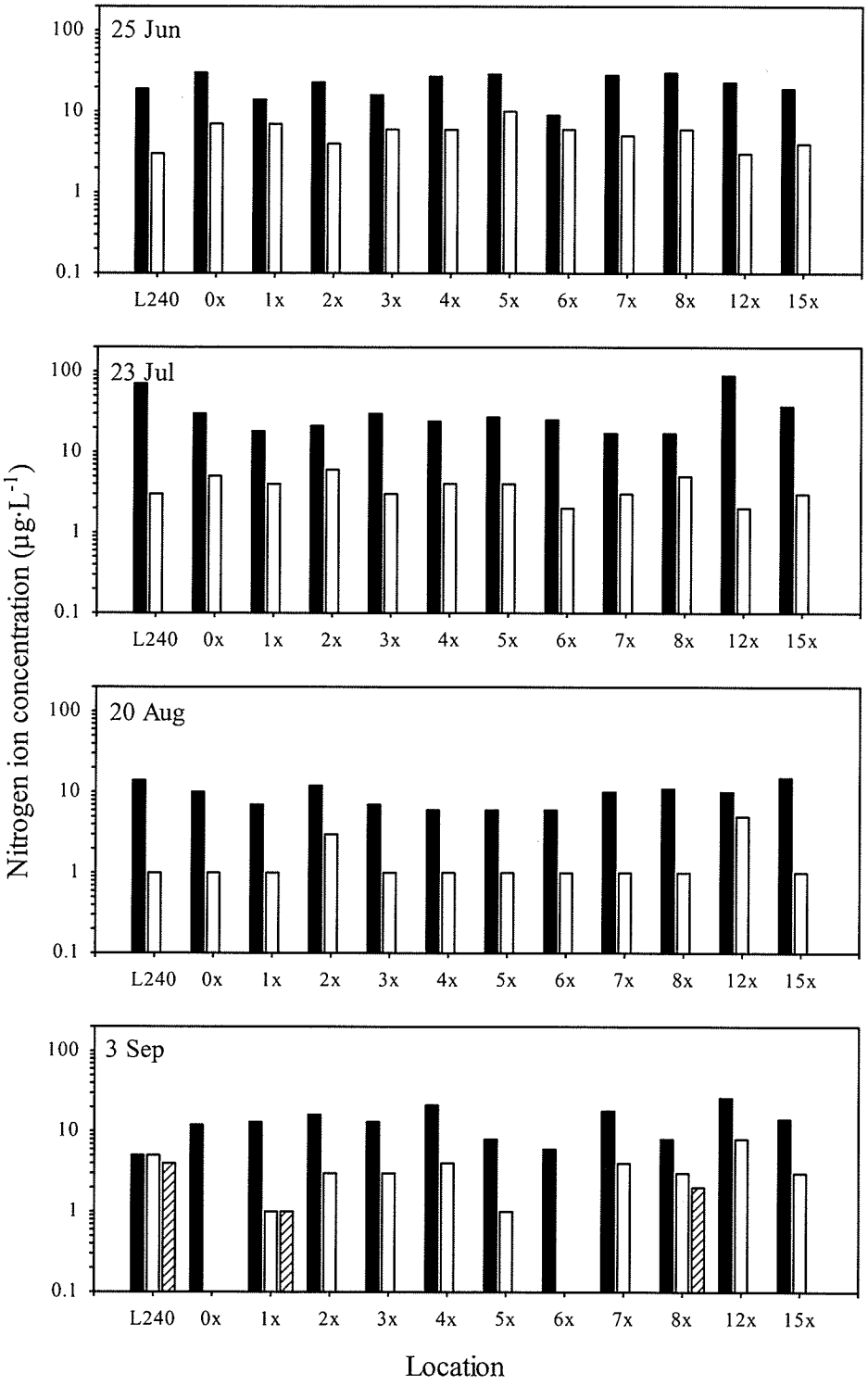

Figure II-17. Comparison of ammonia (solid bars), nitrate (open bars), and nitrite (striped bars) among the mesocosms and Lake 240 on four sampling dates. Nitrite concentrations were below detection limits except for three mesocosms on 3 September. Note that Y-axes are on a log scale.

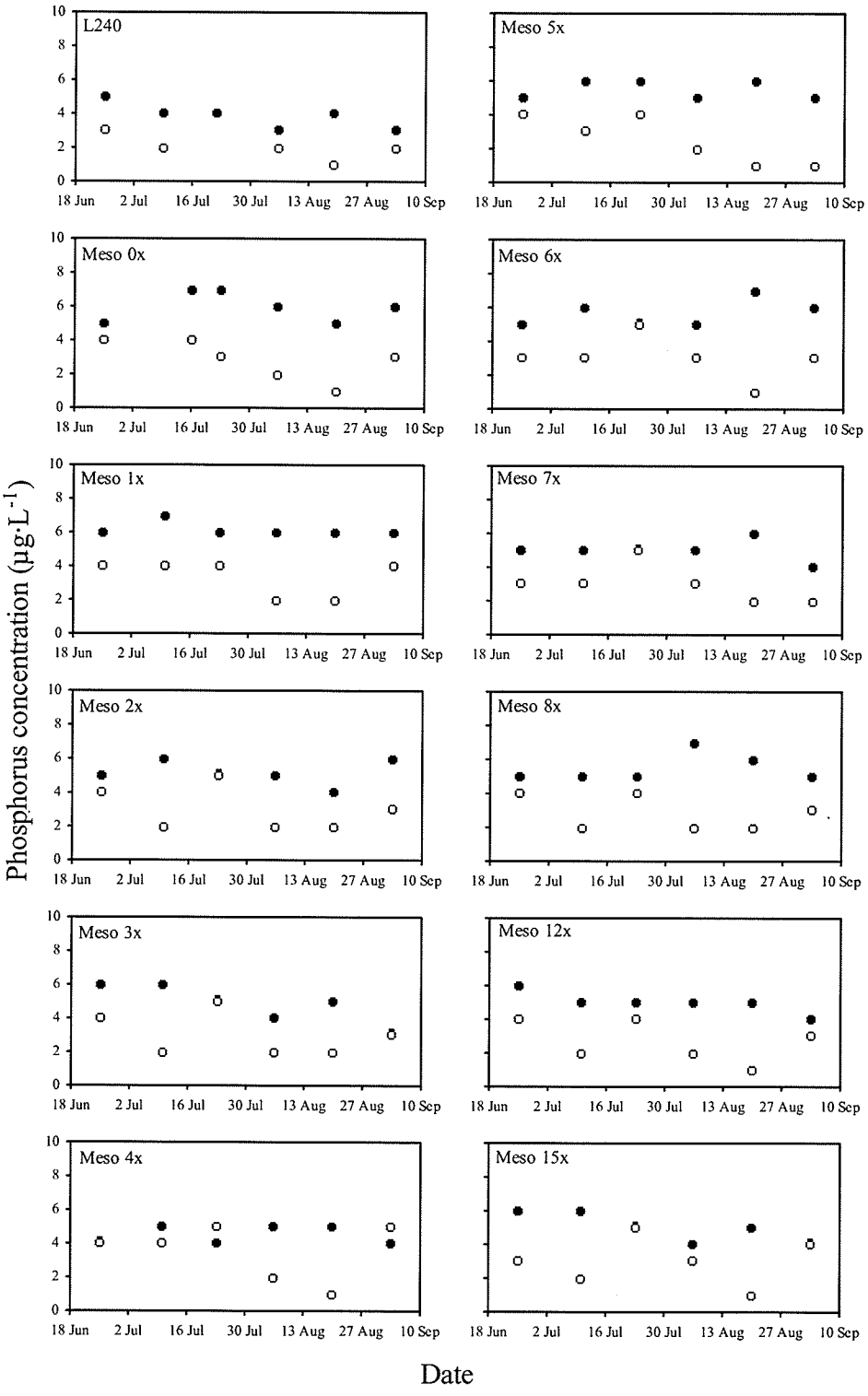

Figure II-18. Temporal changes suspended phosphorus (solid circles) and dissolved phosphorus (open circles) in each mesocosm and Lake 240.

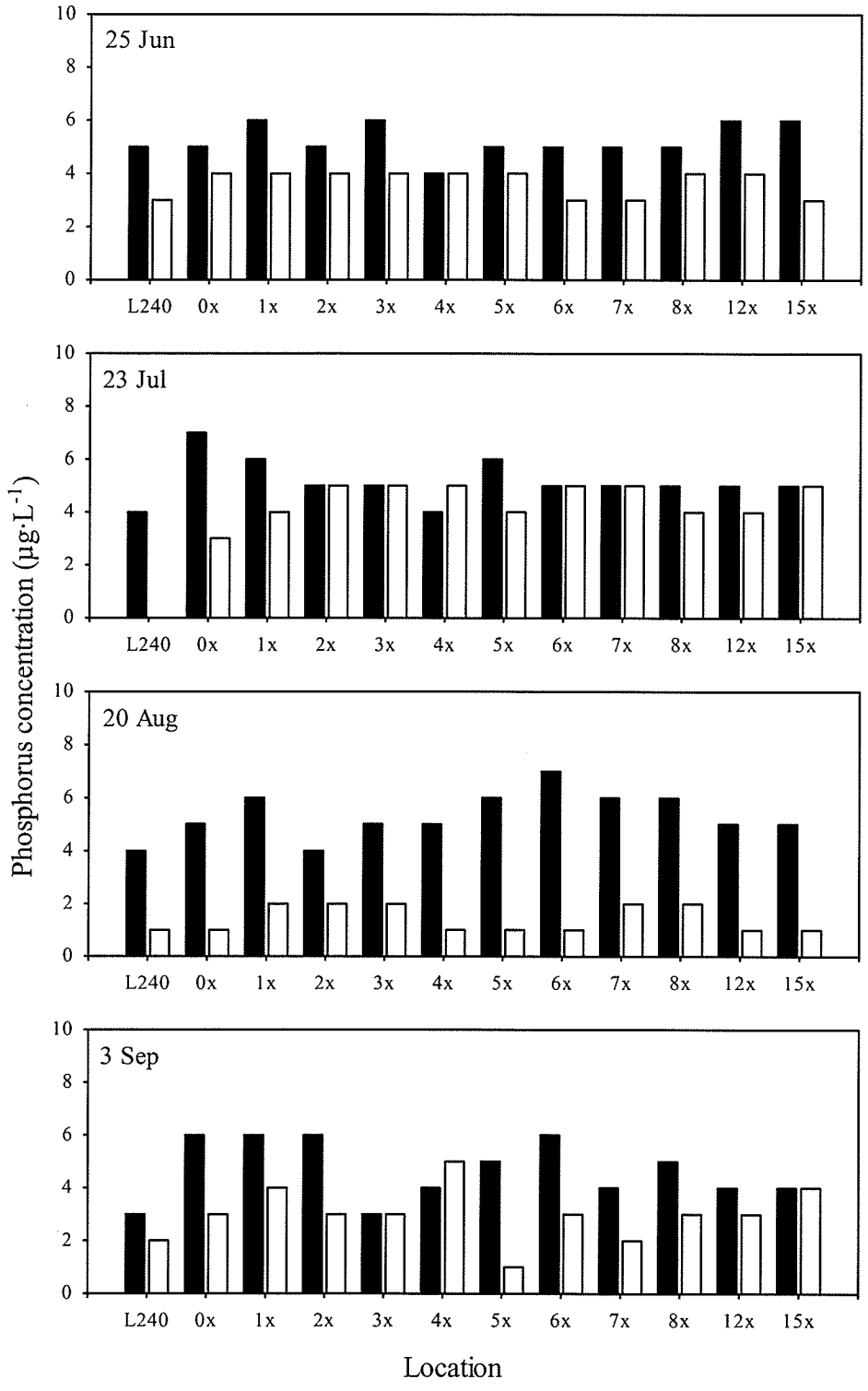

Figure II-19. Comparison of suspended phosphorus (solid bars) and dissolved phosphorus (open bars among the mesocosms and Lake 240 on four sampling dates.

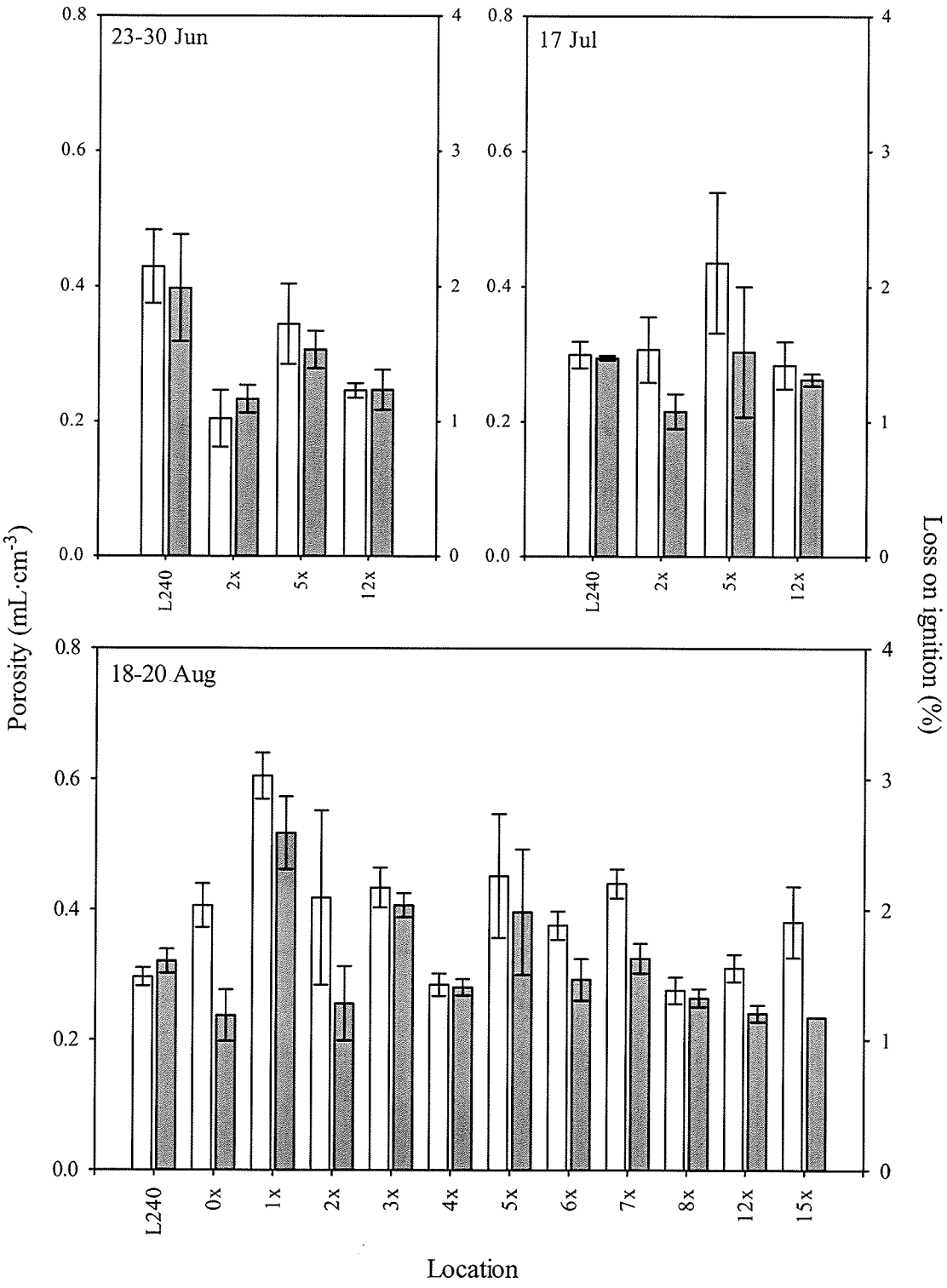

Figure II-20. Mean (± SE) porosity (open bars; left axis) and loss on ignition (solid bars; right axis) of surface sediments (0-2 cm) in the mesocosms and Lake 240 during three sampling periods.

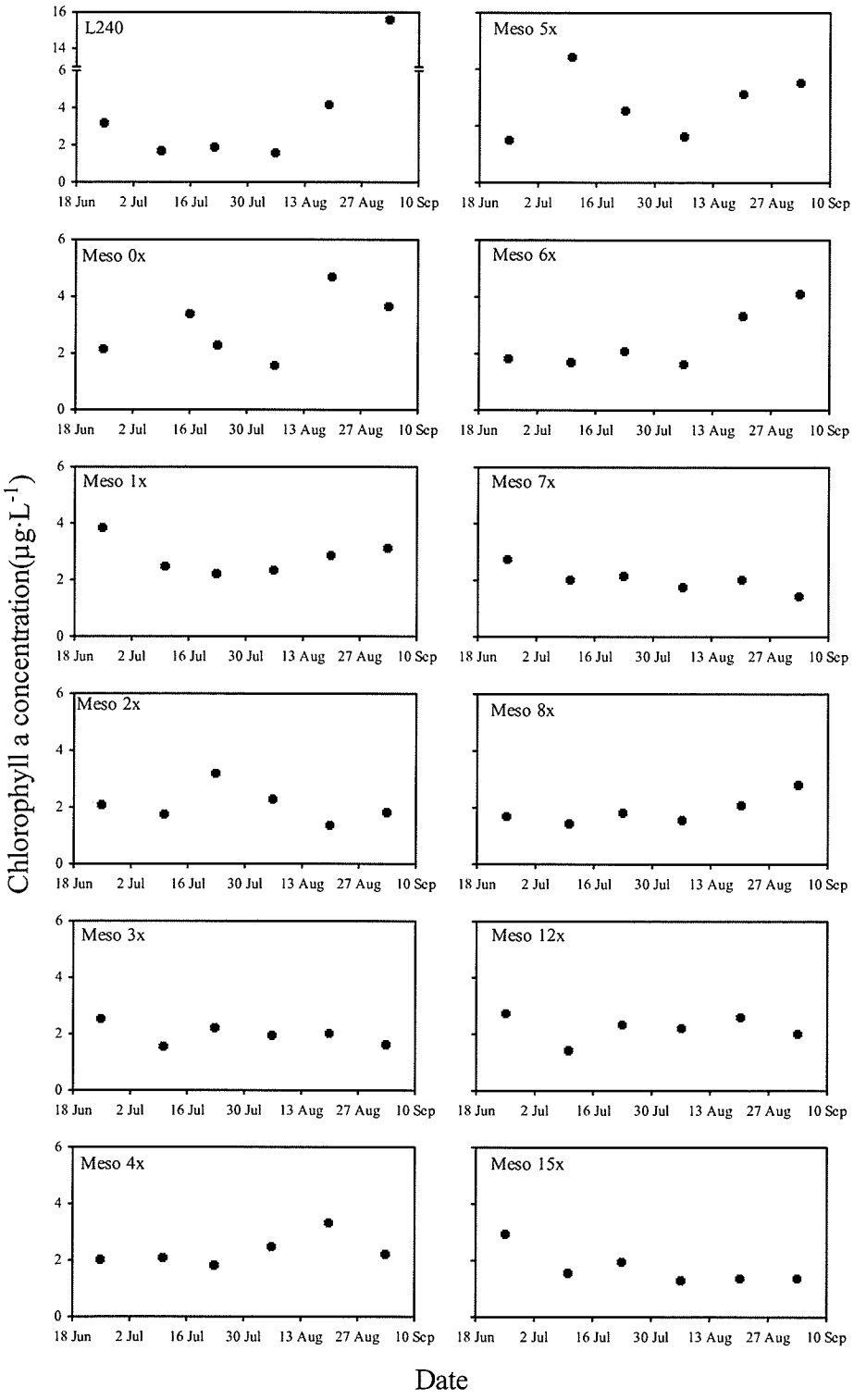

Figure II-21. Chlorophyll *a* concentrations (an indicator of phytoplankton biomass) in Lake 240 and each mesocosm over time. Note the scale break on the top left panel.

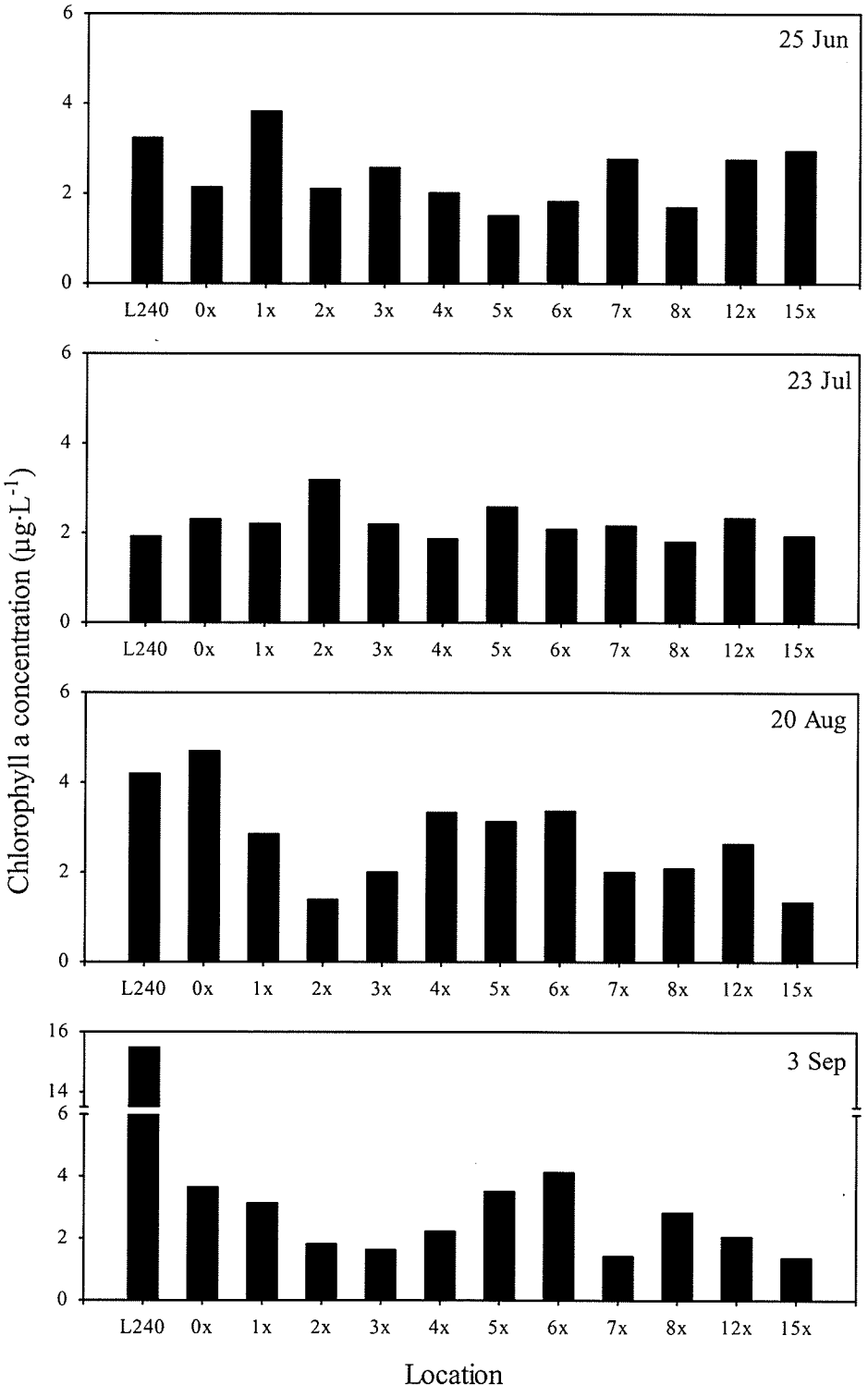

Figure II-22. Chlorophyll *a* concentrations in Lake 240 and each mesocosm on four sampling dates. Note the scale break on the bottom panel.

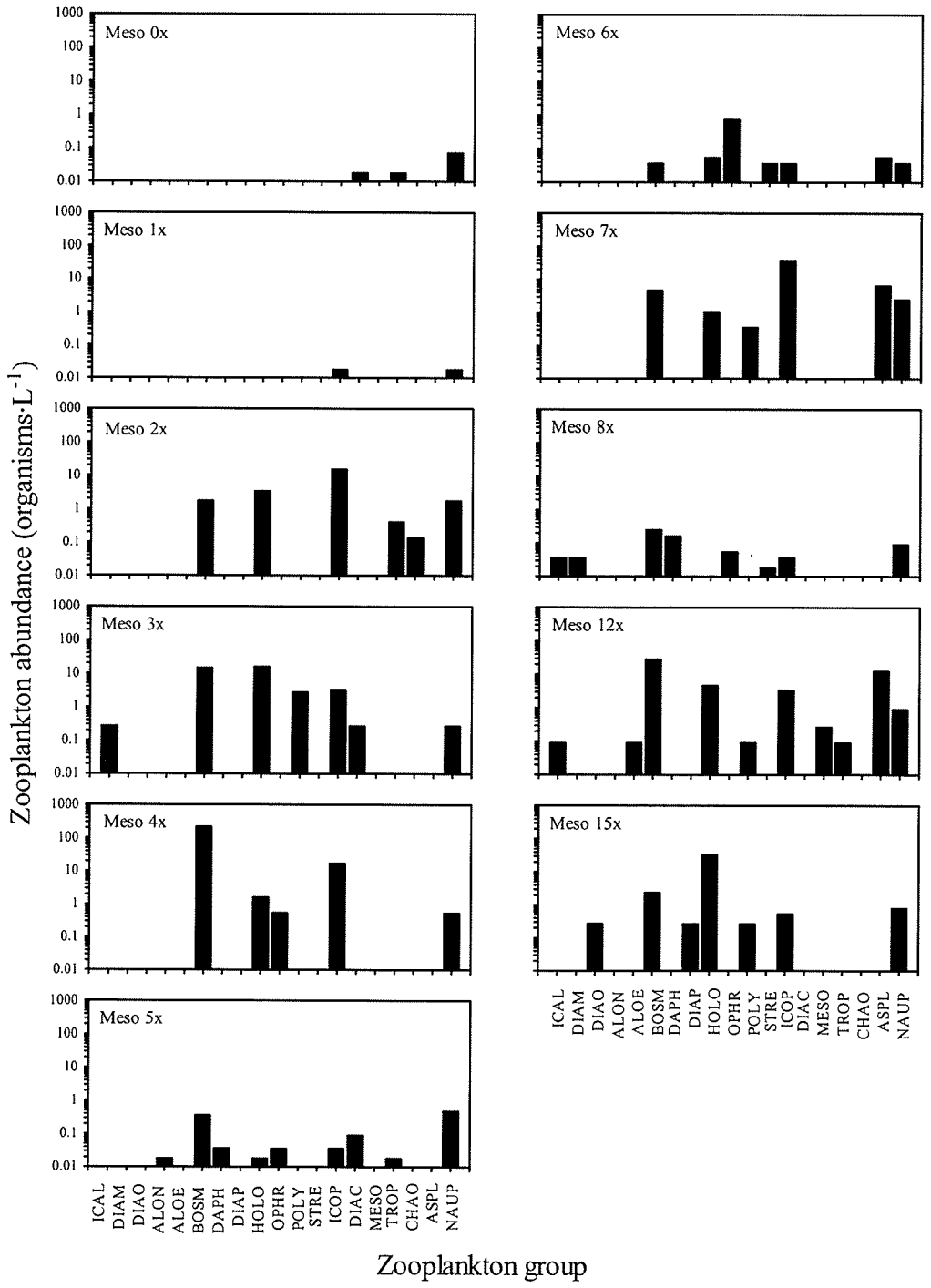

Figure II-23. Abundance of different zooplankton groups in each mesocosm. Samples were collected 29 – 30 September from a depth of 1m. Group codes: ICAL = Immature calanoid; DIAM = *Diaptomus minutus*; DIAO = *Diaptomus oregonensis*; ALON = *Alona* cf. *quadrangularis*; ALOE = *Alonella* sp.; BOSM = *Bosmina longirostris*; DAPH = *Daphnia galeata mendotae*; DIAP = *Diaphanosoma birgei*; HOLO = *Holopedium gibberum*; OPHR = *Ophryoxus gracilis*; POLY = *Polyphemus pediculus*; STRE = *Streblocerus serricaudatus*; ICOP = Immature cyclopoid; DIAC = *Diacyclops bicuspidatus thomasi*; MESO = *Mesocyclops edax*; TROP = *Tropocyclops extensus*; CHAO = *Chaoborus* sp.; ASPL = *Asplanchna* sp.; NAUP = Unidentified nauplius.

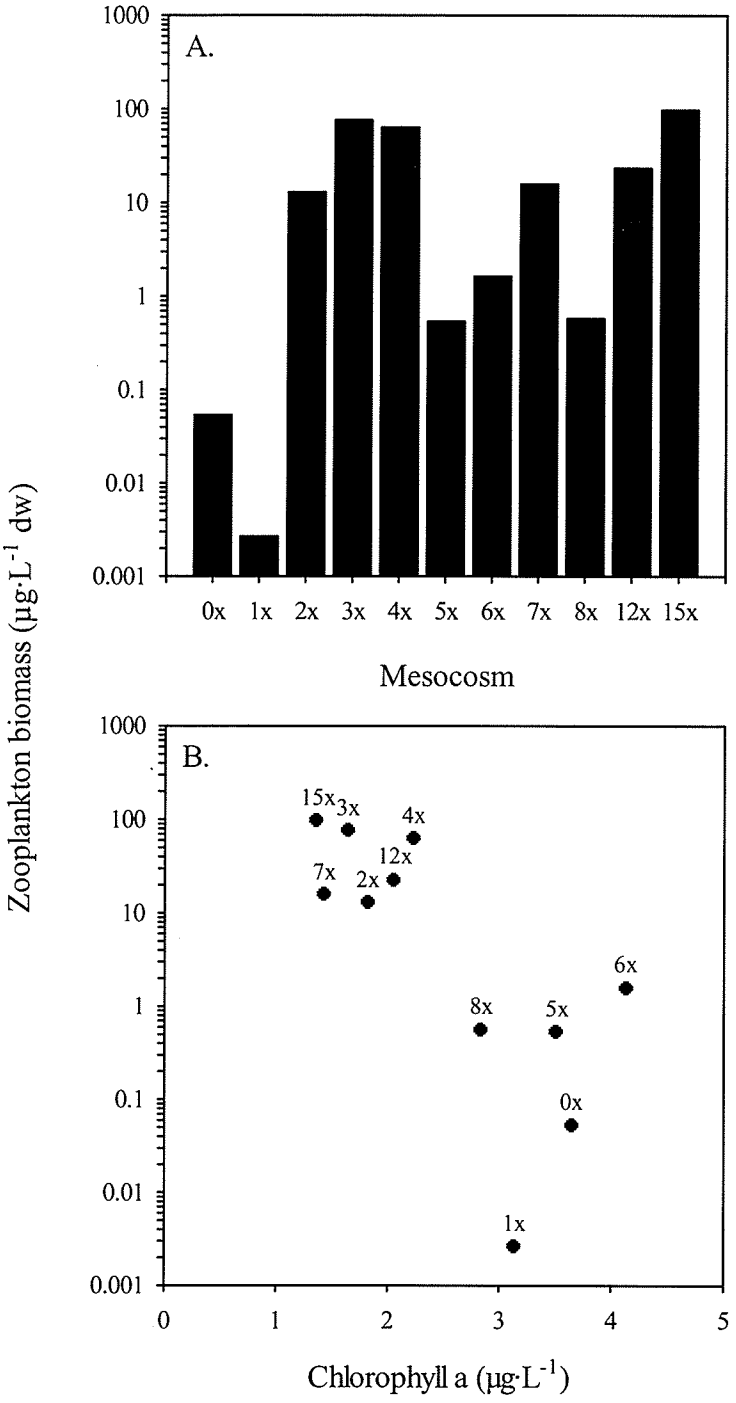

Figure II-24. Estimated zooplankton biomass in each mesocosm, shown in order of Hg loading rate (A). Relationship between chlorophyll *a* and zooplankton biomass in each mesocosm (B). The label above each point in panel B identifies the mesocosm.

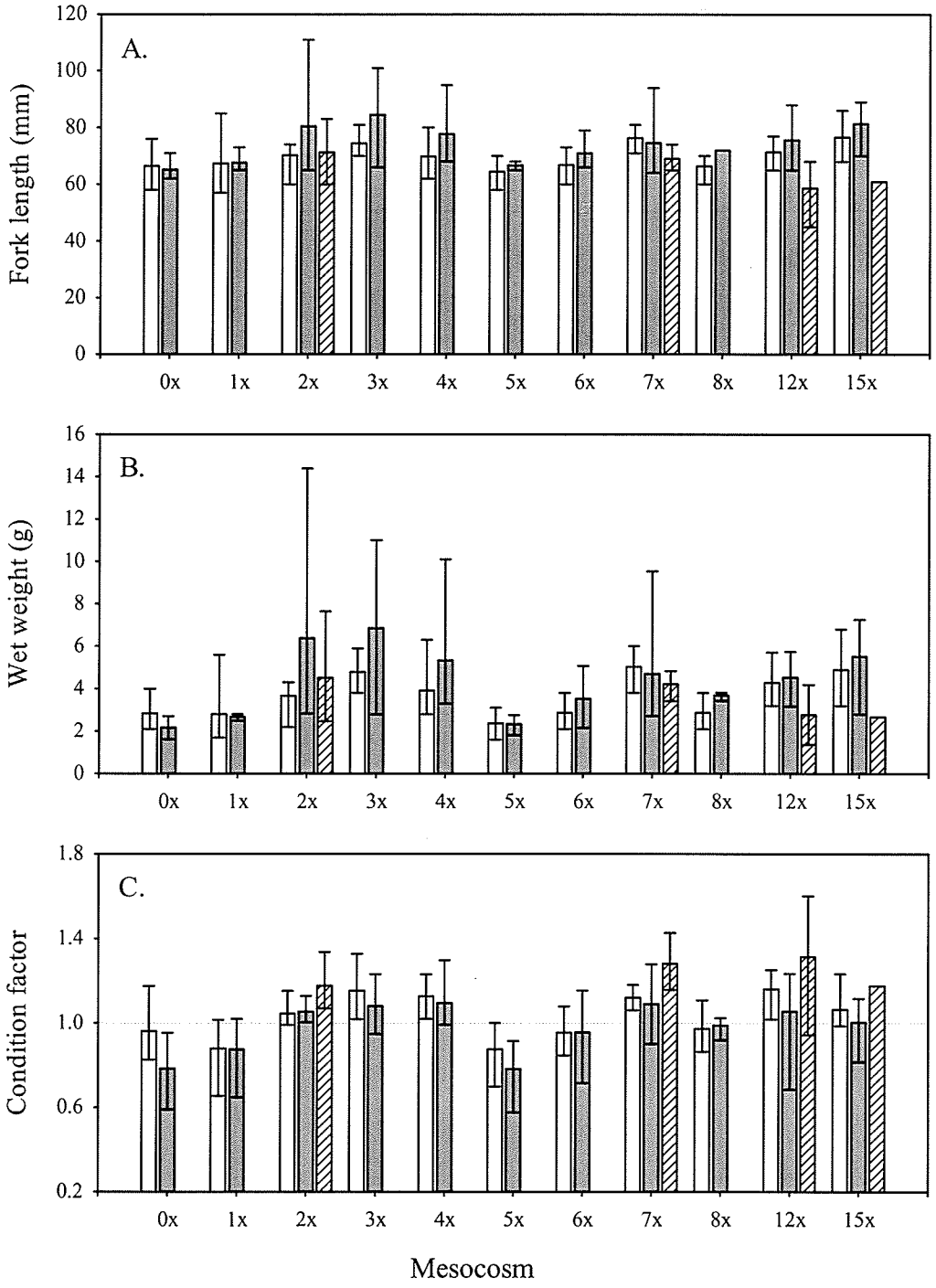

Figure II-25. Average (and range) in fork length (A), weight (B), and condition factor (C) of age 1+ fish captured between 31 July – 2 August (white bars), age 1+ fish captured between 4 – 16 September (grey bars), and age 0+ fish captured between 4 – 16 September (striped bars) in each mesocosm. Age 0+ fish were only captured from four mesocosms during the final sampling period.

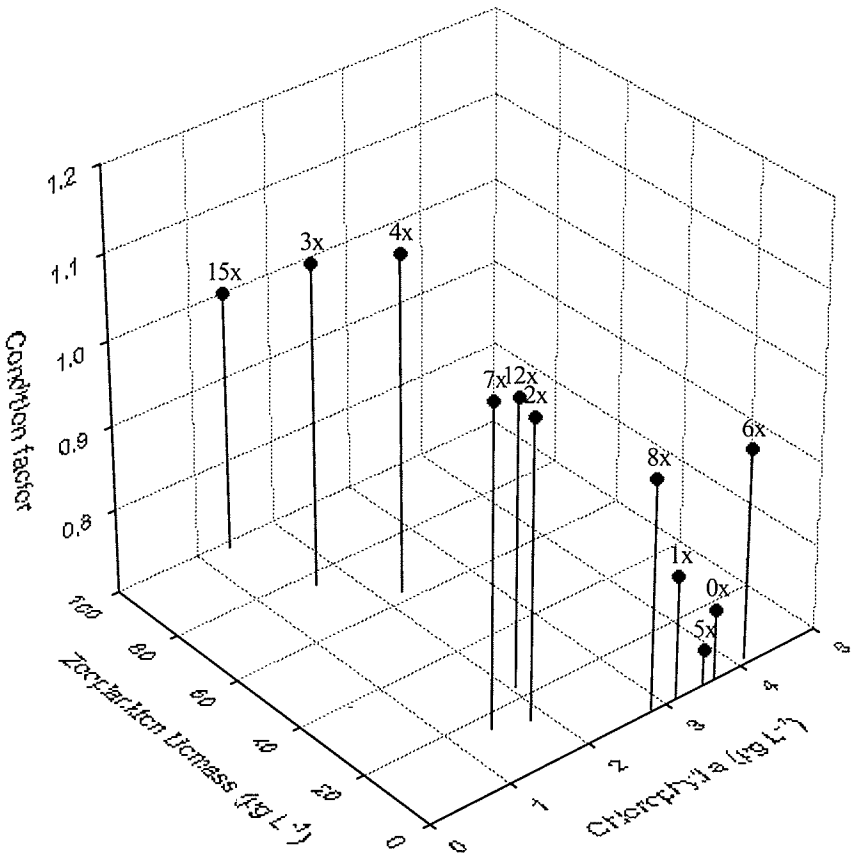

Figure II-26. Average condition factor of age 1 + yellow perch in each mesocosm, shown in relation to chlorophyll *a* (surrogate measure for phytoplankton biomass) and zooplankton biomass. Chlorophyll *a* was measured on 3 September, zooplankton were sampled between 29 – 30 September, and fish were captured between 4 – 16 September. The label above each point identifies the mesocosm.

APPENDIX III. Estimation of mercury evasion

The evasion of dissolved gaseous mercury (DGM) from the intensive mesocosms was estimated by A. Poulain (University of Montreal) based on the thin boundary layer model (Liss and Slater 1974). Evasion of DGM was assumed to be proportional to the concentration gradient of elemental mercury [Hg(0)] across the air-water interface:

$$f = k_{Hg}(\mathrm{DGM} - \mathrm{Hg(0)}_a / H)$$

where f is the flux of DGM to the atmosphere, k_{Hg} is the mass transfer coefficient for Hg(0), DGM is the concentration of Hg(0) in surface water, $Hg(0)_a$ is the concentration of Hg(0) in overlaying atmosphere, and H is Henry's law constant corrected for temperature ($H = 0.0074T + 0.1551$, where T is temperature; Sanemasa (1975)). DGM concentrations measured at noon were assumed to be representative of the 24-h period, based on the observation that daytime and nightime DGM concentrations in a previous enclosure experiment at ELA were similar (Amyot et al. 2004). On days when DGM was not measured, concentrations were estimated using a linear interpolation between the two nearest sampling dates.

The mass transfer coefficient k_{Hg} was estimated by adding an inert gas (SF_6) to the mesocosms and following its decline over time. SF_6 was added to the intensive mesocosms on four dates (1 July, 15 July, 29 July, and 12 August). Briefly, SF_6 gas was injected into evacuated 500 mL plastic bottles containing lake water, shaken vigorously for 2 min, and released underwater in the mesocosms. Following each addition, triplicate surface water samples were collected from each mesocosm over three to four consecutive days. Samples were collected by puncturing 50 mL evacuated serum bottles (containing

5 mL of ultra pure nitrogen). Analyses of SF_6 samples were performed at the Freshwater Institute (Fisheries & Oceans Canada) following the protocol described in Matthews et al. (2003). The mass transfer coefficient for SF_6 was calculated using the formula developed by Ho et al. (2000) :

$$k_{SF_6} = h \cdot \ln(C_i / C_f) / \Delta t$$

where k_{SF_6} is the mass transfer coefficient for SF_6, h is the mean water depth, C_i and C_f are, respectively, the initial and final concentration of the gas over a period of time (Δt). The mass transfer coefficients of Hg and SF_6 were related based on the equation developed by Jahne et al. (1987):

$$k_{Hg} / k_{SF_6} = \left(Sc_{SF_6} / Sc_{Hg}\right)^n$$

where k_{Hg} and k_{SF_6} are, respectively, the mass transfer coefficients of Hg and SF_6, Sc_{Hg} and Sc_{SF_6} are, respectively, the Schmidt numbers for Hg and SF_6, and n is considered to be 2/3 (Crusius and Wanninkhof 2003). The Schmidt numbers for SF_6 and Hg were calculated by formulas developed by Wanninkhof (1992) and Poissant et al. (2000), respectively:

$$Sc_{SF_6} = 3255.3 - 217.13T + 6.8370T^2 - 0.086070T^3$$

$$Sc_{Hg} = (0.017^{-0.025T}) / (6.0^{-7} T + 1.0^{-5})$$

On days when SF_6 was not measured, k_{SF_6} was assumed to be equal to the average k_{SF_6} of the four periods.

To estimate the mass of spike Hg evaded over a particular time period, the amount of Hg evaded each day was added together:

$$F = \sum_{i=1}^{n} f_i$$

where F is the total flux of spike Hg evaded over the time period 1-n and f_i is the flux of spike Hg evaded on day i.

LITERATURE CITED

Amyot, M., G. Mierle, D. R. S. Lean and D. J. McQueen (1994). Sunlight-induced formation of dissolved gaseous mercury in lake waters. Environmental Science and Technology **28**(13): 2366-2371.

Amyot, M., G. Southworth, S. E. Lindberg, H. Hintelmann, J. D. Lalonde, N. Ogrinc, A. J. Poulain and K. A. Sandilands (2004). Formation and evasion of dissolved gaseous mercury in large enclosures amended with $^{200}HgCl_2$. Atmospheric Environment **38**(26): 4279-4289.

Armstrong, F. A. J. and D. P. Scott (1979). Decrease in mercury content of fishes in Ball Lake, Ontario, since imposition of controls on mercury discharges. Journal of the Fisheries Research Board of Canada **36**(6): 670.

Babiarz, C., J. Hurley, D. Krabbenhoft, C. Gilmour and B. Branfireun (2003). Application of ultrafiltration and stable isotopic amendments to field studies of mercury partitioning to filterable carbon in lake water and overland runoff. Science of the Total Environment **304**(1-3): 295-303.

Back, R. C. and C. J. Watras (1995). Mercury in zooplankton of northern Wisconsin lakes - taxonomic and site-specific trends. Water, Air, and Soil Pollution **80**(1-4): 931-938.

Bakir, F., S. F. Damluji, L. Amin-Zaki, M. Murtadha, A. Khadlidi, A.-R. Y., S. Tiktriti, H. I. Dhahir, T. W. Clarkson, J. C. Smith and R. A. Doherty (1973). Methylmercury poisoning in Iraq. Science **181**: 230-240.

Benoit, J. M., C. C. Gilmour, A. Heyes, R. P. Mason and C. L. Miller (2003). Geochemical and biological controls over methylmercury production and degradation in aquatic ecosystems. Biogeochemistry of environmentally important trace elements. **835:** 262 - 297.

Benoit, J. M., C. C. Gilmour and R. P. Mason (2001). The influence of sulfide on solid phase mercury bioavailability for methylation by pure cultures of *Desulfobulbus propionicus* (1pr3). Environmental Science and Technology **35**(1): 127-132.

Benoit, J. M., C. C. Gilmour, R. P. Mason and A. Heyes (1999). Sulfide controls on mercury speciation and bioavailability to methylating bacteria in sediment pore waters. Environmental Science and Technology **33**(10): 1780.

Bloom, N. S. (1992). On the chemical form of mercury in edible fish and marine invertebrate tissue. Canadian Journal of Fisheries and Aquatic Sciences **49**(5): 1010-1017.

Bodaly, R. A., J. W. M. Rudd, R. J. P. Fudge and C. A. Kelly (1993). Mercury concentrations in fish related to size of remote Canadian Shield lakes. Canadian Journal of Fisheries and Aquatic Sciences **50**(5): 980-987.

Boudou, A., M. Delnomdedieu, D. Georgescauld, F. Ribeyre and E. Saouter (1991). Fundamental roles of biological barriers in mercury accumulation and transfer in freshwater ecosystems. Water, Air, and Soil Pollution **56**: 807-822.

Boudou, A. and F. Ribeyre (1981). Comparative study of the trophic transfer of two mercury compounds - $HgCl_2$ and CH_3HgCl - between *Chlorella vulgris* and *Daphnia magna* - influence of temperature. Bulletin of Environmental Contamination and Toxicology **27**(5): 624-629.

Boudou, A. and F. Ribeyre (1983). Contamination of aquatic biocenoses by mercury compounds: an experimental ecotoxicological approach. Aquatic Toxicology. J. O. Nriagu. New York, John Wiley & Sons: 73-116.

Boudou, A. and F. Ribeyre (1985). Experimental study of trophic contamination of *Salmo gairdneri* by two mercury compounds - $HgCl_2$ and CH_3HgCl - analysis at the organism and organ levels. Water, Air, and Soil Pollution **26**(2): 137-148.

Bowles, K. C., S. C. Apte, W. A. Maher, M. Kawei and R. Smith (2001). Bioaccumulation and biomagnification of mercury in Lake Murray, Papua New Guinea. Canadian Journal of Fisheries and Aquatic Sciences **58**(5): 888-897.

Brunskill, G. J. and D. W. Schindler (1971). Geography and bathymetry of selected lake basins, Experimental Lakes Area, northwestern Ontario. Journal of the Fisheries Research Board of Canada **28**(2): 139-155.

Burger, J., K. F. Gaines, C. S. Boring, W. L. Stephens, Jr., J. Snodgrass and M. Gochfeld (2001). Mercury and selenium in fish from the Savannah River: Species, trophic level, and locational differences. Environmental Research **87**(2): 108-118.

Cabana, G., A. Tremblay, J. Kalff and J. B. Rasmussen (1994). Pelagic food chain structure in Ontario lakes: a determinant of mercury levels in lake trout (*Salvelinus namaycush*). Canadian Journal of Fisheries and Aquatic Sciences **51**(2): 381-389.

Carslaw, H. S. and J. C. Jaeger (1959). Conduction of Heat in Solids, Oxford University Press.

Chan, H. M., A. M. Scheuhammer, A. Ferran, C. Loupelle, J. Holloway and S. Weech (2003). Impacts of mercury on freshwater fish-eating wildlife and humans. Human and Ecological Risk Assessment **9**(4): 867-883.

Chen, C. Y. and C. L. Folt (2005). High plankton densities reduce mercury biomagnification. Environmental Science and Technology **39**(1): 115-121.

Choi, S., T. Chase, Jr and R. Bartha (1994). Metabolic pathways leading to mercury methylation in *Desulfovibrio desulfuricans* LS. Applied and Environmental Microbiology **60**(11): 4072-4077.

Choi, S. C. and R. Bartha (1993). Cobalamin-mediated mercury methylation by *Desulfovibrio desulfuricans* LS. Applied and Environmental Microbiology **59**(1): 290-295.

Cizdziel, J., T. Hinners, J. Pollard, E. Heithmar and C. Cross (2002). Mercury concentrations in fish from Lake Mead, USA, related to fish size, condition, trophic level, location, and consumption risk. Archives of Environmental Contamination and Toxicology **43**(3): 309-317.

Clarkson, T. W. (1997). The toxicology of mercury. Critical reviews in clinical laboratory sciences **34**(4): 369-403.

Clarkson, T. W. (2002). The three modern faces of mercury. Environmental Health Perspectives **110**: 11-23.

Cleckner, L. B., C. C. Gilmour, J. P. Hurley and D. P. Krabbenhoft (1999). Mercury methylation in periphyton of the Florida Everglades. Limnology and Oceanography **44**(7): 1815-1825.

Cohen, M., R. Artz, R. Draxler, P. Miller, L. Poissant, D. Niemi, D. Ratte, M. Deslauriers, R. Duval, R. Laurin, J. Slotnick, T. Nettesheim and J. McDonald

(2004). Modeling the atmospheric transport and deposition of mercury to the Great Lakes. Environmental Research **95**(3): 247-265.

Compeau, G. C. and R. Bartha (1985). Sulfate-reducing bacteria: principal methylators of mercury in anoxic estuarine sediment. Applied and Environmental Microbiology **50**(2): 498-502.

Cottingham, K. L., J. T. Lennon and B. L. Brown (2005). Knowing when to draw the line: designing more informative ecological experiments. Frontiers in Ecology and Environment **3**(3): 145-152.

Crusius, J. and R. Wanninkhof (2003). Gas transfer velocities measured at low wind speed over a lake. Limnology and Oceanography **48**(3): 1010-1017.

Cuvin, M. L. A. and R. W. Furness (1988). Uptake and elimination of inorganic mercury and selenium by minnows *Phoxinus phoxinus*. Aquatic Toxicology **13**: 205-216.

Davidson, P. W., G. J. Myers and B. Weiss (2004). Mercury exposure and child development outcomes. Pediatrics **113**(4): 1023-1029.

Dickenson Burrows, W. and P. A. Krenkel (1973). Studies on uptake and loss of methymercury-203 by bluegills (*Lepomis macrochirus* Raf.). Environmental Science and Technology **7**(13): 1127-1130.

Dyrssen, D. and M. Wedborg (1991). The sulfur-mercury(II) system in natural waters. Water, Air, and Soil Pollution **56**: 507-519.

Eckley, C., C. Watras, H. Hintelmann, K. Morrison, A. Kent and O. Regnell (2005). Mercury methylation in the hypolimnetic waters of lakes with and without connection to wetlands in northern Wisconsin. Canadian Journal of Fisheries and Aquatic Sciences **62**(2): 400-411.

Ekstrom, E. B., F. M. M. Morel and J. M. Benoit (2003). Mercury methylation independent of the acetyl-coenzyme a pathway in sulfate-reducing bacteria. Applied and Environmental Microbiology **69**(9): 5414-5422.

Essington, T. and J. Houser (2003). The effect of whole-lake nutrient enrichment on mercury concentration in age-1 yellow perch. Transactions of the American Fisheries Society **132**(1): 57-68.

Fimbreite, N. (1974). Mercury contamination of aquatic birds in northwestern Ontario. Journal of Wildlife Mangement **38**(1): 120-131.

Fitzgerald, W. F. (1998). The case for atmospheric mercury contamination in remote areas. Environmental Science and Technology **32**(1): 1-7.

Fitzgerald, W. F. and T. W. Clarkson (1991). Mercury and monomethylmercury: Present and future concerns. Environmental Health Perspectives **96**: 159-166.

Fitzgerald, W. F. and C. H. Lamborg (2003). Geochemistry of Mercury in the Environment. Treatise on Geochemistry, Elsevier Ltd. **9:** 107-148.

Fitzgerald, W. F., R. P. Mason and G. M. Vandal (1991). Atmospheric cycling and air-water exchange of mercury over midcontinental lacustrine regions. Water, Air, and Soil Pollution **56**: 745-767.

Fjeld, E., T. O. Haugenb and L. A. Vøllestadb (1998). Permanent impairment in the feeding behavior of grayling (*Thymallus thymallus*) exposed to methylmercury during embryogenesis. Science of the Total Environment **213**(1-3): 247.

Fjeld, E. and S. Rognerud (1993). Use of path analysis to investigate mercury accumulation in brown trout (*Salmo trutta*) in Norway and the influence of

environmental factors. Canadian Journal of Fisheries and Aquatic Sciences **50**(6): 1158-1167.

Francesconi, K. A., R. C. J. Lenanton, N. Caputi and S. Jones (1997). Long-term study of mercury concentrations in fish following cessation of mercury-containing discharge. Marine Environmental Research **43**(1-2): 27-40.

Friedmann, A. S., M. C. Watzin, T. Brinck-Johnsen and J. C. Leitera (1996). Low levels of dietary methylmercury inhibit growth and gonadal development in juvenile walleye (*Stizostedion vitreum*). Aquatic Toxicology **35**(3-4): 265.

Futter, M. N. (1994). Pelagic food-web structure influences probability of mercury contamination in lake trout (*Salvelinus namycush*). Science of the Total Environment **145**(1-2): 7-12.

Galli, C. L. and P. Restani (1993). Can methylmercury present in fish affect human health? Pharmacological Research **27**(2): 115-127.

Giblin, F. J. and E. J. Massaro (1973). Pharmocodynamics in rainbow trout (*Salmo gairdneri)*: tissue uptake, distribution, and excretion. Toxicology and Applied Pharmacology **24**: 81-91.

Gilmour, C. C. and E. A. Henry (1991). Mercury methylation in aquatic systems affected by acid deposition. Environmental Pollution **71**(2-4): 131-169.

Gilmour, C. C., E. A. Henry and R. Mitchell (1992). Sulfate stimulation of mercury methylation in fresh-water sediments. Environmental Science and Technology **26**(11): 2281-2287.

Gilmour, C. C., G. S. Riedel, M. C. Ederington, J. T. Bell, J. M. Benoit, G. A. Gill and M. C. Stordal (1998). Methymercury concentrations and production rates across a trophic gradient in the northern Everglades. Biogeochemistry **40**: 327-345.

Glass, G. E., J. A. Sorensen, K. W. Schmidt, G. R. Rapp, D. Yap and D. Fraser (1991). Mercury deposition and sources for the Upper Great Lakes region. Water, Air, and Soil Pollution **56**: 235-249.

Golding, G. R., C. A. Kelly, R. Sparling, P. C. Loewen, J. W. M. Rudd and T. Barkay (2002). Evidence for facilitated uptake of Hg(II) by *Vibrio anguillarum* and *Escherichia coli* under anaerobic and aerobic conditions. Limnology and Oceanography **47**(4): 967-975.

Grandjean, P., P. Weihe, R. F. White, F. Debes, S. Araki, K. Yokoyama, K. Murata, N. Sorensen, R. Dahl and P. J. Jorgensen (1997). Cognitive deficit in 7-year-old children with prenatal exposure to methylmercury. Neurotoxicology and Teratology **19**(6): 417-428.

Greenfield, B. K., T. R. Hrabik, C. J. Harvey and S. R. Carpenter (2001). Predicting mercury levels in yellow perch: use of water chemistry, trophic ecology, and spatial traits. Canadian Journal of Fisheries and Aquatic Sciences **58**(7): 1419-1429.

Grieb, T. M., C. T. Driscoll, S. P. Gloss, C. L. Schofield, C. L. Bowie and D. B. Porcella (1990). Factors affecting mercury accumulation in fish in the upper Michigan peninsula. Environmental Toxicology and Chemistry **9**(7): 919-930.

Hakanson, L., T. Andersson and A. Nilsson (1990). Mercury in fish in Swedish lakes - linkages to domestic and European sources of emission. Water, Air, and Soil Pollution **50**(1-2): 171-191.

Hall, B. D., R. A. Bodaly, R. J. P. Fudge, J. W. M. Rudd and D. M. Rosenberg (1997). Food as the dominant pathway of methylmercury uptake by fish. Water, Air, and Soil Pollution **100**(1-2): 13-24.

Hammerschmidt, C. R. and W. F. Fitzgerald (2005). Methylmercury in mosquitoes related to atmospheric mercury deposition and contamination. Environmental Science and Technology **39**(9): 3034-3039.

Hammerschmidt, C. R., M. B. Sandheinrich, J. G. Wiener and R. G. Rada (2002). Effects of dietary methylmercury on reproduction of fathead minnows. Environmental Science and Technology **36**(5): 877-883.

Harris, H., R. A. Bodaly, M. Amyot, C. Babiarz, K. Beaty, P. Blanchfield, B. Branfireun, C. Gilmour, A. Heyes, H. Hintelmann, J. Hurley, C. Kelly, D. Krabbenhoft, S. Lindberg, R. Mason, M. Paterson, C. Podemski, J. Rudd, G. Southworth and V. St. Louis (2004). METAALICUS Project Interim Report. EPRI, Palo Alto, CA 1005522.

Harris, R. C. and R. A. Bodaly (1998). Temperature, growth and dietary effects on fish mercury dynamics in two Ontario lakes. Biogeochemistry **40**(2-3): 175-187.

Harris, R. C. and W. J. Snodgrass (1993). Bioenergetic simulations of mercury uptake and retention in walleye (*Stizostedion vitreum*) and yellow perch (*Perca flavescens*). Water Pollution Research Journal of Canada **28**(1): 217-236.

Harrison, S. E., J. F. Klaverkamp and R. H. Hesslein (1990). Fates of metal radiotracers added to a whole lake: accumulation in fathead minnow (*Pimphales promelas*) and lake trout (*Salvelinus namaycush*). Water, Air, and Soil Pollution **52**(3-4): 277-293.

Health Canada (2002). Advisory: Information on mercury levels in fish. http://www.hc-sc.gc.ca/english/protection/warnings/2002/2002_41e.htm

Hecky, R. E., D. J. Ramsey, R. A. Bodaly and N. E. Strange (1991). Increased methylmercury contamination in fish in newly formed reservoirs. Advances in Mercury Toxicology. T. Suzuki and e. al. New York, Plenum Press.

Herut, B., H. Hornung, N. Kress and Y. Cohen (1996). Environmental relaxation in response to reduced contaminant input: the case of mercury pollution in Haifa Bay, Isreal. Marine Pollution Bulletin **32**(4): 366-373.

Hill, W. R., A. J. Stewart and G. E. Napolitano (1996). Mercury speciation and bioaccumulation in lotic primary producers and primary consumers. Canadian Journal of Fisheries and Aquatic Sciences **53**(4): 812-819.

Hintelmann, H., R. Ebinghaus and R. D. Wilken (1993). Accumulation of mercury(II) and methylmercury by microbial biofilms. Water Research **27**(2): 237-242.

Hintelmann, H., R. Harris, A. Heyes, J. P. Hurley, C. A. Kelly, D. P. Krabbenhoft, S. Lindberg, J. W. M. Rudd, K. J. Scott and V. L. St Louis (2002). Reactivity and mobility of new and old mercury deposition in a Boreal forest ecosystem during the first year of the METAALICUS study. Environmental Science and Technology **36**(23): 5034-5040.

Hintelmann, H. and H. T. Nguyen (2005). Extraction of methylmercury from tissue and plant samples using acid leaching. Analytical and Bioanalytical Chemistry **381**: 360-365.

Hintelmann, H. and N. Ogrinc (2003). Determination of stable mercury isotopes by ICP/MS and their application in environmental studies. Biogeochemistry of environmentally important trace elements.

Ho, D. T., W. E. Asher, L. F. Bliven, P. Schlosser and E. L. Gordon (2000). On mechanisms of rain-induced air-water gas exchange. Journal of Geophysical Research - Oceans **105**(C10): 24045-24057.

Hrabik, T. R. and C. J. Watras (2002). Recent declines in mercury concentration in a freshwater fishery: isolating the effects of de-acidification and decreased atmospheric mercury deposition in Little Rock Lake. Science of the Total Environment **297**(1-3): 229-237.

Hudson, R. J. M., S. A. Gherini, W. F. Fitzgerald and D. B. Porcella (1995). Anthropogenic influences on the global mercury cycle - a model-based analysis. Water, Air, and Soil Pollution **80**(1-4): 265-272.

Huggett, D. B., J. A. Steevens, J. C. Allgood, C. B. Lutken, C. A. Grace and W. H. Benson (2001). Mercury in sediment and fish from the North Mississippi Lakes. Chemosphere **42**: 923-929.

Hurley, J. P., D. P. Krabbenhoft, C. L. Babiarz and A. W. Andren (1994). Cycling of mercury across the sediment-water interface in seepage lakes. Environmental Chemistry of Lakes and Reservoirs, Advances in Chemistry Series **237**: 425-449.

Jackson, T. A. (1997). Long-range atmospheric transport of mercury to ecosystens, and the importance of anthropogenic emissions - a critical review and evaluation of the published evidence. Environmental Reviews **5**: 99-120.

Jahne, B., K. Munnich and R. Bosinger (1987). On the parameters influencing air-water gas exchange. Journal of Geophysical Research - Oceans **92**(C2): 1937-1949.

James, R., K. Sampath and G. Devakiamma (1993). Accumulation and depuration of mercury in a catfish *Heteropmeustes fossilis* (Pisces: *Heteropneustidae*) exposed to sublethal doses of the element. Asian Fisheries Science **6**: 183-191.

Jarvenpaa, T., M. Tillander and J. K. Miettinen (1970). Methylmercury: half-time elimination in flounder, pike, and eel. Suomen Kemistilehti **43B**: 439-442.

Johnson, M. G. (1987). Trace element loadings to sediments of fourteen Ontario lakes and correlations with concentrations in fish. Canadian Journal of Fisheries and Aquatic Sciences **44**(1): 3-13.

Johnson, W. E. and J. R. Vallentyne (1971). Rationale, background, and development of experimental lake studies in northwestern Ontario. Journal of the Fisheries Research Board of Canada **28**(2): 123-128.

Kelly, C., J. Rudd and M. Holoka (2003). Effect of pH on mercury uptake by an aquatic bacterium: Implications for Hg cycling. Environmental Science and Technology **37**(13): 2941-2946.

Kidd, K., R. H. Hesslein, R. J. P. Fudge and K. A. Hallard (1995). The influence of trophic level as measured by ^{15}N on mercury concentrations in freshwater organisms. Water, Air, and Soil Pollution **80**: 1011-1015.

Kotnik, J., M. Horvat and V. Jereb (2002). Modelling of mercury geochemical cycle in Lake Velenje, Slovenia. Environmental Modelling & Software **17**(7): 593-611.

Krabbenhoft, D. P., J. P. Hurley, M. L. Olson and L. B. Cleckner (1998). Diel variability of mercury phase and species distributions in the Florida Everglades. Biogeochemistry **40**(2-3): 311-325.

Laarman, P. W., W. A. Willford and J. R. Olson (1976). Retention of mercury in the muscle of yellow perch (*Perca flavescens*) and rock bass (*Ambloplites rupestris*). Transactions of the American Fisheries Society **2**: 296-300.

Lamborg, C. H., W. F. Fitzgerald, J. O'Donnell and T. Torgersen (2002). A non-steady-state compartmental model of global-scale mercury biogeochemistry with interhemispheric atmospheric gradients. Geochimica et Cosmochimica Acta **66**(7): 1105-1118.

Lange, T. R., H. E. Royals and L. L. Connor (1994). Influence of water chemistry on mercury concentrations in largemouth bass from Florida lakes. Transactions of the American Fisheries Society **123**(3): 448.

Latif, M. A., R. A. Bodaly, T. A. Johnston and R. J. P. Fudge (2001). Effects of environmental and maternally derived methylmercury on the embryonic and larval stages of walleye (*Stizostedion vitreum*). Environmental Pollution **111**(1): 139.

Lawrence, A. L. and R. P. Mason (2001). Factors controlling the bioaccumulation of mercury and methylmercury by the estuarine amphipod *Leptocheirus plumulosus*. Environmental Pollution **111**(2): 217-231.

Lawson, N. M. and R. P. Mason (1998). Accumulation of mercury in estuarine food chains. Biogeochemistry **40**(2-3): 235-247.

Leaner, J. J. and R. P. Mason (2004). Methylmercury uptake and distribution kinetics in sheepshead minnows, *Cyprinodon variegatus*, after exposure to CH_3Hg-spiked food. Environmental Toxicology and Chemistry **23**(9): 2138-2146.

Lebel, J., D. Mergler, F. Branches, M. Lucotte, M. Amorim, F. Larribe and J. Dolbec (1998). Neurotoxic effects of low-level methylmercury contamination in the Amazonian Basin. Environmental Research **79**(1): 20-32.

Lin, C. J. and S. O. Pehkonen (1999). The chemistry of atmospheric mercury: a review. Atmospheric Environment **33**(13): 2067-2079.

Lindberg, S., A. Vette, C. Miles and F. Schaedlich (2000). Mercury speciation in natural waters: Measurement of dissolved gaseous mercury with a field analyzer. Biogeochemistry **48**(2): 237-259.

Lindberg, S. E. and W. J. Stratton (1998). Atmospheric mercury speciation: concentrations and behavior of reactive gaseous mercury in ambient air. Environmental Science and Technology **32**(1): 49-57.

Lindberg, S. E. and H. Zhang (2000). Air/water exchange of mercury in the Everglades II: measuring and modeling evasion of mercury from surface waters in the Everglades Nutrient Removal Project. Science of the Total Environment **259**(1-3): 135-143.

Lindqvist, O. (1994). Atmospheric cycling of mercury: an overview. Mercury Pollution: Integration and Synthesis. C. J. Watras and J. W. Huckabee. Boca Raton, Lewis Publishers: 181-185.

Lindqvist, O., K. Johansson, M. Aastrup, A. Andersson, L. Bringmark, G. Hovsenius, L. Hakanson, A. Iverfeldt, M. Meil and B. Timm (1991). Mercury in the Swedish Environment - recent research on causes, consequences and corrective measures. Water, Air, and Soil Pollution **55**(1-2): 65-71.

Liss, P. S. and P. G. Slater (1974). Flux of gases across the air-sea interface. Nature **247**: 181-184.

Lockhart, W. L., J. F. Uthe, A. R. Kenney and P. M. Mehrle (1972). Methylmercury in northern pike (*Esox lucius*): distribution, elimination, and some biochemical characteristics of contaminated fish. Journal of the Fisheries Research Board of Canada **29**: 1519-1523.

Lockhart, W. L., P. Wilkinson, B. N. Billeck, R. A. Danell, R. V. Hunt, G. J. Brunskill, J. Delaronde and V. St Louis (1998). Fluxes of mercury to lake sediments in central and northern Canada inferred from dated sediment cores. Biogeochemistry **40**(2-3): 163-173.

Lockhart, W. L., P. Wilkinson, B. N. Billeck, R. V. Hunt, R. Wagemann and G. J. Brunskill (1995). Current and historical inputs of mercury to high-altitude lakes in Canada and to Hudson Bay. Water, Air, and Soil Pollution **80**(1-4): 603-610.

Lorey, P. and C. T. Driscoll (1999). Historical trends of mercury deposition in Adirondack lakes. Environmental Science and Technology **33**(5): 718-722.

MacCrimmon, H. R., C. D. Wren and B. L. Gots (1983). Mercury uptake in lake trout, *Salvelinus namaycush*, relative to age, growth, and diet in Tadenac Lake with comparative data from other Precambrian Shield lakes. Canadian Journal of Fisheries and Aquatic Sciences **40**(2): 114-120.

Marvin-DiPasquale, M., J. Agee , C. McGowan, R. S. Oremland, M. Thomas, D. Krabbenhoft and C. C. Gilmour (2000). Methyl-mercury degradation pathways: A comparison among three mercury-impacted ecosystems. Environmental Science and Technology **34**(23): 4908-4916.

Mason, R. and K. Sullivan (1997). Mercury in Lake Michigan. Environmental Science and Technology **31**(3): 942-947.

Mason, R. P., W. F. Fitzgerald and F. M. M. Morel (1994). The biogeochemical cycling of elemental mercury: anthropogenic influences. Geochimica et Cosmochimica Acta **58**(15): 3191-3198.

Mason, R. P., J. M. Laporte and S. Andres (2000). Factors controlling the bioaccumulation of mercury, methylmercury, arsenic, selenium, and cadmium by freshwater invertebrates and fish. Archives of Environmental Contamination and Toxicology **38**(3): 283-297.

Mason, R. P., F. J. G. Laurier, L. Whalin and G. R. Sheu (2003). The role of ocean-atmosphere exchange in the global mercury cycle. Journal de Physique IV **107**(835-838).

Mason, R. P., J. R. Reinfelder and F. M. M. Morel (1995). Bioaccumulation of mercury and methylmercury. Water, Air, and Soil Pollution **80**(1-4): 915-921.

Mason, R. P., J. R. Reinfelder and F. M. M. Morel (1996). Uptake, toxicity, and trophic transfer of mercury in a coastal diatom. Environmental Science and Technology **30**(6): 1835-1845.

Matthews, C. J. D., V. L. St Louis and R. H. Hesslein (2003). Comparison of three techniques used to measure diffusive gas exchange from sheltered aquatic surfaces. Environmental Science & Technology **37**(4): 772-780.

McCloskey, J. T., I. R. Schultz and M. C. Newman (1998). Estimating the oral bioavailability of methylmercury to channel catfish (*Ictalurus punctatus*). Environmental Toxicology and Chemistry **17**(8): 1524-1529.

McKeown-Eyssen, G. E. and J. Ruedy (1983). Methyl mercury exposure in northern Quebec. I. Neurologic findings in adults. American Journal of Epidemiology **118**(4): 461-469.

McKeown-Eyssen, G. E., J. Ruedy and A. Neims (1983). Methyl mercury exposure in northern Quebec. II. Neurologic findings in children. American Journal of Epidemiology **118**(4): 470-479.

McKim, J. M., G. F. Olson, G. W. Holcombe and E. P. Hunt (1976). Long-term effects of methylmercuric chloride on three generations of brook trout (*Salvalinus fontinalus*): toxicity, accumulation, distribution, and elimination. Journal of the Fisheries Research Board of Canada **33**: 2726-2739.

Meili, M. (1997). Mercury in lakes and rivers. Metal Ions in Biological Systems. A. Sigel and H. Sigel. New York, Marcel Dekker, Inc. **34:** 21-51.

Meyer, M. W., D. C. Evers, J. J. Hartigan and P. S. Rasmussen (1998). Patterns of common loon (*Gavia immer*) mercury exposure, reproduction, and survival in Wisconsin, USA. Environmental Toxicology and Chemistry **17**(2): 184-190.

Mierle, G. (1990). Aqueous inputs of mercury to Precambrian Shield lakes in Ontario. Environmental Toxicology and Chemistry **9**(7): 843-851.

Miles, C. J., H. A. Moye, E. J. Phlips and B. Sargent (2001). Partitioning of monomethylmercury between freshwater algae and water. Environmental Science and Technology **35**(21): 4277-4282.

Monson, B. A. and P. L. Brezonik (1999). Influence of food, aquatic humus, and alkalinity on methylmercury uptake by *Daphnia magna*. Environmental Toxicology and Chemistry **18**(3): 560-566.

Monteiro, L. R., E. J. Isidro and H. D. Lopes (1991). Mercury content in relation to sex, size, age and growth in two scorpionfish (*Helicolenus dactylopterus* and *Pontinus kuhlii*) from Azorean waters. Water, Air, and Soil Pollution **56**: 359-367.

Morel, F. M. M., A. M. L. Kraepiel and M. Amyot (1998). The chemical cycle and bioaccumulation of mercury. Annual review of Ecology and Systematics **29**: 543-566.

Moye, H. A., C. J. Miles, P. E.J., B. Sargent and K. K. Merritt (2002). Kinetics and uptake mechanisms for monomethylmercury between freshwater algae and water. Environmental Science and Technology **36**(16): 3550-3555.

Nocera, J. J. and P. D. Taylor (1998). *In situ* behavioral responses of common loons associated with elevated mercury (Hg) exposure. Conservation Ecology [online] **2**(2): 10-19.

Norstrom, R. J., A. E. McKinnon and S. W. DeFreitas (1976). A bioenergetics-based model for pollutant accumulation by fish. Simulation of PCB and methylmercury residue levels in Ottawa river yellow perch (*Perca flavesencs*). Journal of the Fisheries Research Board of Canada **33**: 248-267.

North American Implementation Task Force on Mercury (2000). North American Regional Action Plan on Mercury: Phase II. http://www.cec.org/programs_projects/pollutants_health/smoc/pdfs/Hgnarap.pdf

O'Driscoll, N. J., S. Beauchamp, S. D. Siciliano, A. N. Rencz and D. R. S. Lean (2003). Continuous analysis of dissolved gaseous mercury (DGM) and mercury flux in two freshwater lakes in Kejimkujik Park, Nova Scotia: Evaluating mercury flux

models with quantitative data. Environmental Science & Technology **37**(10): 2226-2235.

Oliveira Ribeiro, P. C.A., E., , W. C. Pfeiffer and C. Rouleau (2000). Comparative uptake, bioaccumulation, and gill damages of inorganic mercury in tropical and Nordic freshwater fish. Environmental Research **83**(3): 286-292.

Oliveira Ribeiro, C. A., J. R. D. Guimaraes and W. C. Pfeiffer (1996). Accumulation and distribution of inorganic mercury in a tropical fish (*Trichomycterus zonatus*). Ecotoxicology and Environmental Safety **34**(2): 190-195.

Oliveira Ribeiro, C. A., C. Rouleau, E. Pelletier, C. Audet, and and H. Tjälve (1999). Distribution kinetics of dietary methylmercury in the arctic charr (*Salvelinus alpinus*). Environmental Science and Technology **33**(6): 902-907.

Olson, K. R., H. L. Bergman and P. O. Fromm (1973). Uptake of methyl mercuric chloride and mercuric chloride by trout: a study of uptake pathways into the whole animal and uptake by erythrocytes *in vitro*. Journal of the Fisheries Research Board of Canada **30**: 1293-1299.

Olsson, M. (1976). Mercury level as a function of size and age in northern pike, one and five years after the mercury ban in Sweden. Ambio **5**: 73-76.

Ontario Ministry of Environment (2003). Guide to Eating Sport Fish 2003-2004, Queens Printer for Ontario.

Pacyna, E. G. and J. M. Pacyna (2002). Global emission of mercury from anthropogenic sources in 1995. Water, Air, and Soil Pollution **137**(1-4): 149-165.

Parks, J. W., J. A. Sutton, J. D. Hollinger and D. D. Russell (1988). Uptake of mercury by caged crayfish. Applied Organometallic Chemistry **2**: 181-184.

Paterson, M. J., P. Blanchfield, R. Harris, H. H. Hintelmann, C. Podemski, J. W. M. Rudd and K. Sandilands (in prep.). Changes in Hg and methyl Hg bioaccumulation by fish and invertebrates following additions of stable Hg isotopes in large enclosures.

Paterson, M. J., J. W. M. Rudd and V. L. St. Louis (1998). Increases in total and methylmercury in zooplankton following flooding of a peatland reservoir. Environmental Science and Technology **32**(24): 3868-3874.

Pentreath, R. J. (1976). The accumulation of mercury from food by the plaice, *Pleuronectes platessa* L. Journal of Experimental Marine Biology and Ecology **25**: 51-65.

Phillips, G. R. and D. R. Buhler (1978). The relative contributions of methylmercury from food or water to rainbow trout (*Salmo gairdneri*) in a controlled laboratory experiment. Transactions of the American Fisheries Society **107**: 853-861.

Phillips, G. R. and R. W. Gregory (1979). Assimilation efficiency of dietary methylmercury by northern pike. Journal of the Fisheries Research Board of Canada **36**: 1516-1519.

Pickhardt, P. C., C. L. Folt, C. Y. Chen, B. Klaue and J. D. Blum (2002). Algal blooms reduce the uptake of toxic methylmercury in freshwater food webs. Proceedings of the National Academy of Sciences of the United States of America **99**(7): 4419-4423.

Pilgrim, W., W. Schroeder, D. B. Porcella, C. Santos-Burgoa, S. Montgomery, A. Hamilton and L. Trip (2000). Developing consensus: mercury science and policy

in the NAFTA countries (Canada, the United States and Mexico). Science of the Total Environment **261**: 185-193.

Poissant, L., M. Amyot and M. Pilote (2000). Mercury water-air exchange over the Upper St Lawrence River and Lake Ontario. Environmental Science and Technology **34**(15): 30693078.

Porcella, D. B. (1994). Mercury in the environment: biogeochemistry. Mercury Pollution: Integration and Synthesis. C. J. Watras and J. W. Huckabee. Boca Raton, Lewis Publishers: 3-19.

Post, R. P., R. Vandenbos and D. J. McQueen (1996). Uptake rates of food-chain and waterborne mercury by fish: Field measurements, a mechanistic model, and an assessment of uncertainties. Canadian Journal of Fisheries and Aquatic Sciences **53**(2): 395-407.

Power, M., G. M. Klein, K. R. R. A. Guiguer and M. K. H. Kwan (2002). Mercury accumulation in the fish community of a sub-Arctic lake in relation to trophic position and carbon sources. Journal of Applied Ecology **39**(5): 819-830.

Ramlal, R. S., C. A. Kelly, J. W. M. Rudd and A. Furutani (1993). Sites of methyl mercury production in remote Canadian Shield lakes. Canadian Journal of Fisheries and Aquatic Sciences **50**(5): 972-979.

Rasmussen, J. B., D. J. Rowan, D. R. S. Lean and J. H. Carey (1990). Food chain structure in Ontario lakes determines PCB levels in lake trout (*Salvelinus namycush*) and other pelagic fish. Canadian Journal of Fisheries and Aquatic Sciences **47**: 2030-2038.

Reinfelder, J. R. and N. S. Fisher (1991). The assimilation of elements ingested by marine copepods. Science **251**(4995): 794-796.

Riisgard, H. U. and S. Hansen (1990). Biomagnification of mercury in a marine grazing food chain: algal cells *Phaeodactylum tricornutum*, mussels *Mytilus edulis* and flounders *Platichthys flesus* studied by means of a stepwise reduction-CVAA method. Marine Ecology Progress Series **62**(3): 259-270.

Rodgers, D. W. (1994). You Are What You Eat and a Little Bit More: Bioenergetics-Based Models of Methylmercury Accumulation in Fish Revisited. Mercury Pollution: Integration and Synthesis. Watras C.J. and H. J.W., Lewis Publishers, Boca Raton.

Rodgers, D. W. and F. W. H. Beamish (1981). Uptake of waterborne methylmercury by rainbow trout (*Salmo gairdneri)* in relation to oxygen consumption and methylmercury concentration. Canadian Journal of Fisheries and Aquatic Sciences **38**(11): 1309-1315.

Rodgers, D. W. and F. W. H. Beamish (1982). Dynamics of dietary methylmercury in rainbow trout, *Salmo gardneri*. Aquatic Toxicology **2**: 271-290.

Rodgers, D. W. and S. U. Qadri (1982). Growth and mercury accumulation in yearling yellow perch, *Perca flavescens*, in the Ottawa River, Ontario. Environmental Biology of Fishes **7**(4): 377-383.

Rudd, J. and M. Turner (1983). The English-Wabigoon River System: V. Mercury and selenium bioaccumulation as a function of primary productivity. Canadian Journal of Fisheries and Aquatic Sciences **40**(12): 2251-2259.

Rudd, J., M. Turner, A. Furtani, A. Swick and B. Townsend (1983). The English Wabigoon River System: I. A synthesis of recent research with a view toward

mercury amelioration. Canadian Journal of Fisheries and Aquatic Sciences **40**(12): 2206-2217.

Rudd, J. W. M. (1995). Sources of methyl mercury to freshwater ecosystems: a review. Water, Air, and Soil Pollution **80**: 697-713.

Ruohtula, M. and J. K. Miettinen (1975). Retention and excretion of ^{203}Hg-labelled methylmercury in rainbow trout. Oikos **26**: 385-390.

Samson, J. C., R. Goodridge, F. Olobatuyi and J. S. Weis (2001). Delayed effects of embryonic exposure of zebrafish (*Danio rerio*) to methylmercury (MeHg). Aquatic Toxicology **51**(4): 369.

Sandilands, K. A., J. W. M. Rudd, C. A. Kelly, H. Hintelmann, C. C. Gilmour and M. T. Tate (2005). Application of Enriched Stable Mercury Isotopes to the Lake 658 Watershed for the METAALICUS Project, at the Experimental Lakes Ares, Northwestern Ontario, Canada. Canadian Technical Report of Fisheries and Aquatic Sciences **2597**: vii + 48 p.

Sanemasa, I. (1975). The solubility of elemental mercury vapor in water. Bulletin of the Chemical Society of Japan **48**: 1795-1798.

Scheuhammer, A. M. and P. J. Blancher (1994). Potential risk to common loons (*Gavia immer*) from methylmercury exposure in acidified lakes. Hydrobiologia **279/280**: 445-455.

Scheuhammer, A. M., A. H. K. Wong and D. Bond (1998). Mercury and selenium accumulation in common loons (*Gavia immer*) and common mergansers (*Mergus merganser*) from eastern Canada. Environmental Toxicology and Chemistry **17**(2): 197-201.

Schoper, N. J. (1974). The uptake, biotransformation and elimination of elemental mercury by fish. Masters Thesis, University of Georgia.

Schroeder, W. H. and J. Munthe (1998). Atmospheric mercury - An overview. Atmospheric Environment **32**(5): 809-822.

Schuster, P. F., D. P. Krabbenhoft, D. L. Naftz, L. D. Cecil, M. L. Olson, J. F. Dewild, D. D. Susong, J. R. Green and M. L. Abbott (2002). Atmospheric mercury deposition during the last 270 years: A glacial ice core record of natural and anthropogenic sources. Environmental Science and Technology **36**(11): 2303-2310.

Sellers, P., C. A. Kelly and J. W. M. Rudd (2001). Fluxes of methylmercury to the water column of a drainage lake: The relative importance of internal and external sources. Limnology and Oceanography **46**(3): 623-631.

Sellers, P., C. A. Kelly, J. W. M. Rudd and A. R. MacHutchon (1996). Photodegradation of methylmercury in lakes. Nature **380**(6576): 694-697.

Sharpe, M. A., A. S. W. deFreitas and A. E. McKinnon (1977). The effect of body size on methylmercury clearance by goldfish. Environmental Biology of Fishes **2**: 177-183.

Siciliano, S. D., N. J. O'Driscoll and D. R. S. Lean (2002). Microbial reduction and oxidation of mercury in freshwater lakes. Environmental Science & Technology **36**(14): 3064-3068.

Simon, O. and A. Boudou (2001). Direct and trophic contamination of the herbivorous carp *Ctenophatyngodon idella* by inorganic mercury and methylmercury. Ecotoxicology and Environmental Safety **50**(1): 48-59.

Slemr, F. and E. Langer (1992). Increase in global atmospheric concentrations of mercury inferred from measurements over the Atlantic Ocean. Nature **355**(6359): 434-437.

Snodgrass, J. W., C. H. Jagoe, A. L. Bryan, Jr., H. A. Brant and J. Burger (2000). Effects of trophic status and wetland morphology, hydroperiod, and water chemistry on mercury concentrations in fish. Canadian Journal of Fisheries and Aquatic Sciences **57**(1): 171-180.

Sorensen, N., K. Murata, E. Budtz-Jorgensen, P. Weihe and P. Grandjean (1999). Prenatal methylmercury exposure as a cardiovascular risk factor at seven years of age. Epidemiology **10**(4): 370.

Sorenson, J. A., G. E. Glass, K. W. Schmidt, J. K. Huber and J. Rapp (1990). Airborne mercury deposition and watershed characteristics in relation to mercury concentrations in water, sediments, plankton, and fish of eighty northern Minnesota lakes. Environmental Science and Technology **24**(11): 1716-1727.

Spauldling, M. G., R. D. Bjork, G. V. N. Powell and S. F. Sundlof (1994). Mercury and cause of death in great white heron. Journal of Wildlife Mangement **58**(4): 735-739.

St. Louis, V. L., J. W. M. Rudd, C. A. Kelly, K. G. Beaty, N. S. Bloom and R. J. Flett (1994). Importance of wetlands as sources of methyl mercury to boreal forest ecosystems. Canadian Journal of Fisheries and Aquatic Sciences **51**: 1065-1076.

St. Louis, V. L., J. W. M. Rudd, C. A. Kelly, B. D. Hall, K. R. Rolfhus, K. J. Scott, S. E. Lindberg and W. Dong (2001). Importance of the forest canopy to fluxes of methyl mercury and total mercury to boreal ecosystems. Environmental Science and Technology **35**(15): 3089-3098.

Stafford, C. P. and T. A. Haines (2001). Mercury contamination and growth rate in two piscivore populations. Environmental Toxicology and Chemistry **20**(9): 2099-2101.

Stainton, M. P., M. J. Capel and F. A. Armstrong (1977). The chemical analysis of fresh water. DFO Miscellaneous Special Publication **25**: 1-180.

Sunda, W. G. and S. A. Huntsman (1998). Processes regulating cellular metal accumulation and physiological effects: Phytoplankton as model systems. Science of the Total Environment **219**(2-3): 165-181.

Suns, K. and G. Hitchin (1990). Interrelationships between mercury levels in yearling yellow perch, fish condition and water quality. Water, Air, and Soil Pollution **650**: 225-265.

Swain, E. B., D. R. Engstrom, M. E. Brigham, T. A. Henning and P. L. Brezonik (1992). Increasing rates of atmospheric mercury deposition in midcontinental North America. Science **257**(5071): 784-787.

Sweerts, J.-P. A., C. A. Kelly, J. W. M. Rudd, R. H. Hesslein and T. E. Cappenberg (1991). Similarity of whole-sediment molecular diffusion coefficients in freshwater sediments of low and high porosity. Limnology and Oceanography **36**: 335-342.

Takizawa, Y. (1979). Epidemiology of mercury poisoning. The Biogeochemistry of Mercury in the Environment. J. O. Nriagu. New York, Elsevier/North Holland Biomedical Press: 325-365.

Tchounwou, P. B., W. K. Ayensu, N. Ninashvili and D. Sutton (2003). Environmental exposure to mercury and its toxicopathologic implications for public health. Environmental Toxicology **18**(3): 149-175.

Tremblay, A., M. Lucotte and R. Schetagne (1998). Total mercury and methylmercury accumulation in zooplankton of hydroelectric reservoirs in northern Quebec (Canada). Science of the Total Environment **213**(1-3): 307-315.

Trudel, M. and J. B. Rasmussen (1997). Modeling the elimination of mercury by fish. Environmental Science and Technology **31**(6): 1716-1722.

Tseng, C. M., C. Lamborg, W. F. Fitzgerald and D. R. Engstrom (2004). Cycling of dissolved elemental mercury in Arctic Alaskan lakes. Geochimica et Cosmochimica Acta **68**(6): 1173-1184.

Tsui, M. T. K. and W. X. Wang (2004a). Temperature influences on the accumulation and elimination of mercury in a freshwater cladoceran, *Daphnia magna*. Aquatic Toxicology **70**(3): 245-256.

Tsui, M. T. K. and W. X. Wang (2004b). Uptake and elimination routes of inorganic mercury and methylmercury in *Daphnia magna*. Environmental Science and Technology **38**(3): 808-816.

Twining, B. S. and N. S. Fisher (2004). Trophic transfer of trace metals from protozoa to mesozooplankton. Limnology and Oceanography **49**(1): 28-39.

U.S. Environmental Protection Agency (1997). Mercury Study Report to Congress, Volume III: Fate and Transport of Mercury in the Environment.

U.S. Environmental Protection Agency (2004). EPA Fact Sheet: National Listing of Fish Advisories. http://www.epa.gov/waterscience/fish/advisories/factsheet.pdf

U.S. Environmental Protection Agency (2005). Clean Air Mercury Rule. http://www.epa.gov/air/mercuryrule/index.htm

U.S. Food and Drug Administration and U.S. Environmental Protection Agency (2004). What You Need to Know About Mercury in Fish and Shellfish. http://www.epa.gov/waterscience/fish/MethylmercuryBrochure.pdf

Ullrich, S. M., T. W. Tanton and S. A. Abdrashitova (2001). Mercury in the aquatic environment: A review of factors affecting methylation. Critical Reviews in Environmental Science and Technology **31**(3): 241-293.

United Nations Environment Programme (2002). Global Mercury Assessment. http://www.chem.unep.ch/mercury/Report/Final%20Assessment%20report.htm

Vander Zander, M. J. and J. B. Rasmussen (1996). A trophic position model of pelagic food webs: impact on contaminant bioaccumulation in lake trout. Ecological Monographs **66**(4): 451-477.

Verta, M. (1990). Changes in fish mercury concentrations in an intensively fished lake. Canadian Journal of Fisheries and Aquatic Sciences **47**(10): 1888-1897.

Verta, M., T. Matilainen, P. Porvari, M. Niemi, A. Uusi-Rauva and N. S. Bloom (1994). Methylmercury sources in boreal lake ecosystems. Mercury Pollution: Integration and Synthesis. C. J. Watras and J. W. Huckabee. Boca Raton, Lewis Publisher.

Wanninkhof, R., J. (1992). Relationship between wind-speed and gas exchange over the ocean. Journal of Geophysical Research - Oceans **97**(C5): 7373-7382.

Watras, C. J., R. C. Back, S. Halvorsen, R. J. M. Hudson, K. A. Morrison and S. P. Wente (1998). Bioaccumulation of mercury in pelagic freshwater food webs. Science of the Total Environment **219**(2-3): 183-208.

Watras, C. J. and N. S. Bloom (1992). Mercury and methylmercury in individual zooplankton - implications for bioaccumulation. Limnology and Oceanography **37**(6): 1313-1318.

Watras, C. J., N. S. Bloom, R. J. M. Hudson, S. Gherini, R. Munson, S. A. Claas, K. A. Morrison, J. Hurley, J. G. Wiener, W. F. Fitzgerald, R. Mason, G. Vandal, D. Powell, R. Rada, L. Rislov, M. Winfrey, J. Elder, D. Krabbenhoft, A. W. Andren, C. Babiarz, D. B. Porcella and J. W. Huckabee (1994). Sources and Fates of Mercury and Methylmercury in Wisconsin Lakes. Mercury Pollution: Integration and Synthesis. C. J. Watras and J. W. Huckabee. Boca Raton, Lewis Publishers**:** 153-177.

Watras, C. J., K. A. Morrison, R. J. M. Hudson, T. M. Frost and T. K. Kratz (2000). Decreasing mercury in northern Wisconsin: temporal patterns in bulk precipitation and a precipitation-dominant lake. Environmental Science and Technology **34**(19): 4051-4057.

Watras, C. J., K. A. Morrison and T. K. Kratz (2002). Seasonal enrichment and depletion of Hg and SO4 in Little Rock Lake: relationship to seasonal changes in atmospheric deposition. Canadian Journal of Fisheries and Aquatic Sciences **59**(10): 1660-1667.

Webber, H. M. and T. A. Haines (2003). Mercury effects on predator avoidance behavior of a forage fish, golden shiner (*Notemigonus crysoleucas*). Environmental Toxicology and Chemistry **22**(7): 1556-1561.

Weis, J. and P. Weis (1995). Swimming performance and predator avoidance by mummichog (*Fundulus heteroclitus*) larvae after embryonic or larval exposure to methylmercury. Canadian Journal of Fisheries and Aquatic Sciences **42**: 2168-2173.

Wiener, J. G., D. P. Krabbenhoft, G. H. Heinz and A. M. Scheuhammer (2003). Ecotoxicology of mercury. Handbook of Ecotoxicology. D. J. Hoffman, B. A. Rattner, G. A. Burton, Jr. and J. Cairns, Jr. Boca Raton, Lewis Publishers, CRC Press**:** 409-463.

Wiener, J. G. and D. J. Spry (1996). Toxicological Significance of Mercury in Freshwater Fish. Environmental Contaminants in Wildlife: Interpreting Tissue Concentrations. W. N. Beyer, G. H. Heinz and A. W. Redmon-Norwood, Lewis Publishers**:** 297-339.

Winfrey, M. R. and J. W. M. Rudd (1990). Environmental factors affecting the formation of methylmercury in low pH lakes. Environmental Toxicology and Chemistry **9**(7): 853-869.

Wobeser, G. (1976). Mercury poisoning in a wild mink. Journal of Wildlife Diseases **12**: 335-339.

Wolfe, M. F., S. Schwarzbach and R. A. Sulaiman (1998). Effects of mercury on wildlife: A comprehensive review. Environmental Toxicology and Chemistry **17**(2): 146-160.

World Health Organization (1990). Environmental Health Criteria 101 - Methylmercury. Geneva, International Programme on Chemical Safety (IPCS).

WOW (2004). Water on the Web - Monitoring Minnesota Lakes on the Internet and Training Water Science Technicians for the Future - A National On-line

Curriculum using Advanced Technologies and Real-Time Data. http://WaterOntheWeb.org

Wren, C. D. (1985). Probable case of mercury poisoning in a wild otter, *Lutra canadensis*, in northwestern Ontario. Canadian Field-Naturalist **99**: 112-114.

Wren, C. D. and H. R. MacCrimmon (1983). Mercury levels in the sunfish, *Lepomis gibbosus*, relative to pH and other environmental variable of Precambrian Shield lakes. Canadian Journal of Fisheries and Aquatic Sciences **40**(10): 1737-1744.

Wren, C. D., W. A. Scheider and D. L. Wales (1991). Relation between mercury concentrations in walleye (*Stizotedion vitreum vitrieum*) and northern pike (*Esox lucius*) in

Ontario lakes and influence of environmental factors. Canadian Journal of Fisheries and Aquatic Sciences **48**(1): 132-139.

Wright, D. R. and R. D. Hamilton (1982). Release of methyl mercury from sediments - effects of mercury concentration, low-temperature, and nutrient addition. Canadian Journal of Fisheries and Aquatic Sciences **39**(11): 1459-1466.

Yang, H. D., N. L. Rose, R. W. Battarbee and J. F. Boyle (2002). Mercury and lead budgets for Lochnagar, a Scottish mountain lake and its catchment. Environmental Science and Technology **36**(7): 1383-1388.